

THE EXTRUSION AND MELT MODIFICATION OF BIOLOGICALLY DEGRADABLE  
POLYHYDROXYALKANOATES FOR THEIR USE IN PLASTIC ARTICLES

by

GRANT HAYDEN CRANE

(Under the Direction of Jason Locklin)

ABSTRACT

Plastic has become a standard part of modern life and has greatly enhanced the quality of life in many ways. Foods last longer on the shelves, items can be cheaply and safely shipped over large distances, and food can be easily packaged for meals in the fast-food, grocery, and coffee industries that allow a bustling society to continually function. But with all of these benefits comes the downside that when plastic waste is mismanaged it accumulates in the environment with deleterious effects on wildlife. More recently microplastics, which result from either weathering of larger plastic items or from direct release of microparticles, have been shown to accumulate in micro and macro fauna with increasing health concerns for humans as well. There is a pressing need for a viable replacement for current commodity thermoplastics that are used in the single use packaging sector, such as polypropylene (PP), polyethylene (PE), and polyethylene terephthalate (PET), that are biologically degradable into nontoxic components that do not introduce persistent microplastics into the environment.

Polyhydroxyalkanoates (PHA), a class of aliphatic polyesters produced through fermentation, show much promise for meeting that need. PHA copolymers offer a wide variety of melt and mechanical properties depending on the type and amount of random comonomer incorporated. Further melt blending and reactive extrusion with various polyesters, fillers, and nucleating agents were shown to give properties that allow for a broad spectrum of applications to be targeted by a truly biologically degradable material.

INDEX WORDS: polyhydroxyalkanoates, biologically degradable, extrusion, nucleating agent, reactive extrusion, melt blending



THE EXTRUSION AND MELT MODIFICATION OF BIOLOGICALLY DEGRADABLE  
POLYHYDROXYALKANOATES FOR THEIR USE IN PLASTIC ARTICLES

by

GRANT HAYDEN CRANE

B.S., University of Georgia 2014

A Dissertation Submitted to the Graduate Faculty of The University of Georgia in Partial  
Fulfillment of the Requirements for the Degree

DOCTOR OF PHILOSOPHY

ATHENS, GEORGIA

2021

© 2021

Grant Hayden Crane

All Rights Reserved

THE EXTRUSION AND MELT MODIFICATION OF BIOLOGICALLY DEGRADABLE  
POLYHYDROXYALKANOATES FOR THEIR USE IN PLASTIC ARTICLES

by

GRANT HAYDEN CRANE

Major Professor:	Jason Locklin
Committee:	Jonathan Amster
	Hitesh Handa
	Branson Ritchie

Electronic Version Approved:

Ron Walcott  
Vice Provost for Graduate Education and Dean of the Graduate School  
The University of Georgia  
August 2021

## DEDICATION

Soli Deo Gloria: Glory to God alone. God has used this unforeseen PhD program to sanctify me in many ways, but ultimately, I am most thankful that by keeping me in this program he sovereignly orchestrated revealing his Son, Jesus the Christ, to me through the preaching of his Gospel. In those months I came to truly understand that I was a sinner that would face divine judgement for every thought, word and deed that I had ever done and ever would do. Yet God, in his mercy, sent his son to die in my place and take the wrath reserved for me. Not only that but he also granted me his righteousness and adopted me into his family as his son. This is worth far more than any accolade or degree that will fade into dust with me. I must also thank and dedicate to my parents, Terry and Lisa Crane, without them I would not be in nor would I be finishing this program. There are not words that can adequately express the kind of gratitude I feel to them. Thank you for your wisdom, council, and Godly example that you tirelessly set for me through the years. I must also thank Haley, my wife and my glory, for her support and patience while I finished this degree. "An excellent wife who can find, she is far more precious than jewels." (Prov. 31:10) I have indeed obtained the favor of the Lord with you. And to my child who I do not yet know, this work is dedicated to you. For your provision and well-being, Lord willing in 9 months.

## ACKNOWLEDGEMENTS

First, I would like to thank Dr. Locklin for providing so much opportunity to me as a polymer scientist. If he had not taken me into his group or put me on the PHA project when he did, many of the doors that are now open to me would be sealed shut. The lab has shifted a lot over the years that I have been there, but I am thankful for my current lab mates who provide an interesting and pleasant environment to work in. I would also like to thank Demichael and Ethan for providing so many polymers for me to extrude. Both of you have been tremendously helpful. Thank you to the PHA team: Apisata, Scott, Jess, Amanda, and Michael for so much hard work and help as we navigate the challenges that are inherent to this project. Thank you to Dr. Ritchie for the many meetings about the future, for steadfast and sound council, and for all of the help through my program. I have enjoyed our time together immensely. Dr. Carraway thank you for all of the opportunity that you provided through your hard work and creativity. Through your inspiration and drive there is so much opportunity for people like me. Joe, thank you for your positivity and encouragement over the years of my program. I greatly enjoyed the time I spent in your lab during my early years. Dr. Amster, and Dr. Handa, thank you for taking the time to help me through my program and for serving on my committee in this unusual project.

## TABLE OF CONTENTS

	Page
ACKNOWLEDGEMENTS .....	v
LIST OF TABLES .....	vii
LIST OF FIGURES .....	iv
CHAPTER	
1 Introduction and Literature Review .....	1
Plastic Production.....	1
Polyhydroxyalkanoates.....	2
Extrusion Processing.....	6
Reactive Extrusion .....	8
Melt Blending .....	11
Conclusion .....	13
References.....	14
2 Melt Blending and Reactive Extrusion.....	22
Introduction.....	24
Materials and Methods .....	27
Results and Discussion.....	31
Conclusion .....	76
References.....	78

3	Nucleating Agents for PHA .....	84
	Introduction.....	86
	Materials and Methods .....	89
	Results and Discussion.....	92
	Conclusion .....	117
	References.....	121
4	Conclusion and Future Outlook.....	127
	Conclusion .....	127
	Future outlook.....	129
	Final Remarks .....	132

## LIST OF TABLES

	Page
Table 2.1: Elongation at break and Young's modulus of starch and PBAT blended with PHBHHx (6% Hx). Two sizes of talc were also blended as reinforcing fillers. ....	40
Table 2.2: Young's Modulus comparison of reactive extrusion blends with PHBHHx (6% Hx) .....	59
Table 2.3: Elongation at break and Young's modulus for varying molecular weights of PBA blended with PHBHHx (6% Hx).....	61
Table 2.4: Elongation at break and Young's modulus of varying PBSG blends with PHBHHx (6% Hx) .....	63
Table 2.5: Young's Modulus and elongation at break after 15 days with blends of PHBHHx (6% Hx), PHBHHx (10% Hx), and PBSA .....	68
Table 2.6: Young's Modulus and elongation at break after 15 days with blends of REX PHBHHx (6% Hx), PHBHHx (10% Hx), and PBSA .....	69
Table 2.7: Young's modulus and elongation after 15 days of REX blends with PHBHHx (6% Hx), PHBHHx (10% Hx), and PBA.....	72
Table 2.8: Half-life chart of radical initiators used in REX with PHBHHx (6% Hx).....	73
Table 2.9: Elongation at break for REX samples using different multifunctional coagents.....	76
Table 3.1: Peak crystallization temperature and relative crystallinity for various forms of orotic acid heated to different peak temperatures .....	98



Table 3.2: Peak crystallization temperature and relative crystallinity for various forms of orotic acid heated to different peak temperatures .....	101
Table 3.3: Peak crystallization temperatures and relative crystallinity for 0.5, 1, and 2% blends of Ox with PHBHHx (6% Hx) .....	117

## LIST OF FIGURES

	Page
Figure 1.1: General structure of PHA where R is typically 1-5 carbons in length.....	2
Figure 1.2: Crystallinity and melting temperatures for a variety of copolymers of PHB with different HA contents.....	4
Figure 1.3: Thermal depolymerization mechanism for PHB.....	5
Figure 1.4: Representative image for a typical twin-screw extruder .....	6
Figure 1.5: Representative image showing the interfacial compatibilization mechanism through the use of compatibilizing agents.....	11
Figure 2.1: Inside of the Haake minilab conical twin screw extruder showing the backchannel and pressure transducers.....	31
Figure 2.2: Percent elongation of PHBHHx (6% Hx) blends with commercially available polyesters .....	32
Figure 2.3: Young's Modulus of PHBHHx (6% Hx) blends with commercially available polyesters .....	32
Figure 2.4: Melting endotherms of 5, 10, 20, and 30% PBAT blended with PHBHHx (6% Hx) .....	33
Figure 2.5: Crystallization exotherms of 5, 10, 20, and 30% PBAT blended with PHBHHx (6% Hx) .....	35

Figure 2.6: SEM images of cryo-fractured samples showing immiscible PBAT domains (20%) within the PHBHHx matrix.....	36
Figure 2.7: Stress-Strain curves for starch blends using REX_PCL (Left), REX_PBSA (right) with PHBHHx (6% Hx) .....	37
Figure 2.8: SEM image showing starch encapsulated within PBAT when blended with PHBHHx (6% Hx). Image taken from blend one of table 1 .....	38
Figure 2.9: Representative process for the production of high lamellarity talc.....	39
Figure 2.10: SEM images of 5% talc added to PHA. Talc sheets are aligned with the direction of flow (coming out of the page). .....	40
Figure 2.11: SEM images showing Starch:PBAT:Talc blends with PHBHHx (6% Hx).....	41
Figure 2.12: Elongation at break of blends of Polycaprolactone with PHBHHx (6% Hx) ..	42
Figure 2.13: Melting endotherms of 5, 10, 20, and 30% blends of PCL with PHBHHx (6% Hx) .....	42
Figure 2.14: Exothermic transitions for 5, 10, 20, and 30% PCL blends with PHBHHx (6% Hx) .....	43
Figure 2.15: Melting endotherms for 5, 10, 20, and 30 % blends of PBS with PHBHHx (6% Hx) .....	44
Figure 2.16: Elongation at break of 5, 10, 20, and 30% blends of PBSA with PHBHHx (6% Hx) .....	45
Figure 2.17: Crystallization exotherms for 5, 10 ,20 and 30% blends of PBSA with PHBHHx (6%% Hx) .....	45

Figure 2.18: Elongation at break of 5, 10, 20, and 30% blends of PBS with PHBHHx (6% Hx) with and without peroxide.....	46
Figure 2.19: Stress-Strain curves of 5, 10, 20, and 30% REX blends of PBS with PHBHHx (6% Hx) .....	47
Figure 2.20: Melting endotherms for 5, 10, 20, and 30% REX_PBS blends with PHBHHx (6% Hx) .....	48
Figure 2.21: Crystallization exotherms for 5, 10, 20, and 30% REX_PBS blends with PHBHHx (6% Hx) .....	49
Figure 2.22: SEM images of 5, 10, 20, and 30% REX PBS blended with PHBHHx (6% Hx) 50	
Figure 2.23: Elongation at break of 5, 10, 20, and 30% blends of PBS with PHBHHx (6% Hx) with and without peroxide.....	51
Figure 2.24: Melting endotherms of 5, 10, 20, and 30% REX_PCL blends with PHBHHx (6% Hx) .....	52
Figure 2.25: SEM images showing immiscibility and compatibilization of PCL using reactive extrusion (the scale bar is 5 $\mu$ m) .....	53
Figure 2.26: Crystallization exotherms for 5, 10, 20, 30% REX_PCL blends with PHBHHx (6% Hx) .....	54
Figure 2.27: Elongation at break of 5, 10, 20, and 30% Blends of PBSA with PHBHHx (6% Hx) with and without peroxide.....	54
Figure 2.28: SEM images showing compatibilization of PBSA with PHBHHx (6% Hx) through reactive extrusion (scale bar is 5 $\mu$ m).....	55

Figure 2.29: Elongation at break of 5, 10, 20 and 30% blends of PBAT with PHBHHx (6% Hx) with (blue) and without (orange) peroxide.....	57
Figure 2.30: Crystallization exotherms for 5, 10, 20, and 30% blends of REX PBAT with PHBHHx (6% Hx) .....	57
Figure 2.31: SEM images comparing REX of 5, 10, and 20% blends of PBAT with PHBHHx (6% Hx) .....	58
Figure 2.32: Young's Modulus and elongation at break of blends with 30,000 Mw PBA and PHBHHx (6% Hx) .....	60
Figure 2.33: SEM images showing morphology difference in 10% and 20% blends of PBA 55k with PHBHHx (6% Hx) .....	61
Figure 2.34: Schematic of the pathways for aging of PHA. (a) pathway showing development of a rigid amorphous fraction due to secondary crystallization and (b) the pathway showing the development of a constrained amorphous phase that develops a rigid amorphous phase due to secondary crystallization .....	64
Figure 2.35: Crystallization exotherms for rapidly cooled (100°C/min) PHBHHx (6% Hx) alone and blended with PHBHHx (10% Hx) .....	67
Figure 2.36: Stress-Strain curves showing (left) 45° mold and (right) 70°C mold temperatures of REX blends with PHBHHx (6% Hx), PHBHHx (10% Hx), and PBSA.....	70
Figure 2.37: Melting endotherms for 15-day aged blends with PHBHHx (6% Hx), PHBHHx (10% Hx) and PBSA .....	70

Figure 2.38: Elongation at break for increasing peroxide content in blends with PHBHHx (6% Hx) at a mold temperature of 70°C .....	74
Figure 2.39: Chemical structures for crosslinking coagents used in reactive extrusion with Luperox P .....	75
Figure 3.1: Representative image for the effect of spherulite size and crystallization conditions on the final mechanical properties of PHBHHx (6% Hx) .....	92
Figure 3.2: Crystallization exotherms of 2% cyanuric acid blended with PHBHHx (6% Hx) .....	93
Figure 3.3: Crystallization exotherms of 5% cyanuric acid blended with PHBHHx (6% Hx) .....	94
Figure 3.4: Polarized microscopy images comparing blends of 5% and milled 2% cyanuric acid with PHBHHx (6% Hx).....	95
Figure 3.5: Crystallization exotherms for 2% milled cyanuric acid blended with PHBHHx (6% Hx) .....	96
Figure 3.6: Particle size analysis of orotic acid monohydrate before and after milling ...	97
Figure 3.7: Particle size analysis for zinc, magnesium, and calcium orotate.....	100
Figure 3.8: Polarized optical microscopy images of Zinc orotate blends with PHBHHx (6% Hx) cooling from a melt temperature of 200°C.....	101
Figure 3.9: Crystallization exotherms of zinc glycinate blended with PHBHHx (6% Hx) .....	102
Figure 3.10: Polarized optical microscope images of epitaxial nucleation of PHBHHx (6% Hx) on the surface of zinc glycinate crystals.....	103

Figure 3.11: Crystallization exotherms showing 0.1, 0.5, and 1.0% nano boron nitride blends with PHBHHx (6% Hx) .....	104
Figure 3.12: Crystallization exotherms comparing the peak crystallization temperature of a PHB homopolymer against a PHBHHx (6% Hx) copolymer.....	104
Figure 3.13: Crystallization exotherms of 1% nano boron nitride blended with a PHB homopolymer and a PHBHHx (6% Hx) copolymer.....	105
Figure 3.14: Isothermal crystallization at a hold temperature of 105°C comparing nano boron nitride with and without PHB homopolymer against milled cyanuric acid.....	106
Figure 3.15: Crystallization exotherms for blends of 2% pentaerythritol with PHBHHx (6% Hx) .....	108
Figure 3.16: Polarized optical microscope images showing the feather-like recrystallization of PE in blends with PHBHHx (6% Hx) followed by epitaxial nucleation of the polymer component .....	109
Figure 3.17: POM images showing that decreasing concentration of PE allows for finer fibrillar formation that leads to much smaller PHA spherulites.....	110
Figure 3.18: Crystallization exotherms for 1% pentaerythritol blended with PHBHHx (6% Hx) .....	111
Figure 3.19: Polarized optical microscope images showing the morphology of recrystallization for 1% pentaerythritol blended with PHBHHx (6% Hx).....	111
Figure 3.20: Crystallization exotherms for 0.5% pentaerythritol blends with PHBHHx (6% Hx) .....	112

Figure 3.21: POM images showing discrete PE crystals with simultaneous PHA nucleation for blends of 0.5% PE with PHBHHx (6% Hx) .....	113
Figure 3.22: Crystallization exotherms for 1% pentaerythritol melt blend at 165°C with PHBHHx (6% Hx) .....	114
Figure 3.23: Polarized optical microscope images showing 1% pentaerythritol melt blended with PHBHHx (6% Hx) at 165°C .....	115
Figure 3.24: Structure of synthesized, melt miscible, oxalamide nucleating agent (Ox) .....	116
Figure 3.25: Crystallization exotherms for 2% aliphatic oxalamide blended with PHBHHx (6% Hx) .....	117
Figure 3.26: Polarized optical microscope images showing the recrystallization of Ox as small fiber like crystals upon cooling from the melt .....	118



## CHAPTER 1

# BACKGROUND AND LITERATURE REVIEW OF POLYHYDROXYALKANOATES AS A VIABLE BIOLOGICALLY DEGRADABLE ALTERNATIVE TO COMMODITY THERMOPLASTICS FOR EXTRUSION APPLICATIONS

### 1.1 Current Plastic Production

Since the 1950s plastic production has steadily increased and has become a standard part of modern life that has greatly enhanced the quality of life in many ways. Foods last longer on shelves, items can be cheaply and safely shipped over large distances, and food and beverages can be easily packaged for meals in the fast-food, grocery and coffee industries that allow a bustling, modern society to function as it does. But with this growing use of plastic in every aspect of modern life there comes the burden of what to do with it once it is no longer in use. As of 2015, 6300 million metric tons (Mt) of plastic was produced with 79% accumulating in landfills and the environment, 12% being incinerated with and without energy recovery, and only 9% being recycled with 10% of that being recycled more than once.<sup>1</sup> Single use plastics, designed to be used once and then thrown away, are one of the largest contributors in the plastic industry with packaging making up 40% of this category.<sup>2</sup> With this level of plastic production, mismanaged waste is inevitable and it is estimated that 4.8-12.7 Mt has entered the oceans where it has a deleterious effect on both micro and macro fauna.<sup>3</sup> More recently the micronization of plastic has become an increasing concern.<sup>4,5</sup>

As the plastics undergo UV exposure and physical weathering they break down into small particles (<5mm) and can be ingested by small organisms causing adverse effects and death.<sup>6-8</sup> While several technologies look promising for recycling of polyolefins<sup>9-11</sup> or depolymerization to fuels<sup>12, 13</sup> the amount of mismanaged waste is not addressed by chemical or physical recycling, or even incineration and the accumulation in the environment needs to be addressed. There is still a pressing need for a viable replacement for current commodity thermoplastics that are used in the single use packaging sector, such as polypropylene (PP), polyethylene (PE), and polyethylene terephthalate (PET), that are biologically degradable into nontoxic components that do not introduce persistent microplastics into the environment.

## 1.2 Polyhydroxyalkanoates

Currently, biodegradable options for replacements of commodity thermoplastics are rather limited. Many biopolymers such as polylactic acid, a thermoplastic polyester produced through ring opening polymerization of lactide or through fermentation, are not truly biodegradable in all environments and are listed as industrially compostable. But even industrial composting has been found to be an issue for this biopolymer. Mechanically PLA has also been shown to be very brittle and requires plasticization to be effective in many applications. Other biopolymers such as

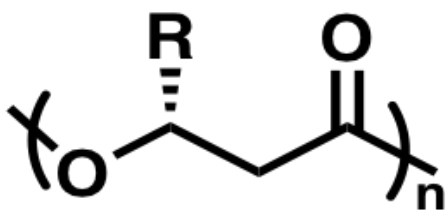


**Figure 1.1:** General structure of PHA where R is typically 1-5 carbons in length

polybutylene succinate (PBS) polybutylene succinate-co-adipate (PBSA), Polybutylene adipate-co-terephthalate (PBAT) and polycaprolactone (PCL) can have excellent

mechanical properties but do not possess the necessary ability to biodegrade in a wide variety of environments. Polyhydroxyalkanoates (PHA), a class of aliphatic polyesters produced through fermentation of plant sugars or oils, is a viable replacement of commodity thermoplastics such as PE and PP for many applications. PHAs are completely biodegradable in a wide variety of environments such as fresh water, marine, soil, home/industrial and anaerobic composting conditions.

Polyhydroxybutyrate (PHB) was first observed and isolated from *bacillus magaterium* by French scientist Maurice Lemoigne in 1926. And in 1974 the copolymers of 3-hydroxyvalerate and 3-hydroxyhexanoate were also identified.<sup>14</sup> PHA is a hydrophobic, granule inclusion made by microorganisms during times of environmental stress that can be depolymerized with the resulting products being used as a carbon source.<sup>15</sup> PHAs are divided into two categories based on the number of carbons in the sidechain. Short chain length (Scl) is when the carbon sidechain is 1-2 carbons in length and medium chain length is when the carbon sidechain is 3 or higher. The side chain length has a large impact on thermal and mechanical properties of the polymer. With its short side chain length and high stereoregularity, due to its biological origin, PHB has a very high crystallinity of up to 65% or higher.<sup>16</sup> This leads to a high melting temperature as well as brittle and stiff mechanical properties. Higher chain length homopolymers and copolymers have been shown to be produced by the addition of specific alkanolic acids into the fermentation media and more recently industrial fermentation has been shown to be a viable production method for random copolymers of PHB with comonomers containing longer side chains by using plant oils with the content and type of

comonomer being dependent on the type of bacteria used as well as the conditions of the fermentation.<sup>17-20</sup> Copolymers of PHB with other hydroxy acids can greatly influence the final mechanical and thermal properties of the PHA. Polyhydroxybutyrate-co-hydroxyvalerate (PHBV) causes a reduction in the melting temperature as well as an increase in the strain at break with increasing content of the valerate comonomer. As

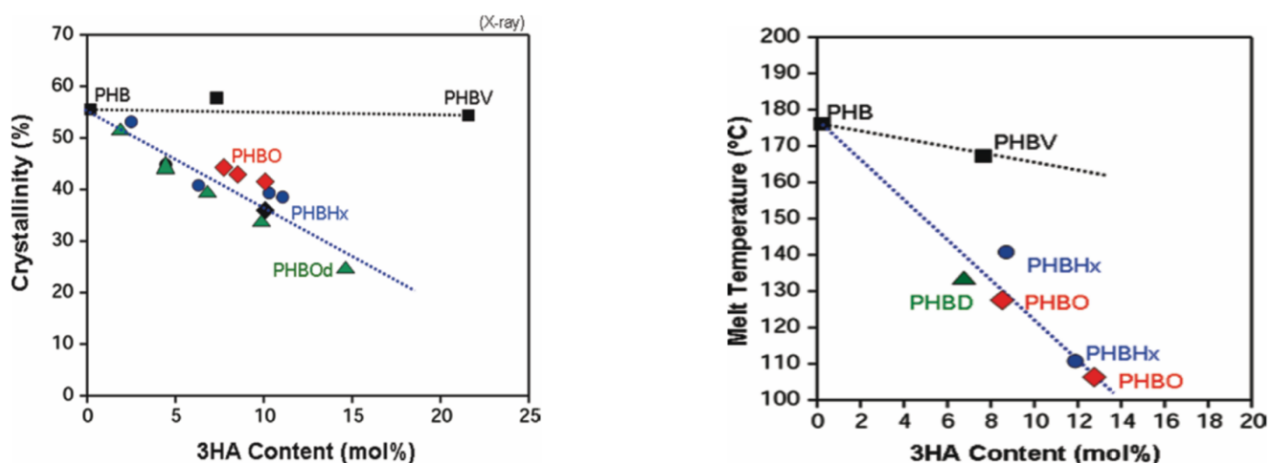


**Figure 1.2:** Crystallinity and melting temperatures for a variety of copolymers of PHB with different HA contents [22]

can be seen in figure 1.2, increasing the side chain length or amount of the comonomer has a larger effect on the reduction in crystallinity and melting temperature as well as increasing the ductility of the blend. PHBV is more readily incorporated into the crystalline lattice of the PHB unit cell and does not start significantly impacting the properties of the copolymer from its exclusion until the mole percent is 40% or more.<sup>21</sup> The longer side chain length of hydroxyhexanoate and hydroxyoctanoate act as chain defects and are excluded from the crystalline lattice resulting in a greater reduction in crystallinity and melting point as well as drastic improvements in the elongation at break.<sup>22</sup> Incorporation of mcl-comonomers also tends to reduce the glass transition

temperature from the range of 4-10°C for PHB to below zero depending on the type and amount of comonomer.<sup>23, 24</sup> The incorporation of longer side chains is very similar to what is done with LLDPE where ethylene is copolymerized with butene, hexene, or octene to have non-crystallizable portions for improved properties especially for film applications.<sup>25</sup> changing the type and amount of comonomer can give a wide variety of mechanical properties with elongation at break being shown to be above 600% for some copolymers of polyhydroxybutyrate-co-hydroxyhexanoate (PHBHHx).<sup>20, 26</sup> This shows much promise for mechanical properties that can be tuned to match those of PP and PE.

### 1.2.1 PHA Thermal Stability

The reduction in melting point and crystallinity is not only beneficial for enhancing the mechanical properties but also for increasing the processability of PHAs. PHB undergoes beta scission involving a six membered ring-like transition state, shown

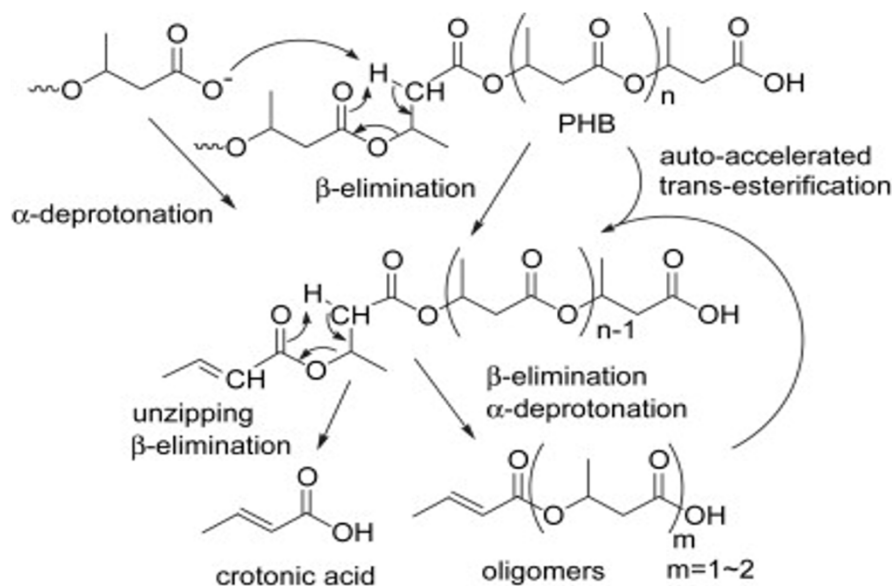


**Figure 1.3:** Thermal depolymerization mechanism for PHB [27]

in figure 1.3, leading to a cascade of thermal degradation pathways with an onset temperature of 185°C which is very close to the processing temperature of approximately 180°C.<sup>27, 28</sup> Thermal degradation leads to discoloration of the extrudate, off gassing of crotonic acid as well as poor mechanical properties due to the loss in molecular weight and chain entanglement. Lowering the melt temperature by incorporating long chain comonomers allows for processing conditions well below the thermal depolymerization onset temperature thus greatly enhancing the applicability of mcl-copolymers for a wide variety of applications.

### 1.3 Extrusion Processing

There are many processing techniques surrounding the single use packaging industry that all typically depend on extrusion for some aspect of the process. Profile

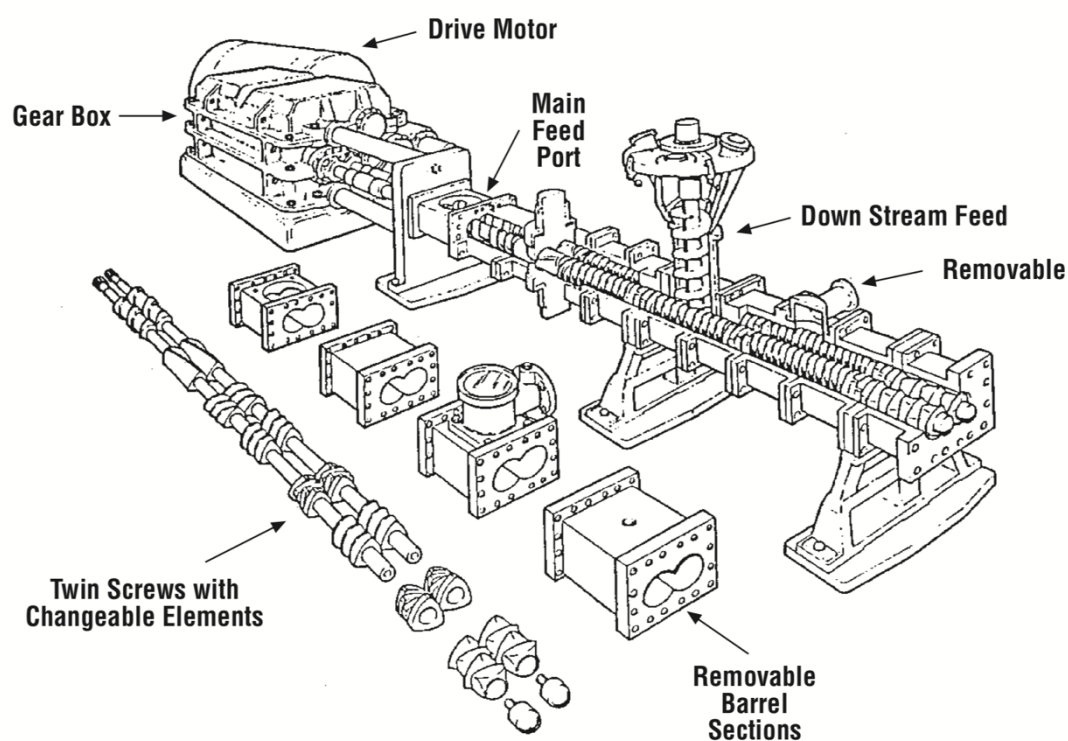


**Figure 1.4:** Representative image for a typical twin-screw extruder [30]

extrusion for items like straws, Injection molding for cutlery and others, extrusion blow molding for containers and bottles, melt blown fibers for non-woven production all rely on the extrusion step for melt processing of the polymers being used. Extrusion processing forces a molten polymer through an exit die using the action of a rotating screw, and originally single screw extruders were used for profile extrusion of polyvinyl chloride pipes.<sup>29</sup> And while single screw flood extruders are common, most modern industrial processing uses some form of twin screw extrusion, especially for polymer formulation and blending. Twin screw extruders can be divided into several categories based on screw rotation and screw design using a variety of removable elements to achieve the desired mixing and residence time required for each application.<sup>30</sup> Co-rotating screws have excellent distributive and dispersive mixing as the molten polymer is transferred from one screw to the other as the screws turn in the same direction. This leads to higher outputs but can hinder devolatilization. Counter rotating screws have added kneading that occurs as polymer is forced between the screws but can have hindered distributive mixing. Intermeshing co-rotating twin screw extruders have been found to function well for continuous reactive extrusion in many systems although screw design and elements play a large role in the final properties of the extruded article.<sup>31</sup> During the processing of a polymer, there can be several extrusion steps that are undergone. The first step can be formulation and melt blending with other polymers, fillers, and chemical modifying agents to produce a resin that will then be used in specific applications. After the initial formulation there can be two or three additional extrusion steps for the formulated resin during the production of the final

article. This requires the incorporation of several additives such as antioxidants and chain extenders that allow for the preservation of molecular weight and mechanical properties of the polymer being used. Several processing steps is especially problematic for PHAs as hydrolysis and beta scission can predominate during extruding leading to a polymer with poor mechanical properties as well as poor crystallization speed. While twin screw extrusion steps can be problematic for the production of PHA it also provides an excellent chamber to do solventless modification of the polymer during the processing step.

### **1.3.1 Reactive Extrusion**

Reactive extrusion (REX) is an excellent, green technique to improve the mechanical properties of polymers as well as increasing the interfacial compatibility of polymer blends by chemically grafting the two polymers together through radical recombination or other reactive chemistries. One of the largest benefits to reactive extrusion processing is the ability to handle the mass transfer problems frequently encountered in batch reactors when the viscosity dramatically increases during the polymerization or while it is quite high during functionalization. An extruder can continuously mix the molten material allowing for solventless modification of the polymer during a relatively short reaction cycle determined by the residence time in the extruder. One of the most common crosslinking methods is the use of organic peroxides as radical initiators for hydrogen abstraction on the polymer backbone. This technique has been extremely common for modification of commodity thermoplastics such as polypropylene and polyethylene but more recently attention has been given to applying



this technique for the improvement in melt and mechanical properties of bio-polyesters. Other reactive chemistries such as epoxide<sup>32, 33</sup>, anhydride<sup>32, 34, 35</sup>, oxazoline<sup>36, 37</sup>, aziridine<sup>34</sup>, phosphite<sup>33, 38-40</sup>, and carbodiimides<sup>33</sup> have been studied particularly with polylactic acid (PLA) and polyethylene terephthalate (PET) but have been less effectively applied to PHB. The difficulty for PHAs increases when medium chain length copolymers are used as the processing temperature is much lower making it difficult for reactive chemistries, such as ring opening of an epoxide, that typically need temperatures in excess of 175°C to reach full conversion during the times required for extrusion processing.

### **1.3.2 Organic Peroxides and Coagents**

Organic peroxides show much promise in reactive modification of PHAs as the processing conditions can be matched by the peroxide half-life to ensure that full conversion takes place. The thermal decomposition pathway of many peroxides is complicated and can lead to a variety of reactions within the bulk polymer leading to branching, chain scission, or crosslinking. Peroxide type has been investigated using PLA and it was shown that peroxide decomposition half-life as well as hydrogen abstraction efficiency are important when determining the cross-linking efficiency of each peroxide. When the half-life is very short, localized decomposition led to higher gel contents while for slower decomposing peroxides the hydrogen abstraction efficiency was directly related to the ability to crosslink PLA. It was also shown that the final molecular architecture for each class of peroxide was different depending on the half-life and abstraction efficiency.<sup>41-43</sup> REX with organic peroxides was furtherer expanded for PLA

by the use of multifunctional coagents. Kontopolou et al showed that the presence of the multifunctional coagent triallyl trimesate (TAM) can significantly increase the crosslinking efficiency of dicumyl peroxide.<sup>44-46</sup> With the addition of the multifunctional coagent it was noted that there was significant increase in strain hardening behavior during extensional viscosity measurements indicating that branching was occurring. Unusually, the crystallization kinetics of the PLA were also greatly increased in comparison to neat PLA and PLA branched with a multifunctional epoxide. While initially attributing this phenomenon to a polymerized, coagent rich phase acting as a nucleating agent or branch points acting as chemical nucleating agents, it is more likely that nano particles of crosslinked polymer are acting as heterogeneous nucleating agents.<sup>47</sup> They also showed that coagent enhanced reactive extrusion was able to compatibilize blends of PLA with PHB. Kolachi et al further expanded this chemistry into the world of PHA by showing the same strain hardening and increased crystallization effect seen with PLA through coagent assisted reactive extrusion of PHB.<sup>48</sup> A significant increase in complex viscosity was seen when compared to REX with DCP alone indicating enhanced crosslinking. The strain hardening behavior also indicates significant levels of branching, but the most unique observation was the increased temperature of recrystallization as well as the decrease in spherulite size. This shows much promise for the production of PHA with high mechanical properties as well as rapid crystallization upon cooling. Reactive extrusion using organic peroxides has also been shown to greatly compatibilize polyester blends through increased interfacial adhesion which can be used for melt blending with PHA for enhanced final mechanical properties.

## 1.4 Melt Blending

Melt blending of two or more polymer components is a low-cost method to modify final polymer properties without the need for new synthetic strategies to create a polymer with the desired properties for a given application. Three criteria dictate the final properties of blended materials: miscibility, compatibility, and morphology. Miscible polymer systems are quite rare and polymers with very similar structures such as polypropylene and polyethylene, differing by a one carbon branch point, are found to be completely immiscible due to the entropic barrier of blending. This leads to a blend with very little intermolecular interactions between the two phases resulting in poor mechanical properties of the blend.<sup>49</sup> Most polymer blends will be heterogeneous but

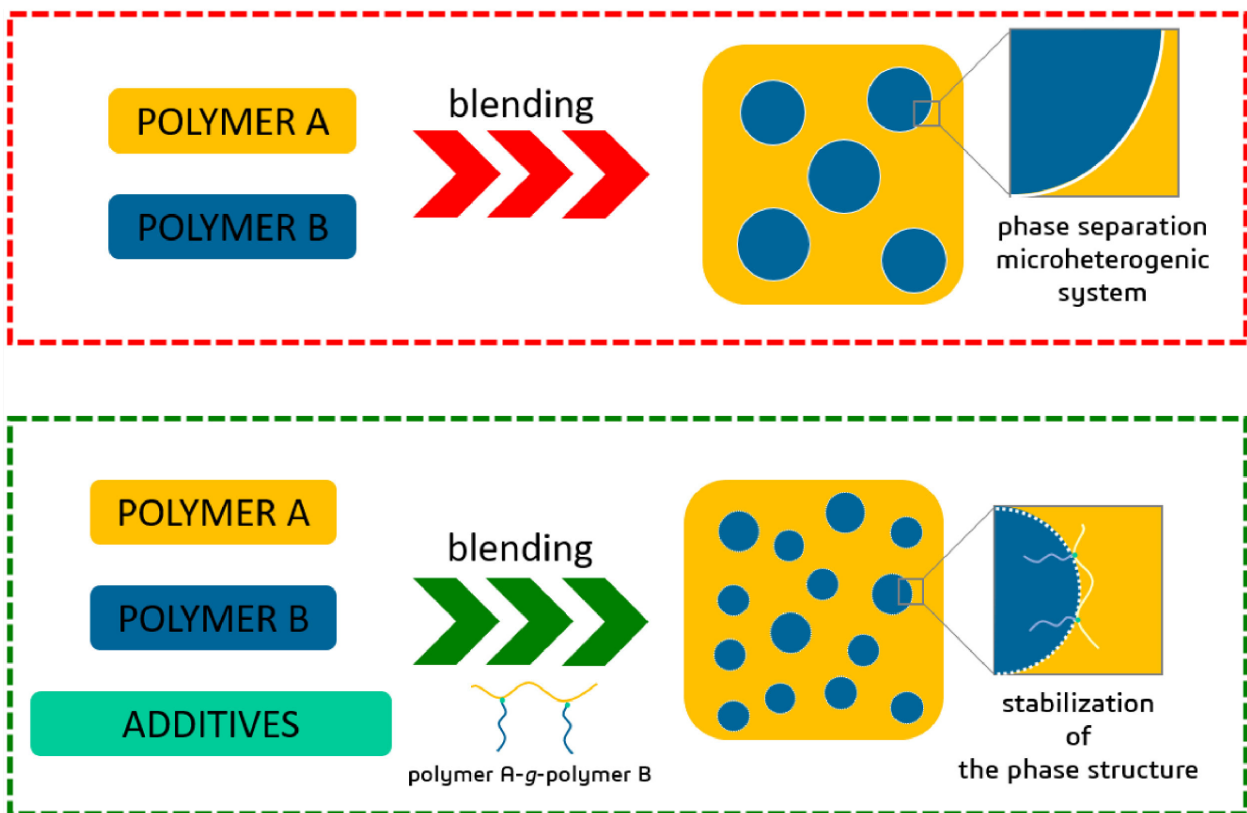


**Figure 1.5:** Representative image showing the interfacial compatibilization mechanism through the use of compatibilizing agents [51]

some may have increased compatibility. A heterogeneous blend that has favorable interactions at the interface of the two components is a compatible blend, and frequently increasing compatibility between two discrete phases is a common method for improving the properties of the final blend.<sup>50</sup> Increasing compatibility has historically been done through the addition of block or graft copolymers, shown in figure 1.5, that will have favorable interactions with both of the polymer components in the blend.<sup>51</sup> Reactive chemistries can also be used and are especially effective in blends with more than two components where a reactive handle can cause interaction between multiple components without the need to synthesize a complicated copolymer compatibilizer for each component. Blend morphology refers to the domain size and shape of the immiscible blended component and is dictated by polymer blend ratios, shear rate and polymer compatibility.<sup>52</sup> PHBHHx, which is of much industrial interest due to its melt properties and scalable production, does not have the required mechanical properties for all applications where it is desired to be used. Melt blending with other biopolymers will be of much interest for the improvement in its final mechanical properties. It is expected that PHA-polyester blends will be immiscible with differing amounts of compatibility depending on the type of biopolymer used for the blending process. There is a broad frontier in exploring blends of PHA with other polymers for improved final mechanical properties as well as reactive extrusion strategies that give enhanced properties for a variety of applications.

## **1.5 Conclusion and Dissertation Outline**

In this dissertation, chapter two deals with the improvement in mechanical properties as well as formulation of PHBHHx by blending with commercially available polyesters such as PBS, PBSA, PBAT and PCL as well as synthesized polyesters such as polybutylene adipate (PBA), polybutylene glutarate (PBG), and polybutylene succinate-co-glutarate (PBSG) with varying molecular weights. Starch was also incorporated into the polymer at high loadings of 10% and Young's modulus was retained in the starch blends by the addition of a high lamellar talc. Chapter two also addresses the impact that reactive extrusion can have on polymer blends using PHBHHx as well as its impact on aging of the blend. The addition of a 10% Hx content PHA was also examined for its ability to prevent embrittle over a period of 15 days. Chapter three examines various heterogenous nucleating agents as well as analyzing the effect on particle size of each added nucleating agent. A previously undescribed melt miscible nucleating agent, pentaerythritol was also compared to a known class of melt miscible nucleating agents (oxalamide). Finally, chapter four presents the final conclusion and future outlook for the work that is presented in this dissertation.

## 1.6 References

1. Geyer, R.; Jambeck, J. R.; Law, K. L., Production, use, and fate of all plastics ever made. *Science Advances* **2017**, 3 (7), e1700782.
2. Chen, Y.; Awasthi, A. K.; Wei, F.; Tan, Q.; Li, J., Single-use plastics: Production, usage, disposal, and adverse impacts. *Science of The Total Environment* **2021**, 752, 141772.
3. Jambeck, J. R.; Geyer, R.; Wilcox, C.; Siegler, T. R.; Perryman, M.; Andrady, A.; Narayan, R.; Law, K. L., Plastic waste inputs from land into the ocean. *Science* **2015**, 347 (6223), 768-771.
4. Law, K. L.; Thompson, R. C., Microplastics in the seas. *Science* **2014**, 345 (6193), 144.
5. Shim, W. J.; Thomposon, R. C., Microplastics in the Ocean. *Archives of Environmental Contamination and Toxicology* **2015**, 69 (3), 265-268.
6. Goldstein, M. C.; Goodwin, D. S., Gooseneck barnacles (*Lepas* spp.) ingest microplastic debris in the North Pacific Subtropical Gyre. *PeerJ* **2013**, 1, e184.
7. White, E. M.; Clark, S.; Manire, C. A.; Crawford, B.; Wang, S.; Locklin, J.; Ritchie, B. W., Ingested Micronizing Plastic Particle Compositions and Size Distributions within Stranded Post-Hatchling Sea Turtles. *Environmental Science & Technology* **2018**, 52 (18), 10307-10316.
8. Meaza, I.; Toyoda, J. H.; Wise Sr, J. P., Microplastics in Sea Turtles, Marine Mammals and Humans: A One Environmental Health Perspective. *Frontiers in Environmental Science* **2021**, 8, 298.

9. Eagan, J. M.; Xu, J.; Di Girolamo, R.; Thurber, C. M.; Macosko, C. W.; LaPointe, A. M.; Bates, F. S.; Coates, G. W., Combining polyethylene and polypropylene: Enhanced performance with PE/iPP multiblock polymers. *Science* **2017**, *355* (6327), 814-816.
10. Klimovica, K.; Pan, S.; Lin, T.-W.; Peng, X.; Ellison, C. J.; LaPointe, A. M.; Bates, F. S.; Coates, G. W., Compatibilization of iPP/HDPE Blends with PE-g-iPP Graft Copolymers. *ACS Macro Letters* **2020**, *9* (8), 1161-1166.
11. Xu, J.; Eagan, J. M.; Kim, S.-S.; Pan, S.; Lee, B.; Klimovica, K.; Jin, K.; Lin, T.-W.; Howard, M. J.; Ellison, C. J.; LaPointe, A. M.; Coates, G. W.; Bates, F. S., Compatibilization of Isotactic Polypropylene (iPP) and High-Density Polyethylene (HDPE) with iPP-PE Multiblock Copolymers. *Macromolecules* **2018**, *51* (21), 8585-8596.
12. Goldman, A. S.; Roy, A. H.; Huang, Z.; Ahuja, R.; Schinski, W.; Brookhart, M., Catalytic alkane metathesis by tandem alkane dehydrogenation-olefin metathesis. *Science* **2006**, *312* (5771), 257-61.
13. Jia, X.; Qin, C.; Friedberger, T.; Guan, Z.; Huang, Z., Efficient and selective degradation of polyethylenes into liquid fuels and waxes under mild conditions. *Science Advances* **2016**, *2* (6), e1501591.
14. Choi, S. Y.; Cho, I. J.; Lee, Y.; Kim, Y.-J.; Kim, K.-J.; Lee, S. Y., Microbial Polyhydroxyalkanoates and Nonnatural Polyesters. *Advanced Materials* **2020**, *32* (35), 1907138.
15. Możejko-Ciesielska, J.; Kiewisz, R., Bacterial polyhydroxyalkanoates: Still fabulous? *Microbiological Research* **2016**, *192*, 271-282.

16. Owen, A. J.; Heinzl, J.; Škrbić, Ž.; Divjaković, V., Crystallization and melting behaviour of PHB and PHB/HV copolymer. *Polymer* **1992**, 33 (7), 1563-1567.
17. Budde Charles, F.; Riedel Sebastian, L.; Willis Laura, B.; Rha, C.; Sinskey Anthony, J., Production of Poly(3-Hydroxybutyrate-co-3-Hydroxyhexanoate) from Plant Oil by Engineered *Ralstonia eutropha* Strains. *Applied and Environmental Microbiology* **2011**, 77 (9), 2847-2854.
18. Brandl, H.; Gross, R. A.; Lenz, R. W.; Fuller, R. C., *Pseudomonas oleovorans* as a Source of Poly(beta-Hydroxyalkanoates) for Potential Applications as Biodegradable Polyesters. *Applied and environmental microbiology* **1988**, 54 (8), 1977-1982.
19. Chen, G.; Zhang, G.; Park, S.; Lee, S., Industrial scale production of poly(3-hydroxybutyrate-co-3-hydroxyhexanoate). *Applied Microbiology and Biotechnology* **2001**, 57 (1), 50-55.
20. Doi, Y.; Kitamura, S.; Abe, H., Microbial Synthesis and Characterization of Poly(3-hydroxybutyrate-co-3-hydroxyhexanoate). *Macromolecules* **1995**, 28 (14), 4822-4828.
21. Marchessault, R. H.; Yu, G.-e., Crystallization and Material Properties of Polyhydroxyalkanoates PHAs). In *Biopolymers Online*, 2005.
22. Noda, I.; Green, P. R.; Satkowski, M. M.; Schechtman, L. A., Preparation and Properties of a Novel Class of Polyhydroxyalkanoate Copolymers. *Biomacromolecules* **2005**, 6 (2), 580-586.
23. Feng, L.; Watanabe, T.; Wang, Y.; Kichise, T.; Fukuchi, T.; Chen, G.-Q.; Doi, Y.; Inoue, Y., Studies on Comonomer Compositional Distribution of Bacterial Poly(3-



hydroxybutyrate-co-3-hydroxyhexanoate)s and Thermal Characteristics of Their  
Factions. *Biomacromolecules* **2002**, 3 (5), 1071-1077.

24. Feng, L.; Yoshie, N.; Asakawa, N.; Inoue, Y., Comonomer-Unit Compositions,  
Physical Properties and Biodegradability of Bacterial Copolyhydroxyalkanoates.  
*Macromolecular Bioscience* **2004**, 4 (3), 186-198.

25. Satkowski, M. M.; Melik, D. H.; Autran, J.-P.; Green, P. R.; Noda, I.;  
Schechtman, L. A., Physical and Processing Properties of Polyhydroxyalkanoate (PHA)  
Copolymers. In *Biopolymers Online*, 2005.

26. Alata, H.; Aoyama, T.; Inoue, Y., Effect of Aging on the Mechanical Properties of  
Poly(3-hydroxybutyrate-co-3-hydroxyhexanoate). *Macromolecules* **2007**, 40 (13), 4546-  
4551.

27. Ariffin, H.; Nishida, H.; Shirai, Y.; Hassan, M. A., Determination of multiple  
thermal degradation mechanisms of poly(3-hydroxybutyrate). *Polymer Degradation and  
Stability* **2008**, 93 (8), 1433-1439.

28. Xiang, H.; Wen, X.; Miu, X.; Li, Y.; Zhou, Z.; Zhu, M., Thermal depolymerization  
mechanisms of poly(3-hydroxybutyrate-co-3-hydroxyvalerate). *Progress in Natural  
Science: Materials International* **2016**, 26 (1), 58-64.

29. Hyvärinen, M., Jabeen, Rowshni, Kärki, Timo, The Modelling of Extrusion  
Processes for Polymers—A Review. *Polymers* **2020**, 12 (6).

30. Whelan, T. A.; Whelan, T.; Dunning, D.; Dynisco, I., *The Dynisco Extrusion  
Processors Handbook*. Dynisco Incorporated: 1988.

31. Tzoganakis, C., Reactive extrusion of polymers: A review. *Advances in Polymer Technology* **1989**, 9 (4), 321-330.
32. Yahyaee, N.; Javadi, A.; Garmabi, H.; Khaki, A., Effect of Two-Step Chain Extension using Joncryl and PMDA on the Rheological Properties of Poly (lactic acid). *Macromolecular Materials and Engineering* **2020**, 305 (2), 1900423.
33. Najafi, N.; Heuzey, M. C.; Carreau, P. J.; Wood-Adams, P. M., Control of thermal degradation of polylactide (PLA)-clay nanocomposites using chain extenders. *Polymer Degradation and Stability* **2012**, 97 (4), 554-565.
34. Gu, L.; Xu, Y.; Fahnhorst, G. W.; Macosko, C. W., Star vs long chain branching of poly(lactic acid) with multifunctional aziridine. *Journal of Rheology* **2017**, 61 (4), 785-796.
35. Awaja, F.; Daver, F.; Kosior, E.; Cser, F., The effect of chain extension on the thermal behaviour and crystallinity of reactive extruded recycled PET. *Journal of Thermal Analysis and Calorimetry* **2004**, 78 (3), 865-884.
36. Berg, D.; Schaefer, K.; Moeller, M., Impact of the chain extension of poly(ethylene terephthalate) with 1,3-phenylene-bis-oxazoline and N,N'-carbonylbiscaprolactam by reactive extrusion on its properties. *Polymer Engineering & Science* **2019**, 59 (2), 284-294.
37. Karayannidis, G. P.; Psalida, E. A., Chain extension of recycled poly(ethylene terephthalate) with 2,2'-(1,4-phenylene)bis(2-oxazoline). *Journal of Applied Polymer Science* **2000**, 77 (10), 2206-2211.

38. Meng, X.; Shi, G.; Wu, C.; Chen, W.; Xin, Z.; Shi, Y.; Sheng, Y., Chain extension and oxidation stabilization of Triphenyl Phosphite (TPP) in PLA. *Polymer Degradation and Stability* **2016**, *124*, 112-118.
39. Cavalcanti, F. N.; Teófilo, E. T.; Rabello, M. S.; Silva, S. M. L., Chain extension and degradation during reactive processing of PET in the presence of triphenyl phosphite. *Polymer Engineering & Science* **2007**, *47* (12), 2155-2163.
40. Wang, L.; Ma, W.; Gross, R. A.; McCarthy, S. P., Reactive compatibilization of biodegradable blends of poly(lactic acid) and poly( $\epsilon$ -caprolactone). *Polymer Degradation and Stability* **1998**, *59* (1), 161-168.
41. Takamura, M.; Nakamura, T.; Takahashi, T.; Koyama, K., Effect of type of peroxide on cross-linking of poly(l-lactide). *Polymer Degradation and Stability* **2008**, *93* (10), 1909-1916.
42. Takamura, M.; Sugimoto, M.; Kawaguchi, S.; Takahashi, T.; Koyama, K., Influence of extrusion temperature on molecular architecture and crystallization behavior of peroxide-induced slightly crosslinked poly(L-lactide) by reactive extrusion. *Journal of Applied Polymer Science* **2012**, *123* (3), 1468-1478.
43. Takamura, M.; Nakamura, T.; Kawaguchi, S.; Takahashi, T.; Koyama, K., Molecular characterization and crystallization behavior of peroxide-induced slightly crosslinked poly(L-lactide) during extrusion. *Polymer Journal* **2010**, *42* (7), 600-608.
44. Tiwary, P.; Kontopoulou, M., Tuning the Rheological, Thermal, and Solid-State Properties of Branched PLA by Free-Radical-Mediated Reactive Extrusion. *ACS Sustainable Chemistry & Engineering* **2018**, *6* (2), 2197-2206.

45. Nerkar, M.; Ramsay, J. A.; Ramsay, B. A.; Kontopoulou, M., Dramatic Improvements in Strain Hardening and Crystallization Kinetics of PLA by Simple Reactive Modification in the Melt State. *Macromolecular Materials and Engineering* **2014**, 299 (12), 1419-1424.
46. Nerkar, M.; Ramsay, J. A.; Ramsay, B. A.; Vasileiou, A. A.; Kontopoulou, M., Improvements in the melt and solid-state properties of poly(lactic acid), poly-3-hydroxyoctanoate and their blends through reactive modification. *Polymer* **2015**, 64, 51-61.
47. Zhang, Y.; Tiwary, P.; Gui, H.; Kontopoulou, M.; Parent, J. S., Crystallization of Coagent-Modified Polypropylene: Effect of Polymer Architecture and Cross-Linked Nanoparticles. *Industrial & Engineering Chemistry Research* **2014**, 53 (41), 15923-15931.
48. Kolahchi, A. R.; Kontopoulou, M., Chain extended poly(3-hydroxybutyrate) with improved rheological properties and thermal stability, through reactive modification in the melt state. *Polymer Degradation and Stability* **2015**, 121, 222-229.
49. Zainal, N. F. A.; Chan, C. H., Chapter 14 - Crystallization and melting behavior of compatibilized polymer blends. In *Compatibilization of Polymer Blends*, A.R, A.; Thomas, S., Eds. Elsevier: 2020; pp 391-433.
50. Muthuraj, R.; Misra, M.; Mohanty, A. K., Biodegradable compatibilized polymer blends for packaging applications: A literature review. *Journal of Applied Polymer Science* **2018**, 135 (24), 45726.

51. Przybysz-Romatowska, M.; Haponiuk, J.; Formela, K., Reactive extrusion of biodegradable aliphatic polyesters in the presence of free-radical-initiators: A review. *Polymer Degradation and Stability* **2020**, *182*, 109383.
52. Utracki, L. A., Introduction to Polymer Blends. In *Polymer Blends Handbook*, Utracki, L. A., Ed. Springer Netherlands: Dordrecht, 2003; pp 1-122.

## CHAPTER 2

### MELT BLENDING AND REACTIVE OF EXTRUSION OF POLYHYDROXYBUTYRATE-CO- HYDROXYHEXANOATE<sup>1</sup>

---

<sup>1</sup> Crane, Grant Stinchcomb, Ethan Winfield, Demichael. To be submitted to Macromolecular Materials and Engineering

## ABSTRACT

Polyhydroxyalkanoates present a viable, biologically degradable replacement for current commodity thermoplastics such as polypropylene. They are typically a random copolymer of hydroxy butyric acid and other comonomers such as hydroxy hexanoic, and octanoic acid with their thermal and mechanical properties being dependent on the type and amount of comonomer incorporated into the polymer. For polyhydroxybutyrate-co-hydroxyhexanoate (PHBHHx), increasing the mole percent of hexanoate reduces the melting temperature, and Young's modulus while increasing the strain at break, and while this adds some ductility it comes at the cost of reducing the crystallization rate of the copolymer. Melt blending of PHBHHx with other degradable/compostable polyesters as well as with high hexanoate content copolymers can greatly enhance the elongation at break of the blend while maintaining adequate crystallization rate as well as stiffness of the extruded article. Reactive extrusion, using organic peroxides, can also be used to further increase the mechanical properties of the raw polymer or of the polymer blend.

## Introduction

Polyhydroxyalkanoates (PHA's) can be divided into two groups: short chain length (scl) where R is C1 to C2 and medium chain length (mcl) where R is C3 and higher. Polyhydroxybutyrate (PHB) a type of PHA shows much promise for being a biologically degradable alternative to common plastics such as polypropylene and polyethylene. Though attractive in many ways PHB is too brittle to be used for many applications where high toughness is needed such as single use items and plastic packaging. PHB, due to its high crystallinity, has a melting point very near its onset of thermal degradation (185°C) which makes processing challenging as well. Introduction of comonomers can change the mechanical and thermal properties as well as crystallinity of the random copolymer. Introduction of valerate into the copolymer adds some toughness although the short sidechain is more readily incorporated into the crystal lattice of the PHB unit cell thus causing little reduction in melt temperature and crystallinity.<sup>1</sup> When hexanoate is incorporated into the random copolymer the longer side chain length of three carbons is less readily incorporated into the crystalline lattice thus acting as chain defects that reduce the overall crystallinity of the copolymer with increasing mole percent of the hexanoate monomer.<sup>2</sup> This leads to a reduction in melt temperature and an increase in the elongation at break of the copolymer which allows for a wide variety of thermal and mechanical properties to be achieved by varying the amount of comonomer. PHAs, while having a wide variety of mechanical properties with incorporation of even a small amount of comonomer, still suffer from severe embrittlement caused by secondary crystallization over time leading to a rigid



amorphous region<sup>3, 4</sup> Increasing the mole percent above a 10% threshold, in the case of hydroxy hexanoate, causes a large reduction in the embrittlement due to the thicker interlamellar amorphous regions preventing secondary crystallization from significantly affecting the mechanical properties.<sup>5</sup> While a high Hx percent is advantageous for preventing embrittlement over time, a drastic reduction in crystallization and melting takes place which can greatly disrupt the applicability of a high Hx copolymer for many extrusion applications where a rapid crystallization rate is needed. Typically, mechanical and thermal properties of copolymers or pure homopolymers have been shown, but there has been little work done on how blending of low weight loadings of a higher Hx PHA affects the mechanical properties, over time, of a lower Hx PHA that would typically embrittle. Further work is also needed in how ternary blends of high Hx and low Hx PHA with polyesters such as PBSA, PBS, PBAT, and PCL affect the embrittlement phenomenon common to PHA.

While PHBHHx has better elongation than PHB homopolymer, for many applications the toughness of the article requires that the mechanical properties be further improved. Melt blending with other polymers provides a viable way of improving the toughness of PHBHHx. While blending of scl-PHAs has been studied with many different polyesters such as PBAT, PBS, and PCL.<sup>6-9</sup> There has been little to no work done characterizing the thermal and mechanical properties of PHBHHx polyester blends. Furthermore, investigating how these blends affect the embrittlement that PHA is susceptible to over time would be of much interest.

Reactive extrusion (REX) is an attractive technique for the modification of polymers in the melt without the use of solvent or post processing purification and has been used extensively to modify the properties of polyolefins and polyesters. The reaction is typically carried out using an intermeshing twin screw extruder that allows, based on the screw design, both dispersive and distributive mixing. The chemistries available for reactive extrusion are typically tuned to the extrusion environment based on the relatively short residence time for the reactive modifications to take place.<sup>10</sup> REX can be used for a variety of processes for the modification of polymers such as extrusion polymerization,<sup>11, 12</sup> grafting<sup>13-16</sup>, and branching.<sup>17, 18</sup> The use of organic peroxides for the controlled production of radicals during the extrusion process to induce long chain branching and slight crosslinking is a common method for the melt modification of polymers within a twin screw extruder. Investigation into peroxide type and reactive co-agent use for the improvement in mechanical properties of PHBHHx would be of great interest for the production of high PHA content articles that have mechanical properties amenable to high stress applications such as bottles or fibers. While blending with other polyesters presents an attractive way for the improvement in mechanical properties of PHAs, reactive extrusion using organic peroxides is also a viable method for the improvement in mechanical, and melt properties of PHA only, or high PHA content blends. Dicumyl peroxide has been shown to effectively compatibilize blends of PHBV and PBS.<sup>7</sup> DCP was also used to compatibilize blends with PHB and PBAT although the impact on mechanical properties was neglected in this study.<sup>8</sup> More recently PHBV was blended with PCL in the presence of a multifunctional coagent and DCP with limited

success on improvement in mechanical properties.<sup>6</sup> A broader study incorporating multiple polymer additives as well as high Hx comonomers with PHA would be of much value for the production of biologically degradable plastic items that have mechanical properties equivalent or better than current commodity polyolefin competitors.

## **Materials and Methods**

### *Materials*

Polyhydroxybutyrate-co-hydroxyhexanoate (6% Hx) with a molecular weight of 930,000 daltons and polyhydroxybutyrate-co-hydroxyhexanoate (11% Hx) were produced through fermentation and were both supplied by the New Materials Institute at the University of Georgia. Polycaprolactone (CAPA 6800) was purchased from Perstorp as white pellets. Polybutylene succinate (FD91) and polybutylene succinate-co-adipate (FD92) were purchased from ptt MCC Biochem as white pellets. Polybutylene adipate-co-terephthalate (Ecoflex C1200 F) in the form of white pellets was a gift from RWDC industries. Adipic acid was purchased from Oakwood Chemical. Starch in the form of translucent, pre-plasticized pellets (BiologiQ GP100) was a gift from RWDC industries. Talc (3CA) was purchased from Imerys and had a d<sub>50</sub> of 1 µm. Glutaric acid and 1,4-butanediol were both purchased from Sigma Aldrich. Luperox P (tert-Butyl peroxybenzoate), Luperox LP (lauroyl peroxide), Luperox 101 (2,5-Bis(*tert*-butylperoxy)-2,5-dimethylhexane), Dicumyl peroxide, Luperox 231 (1,1-Bis(*tert*-butylperoxy)-3,3,5-trimethylcyclohexane), and Benzoyl peroxide were all purchased from Sigma Aldrich and

used without purification. Triallyl Cyanurate, Pentaerythritol tetraacrylate, and 1,6-Hexanediol diacrylate were all purchased from Sigma Aldrich and used as received.

#### *Peroxide Masterbatch Preparation*

10g of PHA powder was suspended in approximately 100ml of acetone in a 250ml round bottom flask. 0.4g of peroxide was dissolved in 20ml of acetone and added to the round bottom flask. The scintillation vial was rinsed 2x with 20ml of acetone to ensure all peroxide was transferred to the PHA/acetone suspension. The mixture was then briefly sonicated to break up any large PHA particles. The acetone was then removed under reduced pressure with the temperature not exceeding 35°C and placed on high vacuum overnight to remove any residual solvent. The compounded mixture was then ground into a fine powder in a mortar and pestle to give a masterbatch of PHA containing 4wt% peroxide.

#### *Extrusion procedure*

6.5g total formulation was added to a Haake minilab II corotating twin screw extruder using a manual feeder. Melt blending was carried out at 150°C, 100 rpm screw speed, and a cycle time of 6 minutes to ensure adequate blending or peroxide decomposition. Type V tensile bars were injection molded from a 150°C cylinder using 660 bar of pressure for 5 seconds into a 45°C or 70°C mold. Tensile bars were aged for at least 24 hours prior to testing unless otherwise stated.

### *Mechanical and Thermal Properties*

Tensile testing was done using a Shimadzu AGS-X tensile tester. Type V dogbones were tested at a strain rate of 5 mm/min. All samples were aged for 24 hours prior to testing unless otherwise stated. Thermal properties were measured using a TA Discovery 250 differential scanning calorimeter. Samples were taken from the bottom portion of the tensile bar after testing to best represent the crystallinity of the injection molded sample. Samples were heated at 10°C/min to 180°C and cooled at 10°C/min to -20°C. For samples where nucleation was being examined the first heating run was done to 200°C to melt any inherent PHB found in the sample. Melting enthalpy, melting peak temperature, and percent crystallinity were calculated using TA software on the instrument. Percent crystallinity was calculated using equation 1.

$$X_c (\%) = \frac{\Delta H}{\Delta H_c * \phi} * 100 \quad (1)$$

Where  $\Delta H$  is the specific enthalpy of fusion of the sample taken from the peak area on the program software (J/g), and  $\Delta H_c$  is the enthalpy of fusion for a 100% crystalline material (assumed to be 146 J/g for PHB)<sup>19</sup> and  $\phi$  is the weight fraction of the polymer. Crystallization was observed using a Nikon polarized optical microscope. Small samples were cut from the extruded article and were heated to a peak temperature of 180°C or 200°C and cooled at a rate of 20°C/min to observe blend morphology, crystallization and spherulite morphology.

### *GPC*

Molecular weight was taken using a Shimadzu prominence UFLC GPC. The samples were dissolved in chloroform at 5mg/ml and passed through a 0.22 $\mu$ m PTFE syringe filter and the molecular weights were calculated in comparison to a polystyrene standard.

### *SEM*

Blend morphology was examined using a FEI Teneo field emission SEM at an accelerating voltage of 2-5kV with a spot size of 8. Samples were cryo-fractured by immersing in liquid nitrogen for 10 minutes prior to breaking. The fractured surfaces were sputter coated (13nm thickness) using gold-palladium with a LEICA EM ACE200 coater. All images were taken with a sample height of 10-13mm.

### *Synthesis of Polybutylene adipate*

Adipic acid (mmol), and butanediol (mmol) were added to a 3-neck round bottom flask equipped with an overhead stirrer. The reaction vessel was heated to 200°C under a flow of nitrogen for 6 hours. The reaction was continued for another 12 hours under vacuum (175-400 millitorr). 1 mol% of zirconium butoxide was then added in 2ml of dry toluene and the reaction was continued for another 3 hours. The polymer was poured onto a tray to cool and collected as an off-white solid and was used without further purification.

### *Synthesis of Polybutylene succinate-co-glutarate*

Succinic acid, glutaric acid, and butanediol were added to a 3-neck round bottom flask equipped with an overhead stirrer. The reaction vessel was heated to 190°C for 3 hours under a flow of nitrogen. Vacuum was pulled at a rate of 100 millitorr/min to

reduce oligomer sublimation. The reaction was continued between 200-500 millitorr for 16 hours. Titanium butoxide was added in dry toluene. Vacuum was again pulled at 100 millitorr/min to reduce foaming and the reaction was continued for 8h. The off-white polymer was poured onto a tray and allowed to cool.

## Results and Discussion

Initially PHBHHx (6% Hx) was blended with four commercially available polyesters: Polycaprolactone (PCL), Polybutylene Succinate (PBS), Polybutylene Succinate-co-adipate (PBSA), and Polybutylene adipate-co-terephthalate (PBAT). The blending was done using a haake minilab conical corotating twin screw extruder which allows for cycling of the polymer melt for a desired amount of time as well as

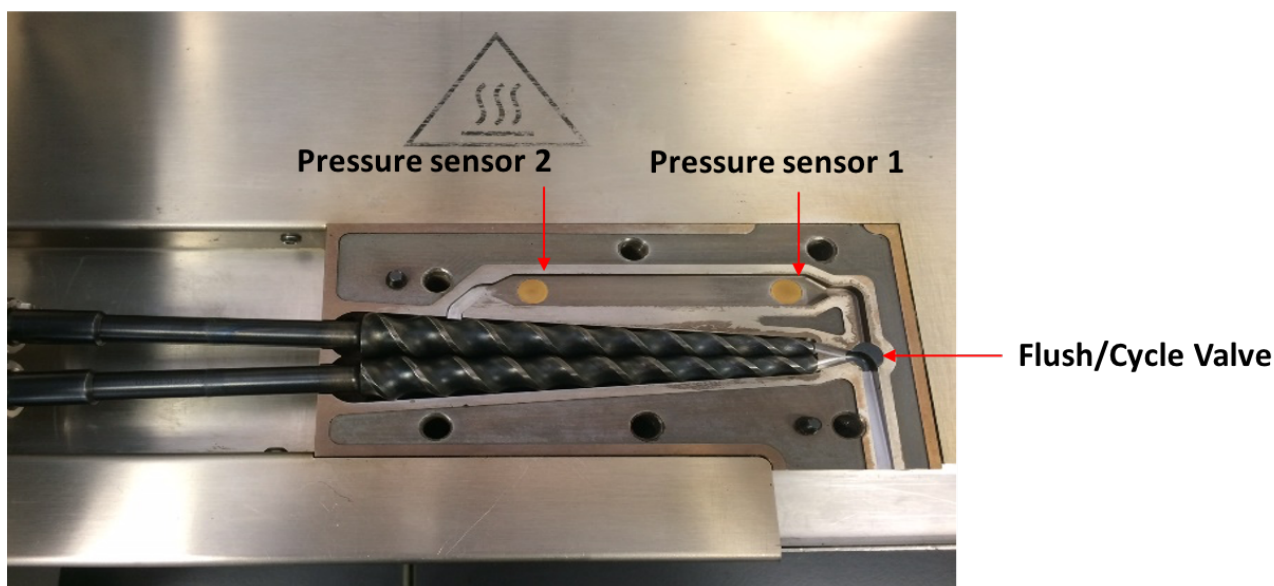


**Figure 2.1:** Inside of the Haake minilab conical twin screw extruder showing the backchannel and pressure transducers monitoring the torque response from the screws as well as the pressure response in two different zones of the back channel. This allows for monitoring of the blending process as well as the pressure response when reactions are carried out within the extruder. As can be expected the addition of immiscible polymers into the PHA matrix causes a

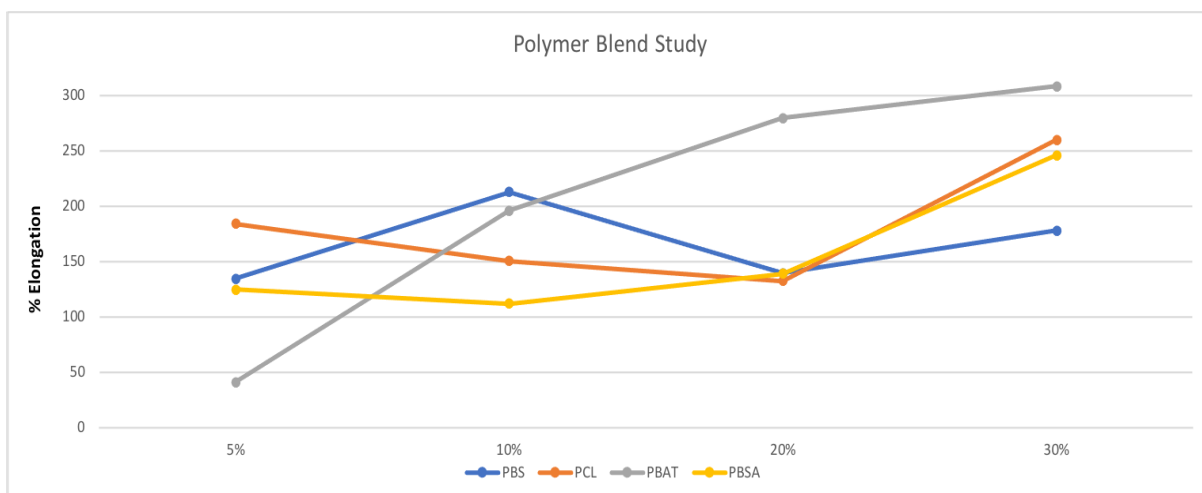


**Figure 2.2:** Percent elongation of PHBHHx (6% Hx) blends with commercially available polyesters

reduction in the Young's modulus shown in figure 2.3 although only slightly so in the case of PBS. Noticeably PBAT behaves very differently from PBS, PCL and PBSA. While these polymers have only a slight impact on the stiffness of the PHA they greatly enhance the elongation at break with even small loadings. PBAT shows little improvement in elongation at lower loadings (41%) but upon increasing the weight loading a significant improvement in elongation is seen (308%). Increasing the weight loading also significantly reduced the modulus of the PHA. DSC analysis was used to probe the thermal properties of the blends, and PBAT showed a distinct difference by

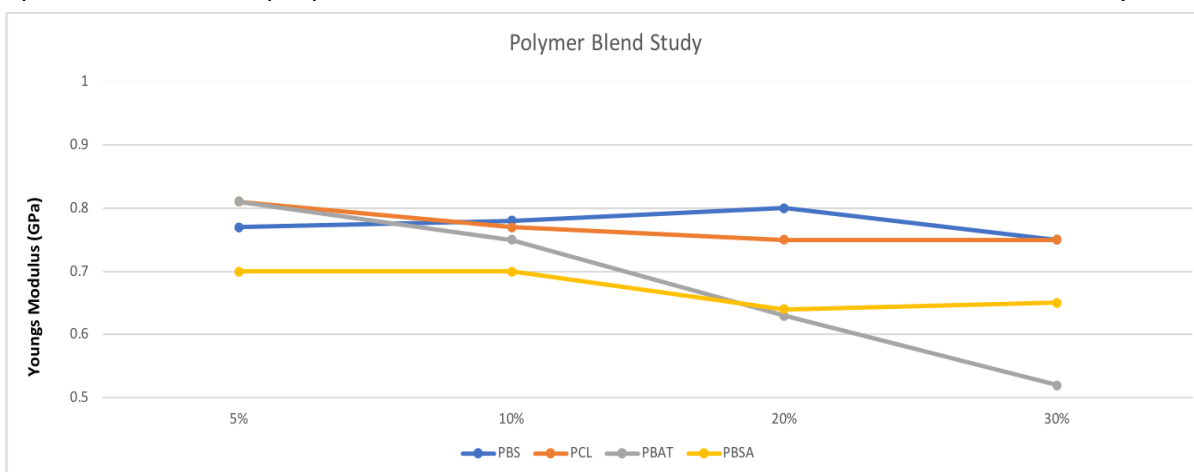


**Figure 2.3:** Young's Modulus of PHBHHx (6% Hx) blends with commercially available polyesters



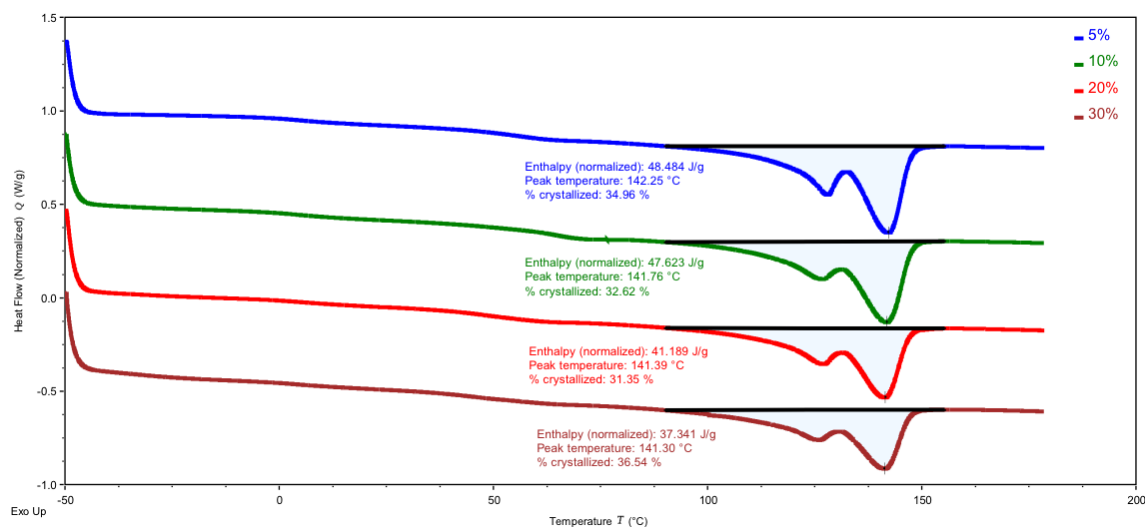


**Figure 2.4:** Melting endotherms of 5, 10, 20, and 30% PBAT blended with PHBHHx (6% Hx)

lacking any visible melting or crystallization transition. The other polymers have clear transitions especially at higher loadings indicating immiscible semicrystalline blends. As can be seen in figure 2.4 there is no melting transition seen for PBAT in the first heating cycle seemingly indicating that there is no crystalline material in the tensile bar even in the 30% blend. However, the relative percent crystallinity of the PHA fraction increases significantly with the 5% and 30% blends. For the blends using 10% and 20% PBAT the crystallinity remains around 31-32% which is what is expected for this PHA with 6% hexanoate comonomer. The melting transition for PBAT is expected in the range of 110-120°C which could be hidden in the melting endotherm of the PHA. Likely this is why the crystallinity increases to 37% for the 30% blend. There is an overestimation of the PHA crystallinity based on melting of the PBAT portion that is within the peak area of what is thought to be the PHA melting transition. Although, the 5% PBAT blend increases the crystallinity to 35% which is several percent higher than the 10 and 20% blends indicating that PBAT may increase the extent to which the PHA can crystallize at low

loadings. The additional percent seen in the 30% blend could come from a small amount of semi-crystalline PBAT that is hidden within the melting transition of the PHA. Noteworthy is that the shape of the melting transition of the PHA remains the same at all loadings of PBAT even though the relative crystallinity does increase with increasing weight percent of PBAT indicating that it remains largely amorphous within the blend. The amorphous nature of PBAT above its glass transition temperature causes it to act as a rubbery additive for the improvement of PHA's mechanical properties. It is hypothesized that the amorphous PBAT is forced out of the crystalline lamellae of the PHA causing rich domains of immiscible rubbery polymer. The cooling curve on the DSC also shows that even though the peak crystallization temperature of the PHBHHx is reduced to 89°C there is no further reduction with increased loading of PBAT. As PBAT is forced out the growing crystallization front it is accumulated in amorphous zones either in the inter-spherulitic, interfibrillar region, or between the lamellar stacks.<sup>20</sup> This hinders the complete crystallization of the PHBHHx which is similar to when high Hx comonomers are incorporated into PHA and are excluded from the crystalline lamellae forming thicker amorphous fractions that are less prone to the effects of secondary crystallization and aging.<sup>5</sup> This phenomenon is also seen with PHBHHx : PBAT blends that do not grow brittle over time. Although, for PBAT the amorphous fractions are localized into large immiscible zones and for high Hx blends there is no visible

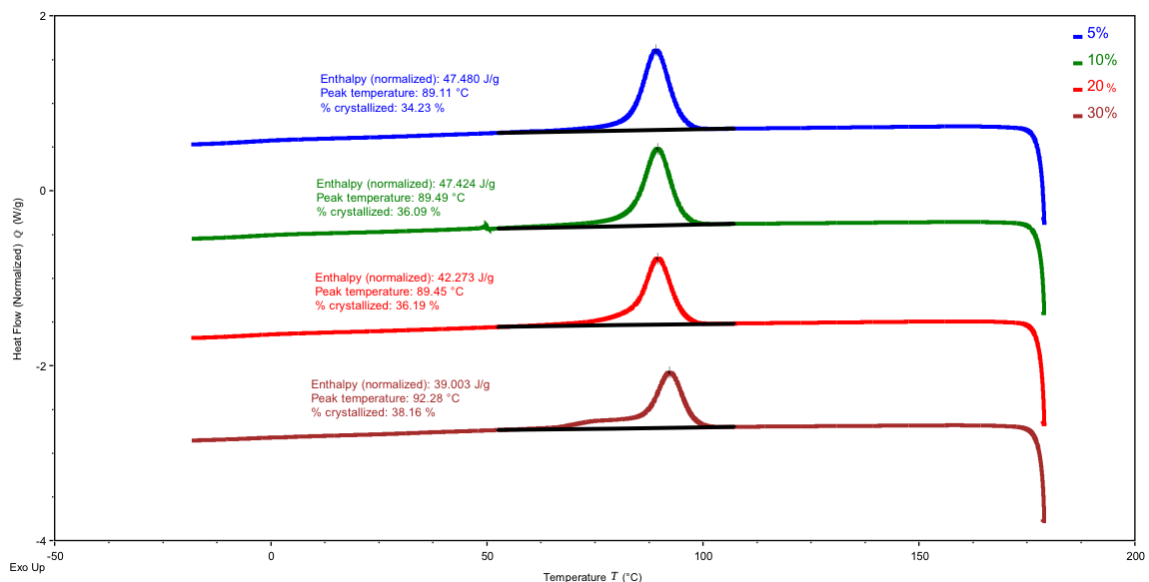


**Figure 2.5:** Crystallization exotherms of 5, 10, 20, and 30% PBAT blended with PHBHHx (6% Hx)

immiscibility between the fractions. For the 30% blend of PBAT a separation in the crystallization exotherm is evident. The peak crystallization of the PHA portion shifts back to its normal temperature of 92°C with a broad tail. Likely, at this loading, the amorphous enriched zones of PBAT have become large enough that some crystallization has taken place which is also supported by the increasing in relative crystallinity seen when calculated from the melting transition. This has previously been observed in blends of PHB with PBAT although loadings above 40% began to show a melting endotherm for the PBAT portion.<sup>8</sup>

SEM was used to confirm the existence of immiscible droplets of blended polymer within the PHBHHx matrix. While the morphology, shown in figure 2.6, is not very different from what is seen with PBS, PBSA, and PCL the large change in mechanical property trends can be ascribed to PBAT remaining amorphous. Rubber Toughening is a method that has been used extensively to effectively toughen polymer systems with the

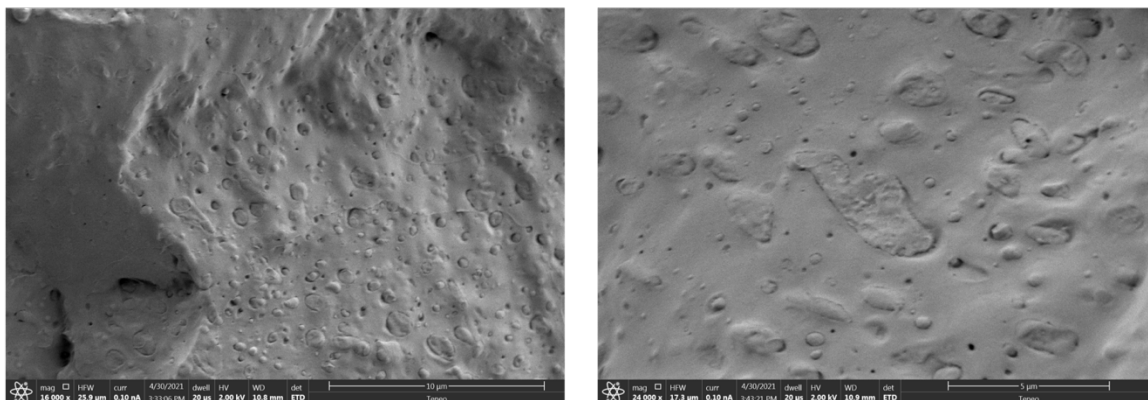


**Figure 2.6:** SEM images of cryo-fractured samples showing immiscible PBAT domains (20%) within the PHBHHx matrix

most famous example being high impact polystyrene (HIPS).<sup>21, 22</sup> While the mechanism of rubber toughening can vary with polymer systems and additive, it is believed that PBAT behaves in a similar manner while remaining mostly amorphous within the PHA matrix.

PBAT also shows much promise in incorporation of high starch loadings into a PHA blend. Starch is a beneficial additive to include in a PHA formulation as it reduces the overall cost of the resin as well as potentially increasing the biodegradation time for the end use article. Blending of starch with PHA proved to be notoriously difficult as phase separation took place which led to extremely poor mechanical properties as well as melt fracture as the polymer exited the die. Several reactive strategies were attempted to increase the compatibility between the PHA and starch components including the use of organic peroxides, but adequate compatibilization could not be achieved in a blend with just PHA and starch. One of the largest barriers is the low processing window for PHA. The starch used has an optimal processing temperature of 166°C-180 which starts to induce severe degradation in the PHA. Also, the use of a

nucleating agent is necessary at these temperatures as any inherent PHB is melted. The starch component showed better compatibility with PBSA and PCL, but organic peroxides were needed when blending the starch/polyester master batch with PHA to increase the compatibility and improve the elongation at break of the blend. The starch polyester masterbatches were made by pre-blending the components at a 30:70 ratio respectively while using a melt temperature of 165°C. The pre-blends of 50:50 produced a brittle masterbatch that needing diluting by more polyester before undergoing reactive extrusion with PHA. The masterbatches were then used in reactive extrusion of a PHA blend using Luperox P as the radical initiator and triallyl cyanurate as a coagent to increase the crosslinking efficiency of the peroxide. Both blends were able to incorporate 10% starch by using a loading of 20% of the polyester. As can be seen in figure 2.7, PCL shows much better elongation at break (308%) than PBSA (240%). While

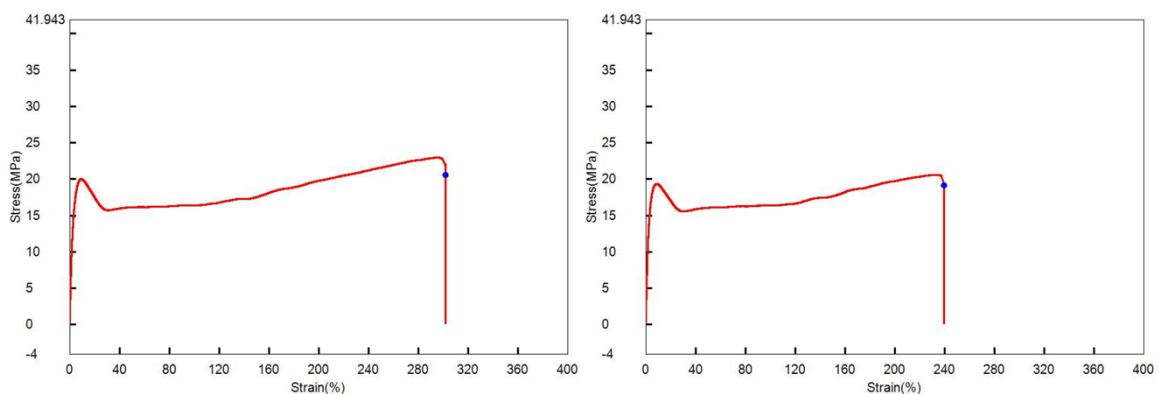


**Figure 2.7:** Stress-Strain curves for starch blends using REX\_PCL (Left), REX\_PBSA (right) with PHBHHx (6% Hx)

PBSA would be suspected as blending better with starch as well as giving the best elongation at break, likely the peroxide in combination with the coagent produced too much crosslinking in comparison to the PCL blend. PBAT was able to be pre-blended using a 50:50 ratio producing a flexible and tough masterbatch that could then be used

in further processing indicating a greater interfacial adhesion with PBAT. When the masterbatch was blended with PHA the poor compatibility is able to be overcome through encapsulating the starch within the PBAT component as seen in figure 2.8. The starch component forms a core shell morphology of small droplets within the PBAT droplet which is why such high loading of starch is able to be achieved. When the PBAT component was lowered to 10% the elongation at break decreased significantly and gave a brittle failure. It is hypothesized that the core shell structure begins to fall apart as the PBAT component is too low to encapsulate the starch component and more starch is exposed to the PHA matrix with poor interfacial adhesion causing poor elongation at break like what is seen with a pure starch PHA blend. It is unknown how

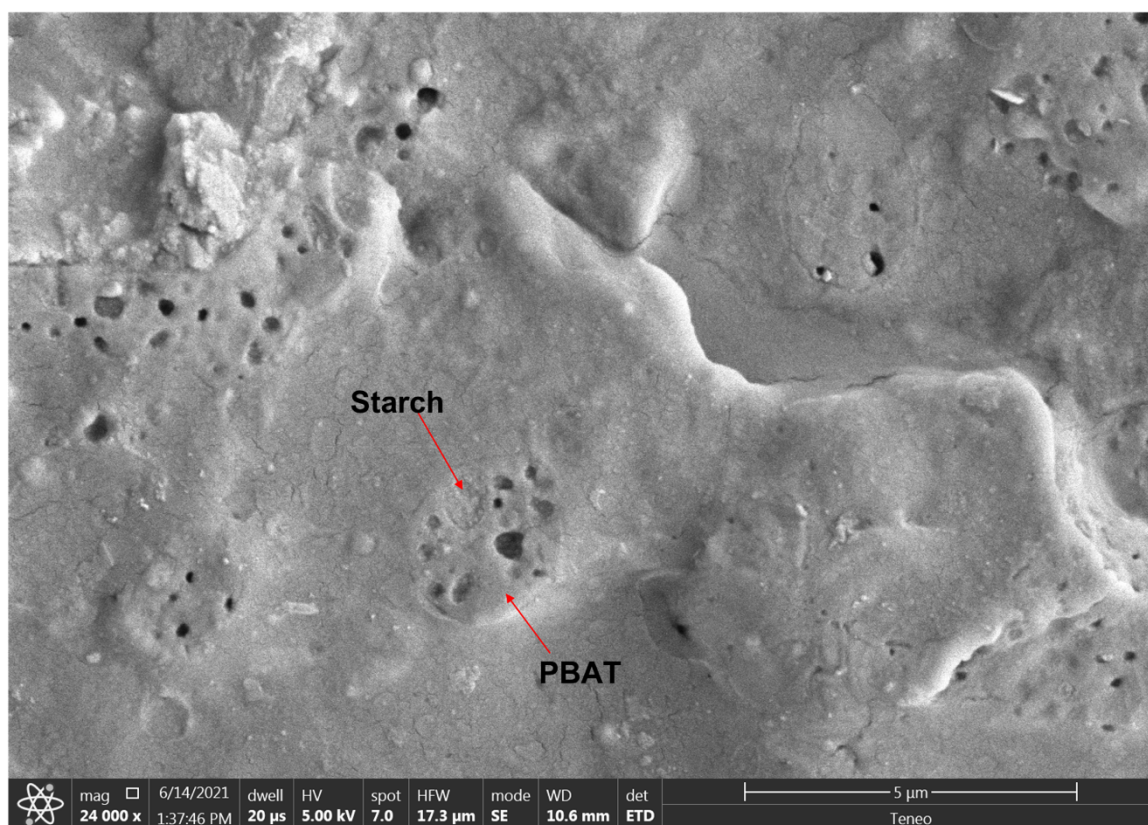


**Figure 2.8:** SEM image showing starch encapsulated within PBAT when blended with PHBHHx (6% Hx). Image taken from blend one of table 1

this core shell morphology will affect end of life testing for PBAT encapsulated starch blends as the starch will not be as readily accessible to microbial decomposition until the PBAT shell is degraded. Increasing the PBAT component too high (30%) gave good elongation of 322% but at the cost of dropping the Young's modulus to 0.44 GPa as well as reducing the tensile strength of the material. Talc, a reinforcing filler that has been extensively studied in many commodity thermoplastics such as polypropylene, was added to enhance the stiffness of this blend.<sup>23,24,25</sup> Talc can have high lamellarity from its composition of magnesium sandwiched between two  $\text{Si}_2\text{O}_5$  sheets and can act as a reinforcing filler for many polymers depending on the structure of the talc used. Very high lamellarity is desirable as it increases the surface area of each individual talc sheet while talc with a very small particle size is better used at lower loadings as a nucleating agent rather than a reinforcing filler at higher loadings. As shown in figure 2.9 and 2.10, 3CA talc has a very platy structure as well as a small particle size with a d50 of 1  $\mu\text{m}$ . the proprietary process coined "Jetfine delamination" allows for the retention of the platy

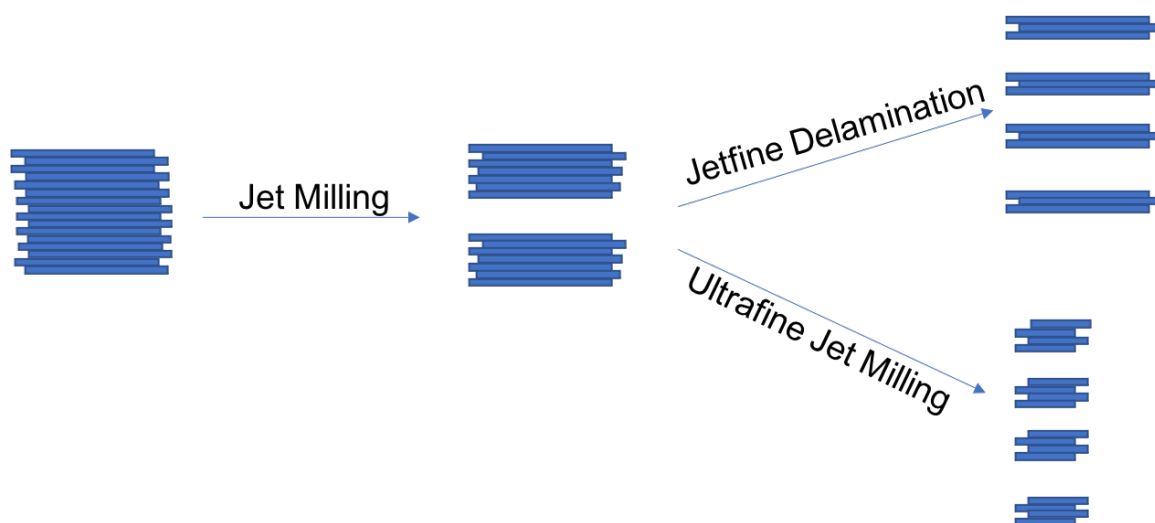


**Figure 2.9:** Representative process for the production of high lamellarity talc

Blend	PHA	PBAT	Starch	Talc	Elongation (%)	Young's Modulus (GPa)
1	60	30	10	0	322	0.44
2	55	30	10	5 (3CA)	319	0.63
3	65	20	10	5 (3CA)	289	0.67
4	75	10	10	5 (3CA)	40	0.66
5	55	30	10	5 (micro)	336	0.48
6	65	20	10	5 (micro)	307	0.60
7	75	10	10	5 (micro)	35	0.67

**Table 2.1:** Elongation at break and Young's modulus of starch and PBAT blended with PHBHHx (6% Hx). Two sizes of talc were also blended as reinforcing fillers.

structure while reducing the talc down to a small particle size. Normal ultrafine jet milling can produce a very small particle size ( $d_{50} < 1 \mu\text{m}$ ) at the expense of the plate like structure that is needed for reinforcement of the polymer. The added talc aligns with the direction of flow, as seen in figure 2.11, causing it to have high surface area in the transverse direction which gives a reinforcing effect. Introduction of just 5% 3CA talc into the PHA/PBAT/Starch blend was able to increase the modulus of the material to 0.63 GPa from 0.44 GPa while maintaining the elongation at break at 319%. Decreasing

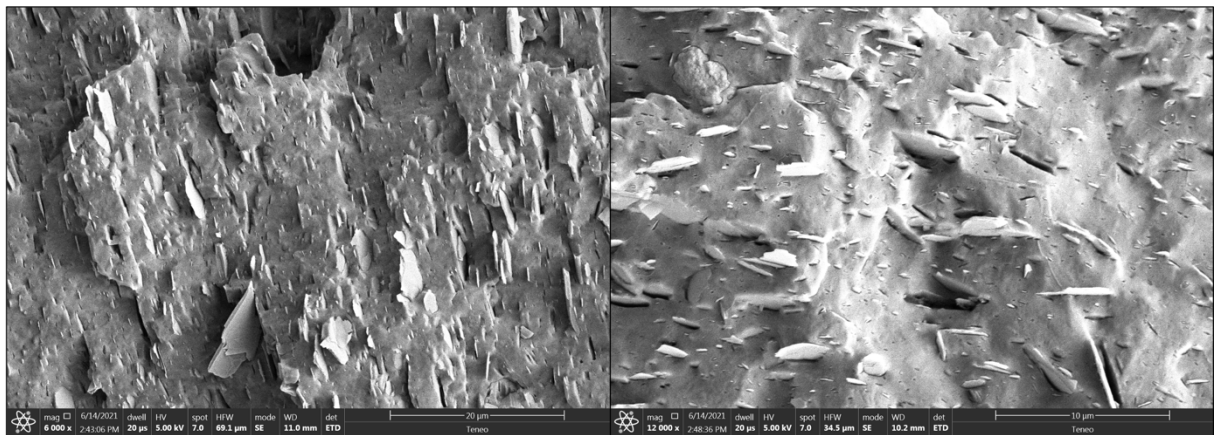


**Figure 2.10:** SEM images of 5% talc added to PHA. Talc plates are aligned with the direction of flow (coming out of the page).



the amount of PBAT in the same blend using talc reduced the elongation at break to 289% while increasing the Young's modulus to 0.67 GPa. The increase in Young's modulus also indicates good compatibility between the talc and PHA components as the greatest impact on stiffness is typically flexural rather than elongational. Interestingly these blends were tested after 72 hours rather than 24 indicating that PBAT is able to inhibit embrittlement, which is usually observed after 72 hours, even with starch added to the formulation. The same formulations were repeated using a different talc grade with a much smaller particle size. While the elongation at break for the 30% and 20% PBAT blends remained quite high, 336% and 307% respectively. The talc added was not able to provide the increase in modulus that was seen for the high lamellarity grade. For the 30% PBAT blend the Young's modulus was 0.48 GPa which is very similar to the blend without any talc. When PBAT was reduced to 20% of the overall blend the Young's modulus was 0.60 GPa indicating that the talc with such a small particle size was not able to sufficiently stiffen the blends as well as a talc with high lamellarity. Alternatively, these samples were tested after 24 hours which could also account for some of the discrepancy between the talc grades as the samples that were aged could have a higher

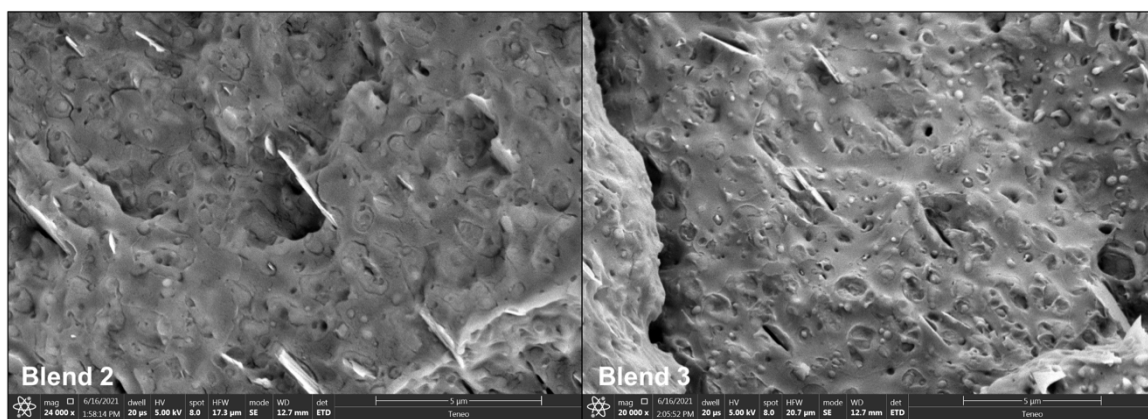


**Figure 2.11:** SEM images showing Starch:PBAT:Talc blends with PHBHHx (6% Hx)

stiffness as secondary crystallization of the PHA portion could have taken place over 72 hours. Although, a change of nearly 400 MPa is usually not observed after 72 hours.

Polycaprolactone showed excellent improvement in the elongation at break of the polymer blend at low loadings of 5%. The elongation reduces as weight percent increases past the critical point of 20% before beginning to increase again. This trend

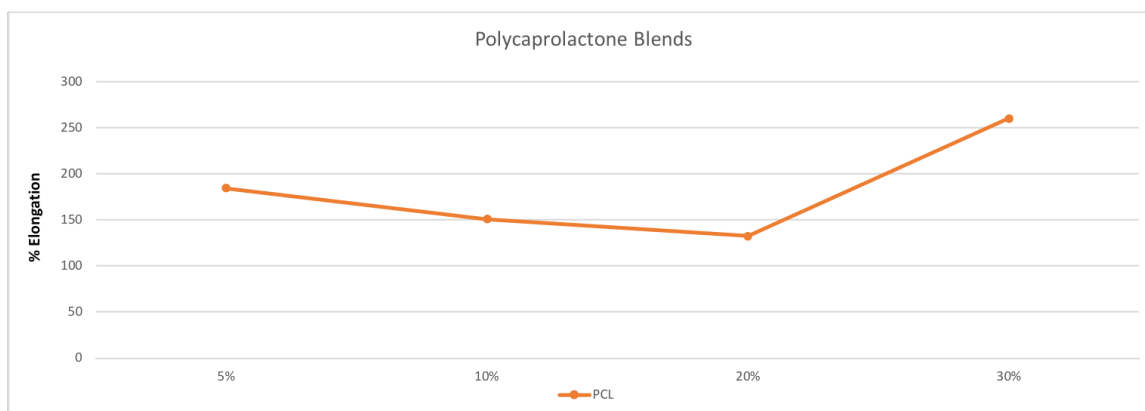


**Figure 2.12:** Elongation at break of blends of Polycaprolactone with PHBHHx (6% Hx)

has been noticed with PBS as well. As the weight percent increases beyond 20% the mechanical properties are greatly enhanced depending on the mechanical properties of the polymer added. While 30% still shows immiscible droplet formation the weight

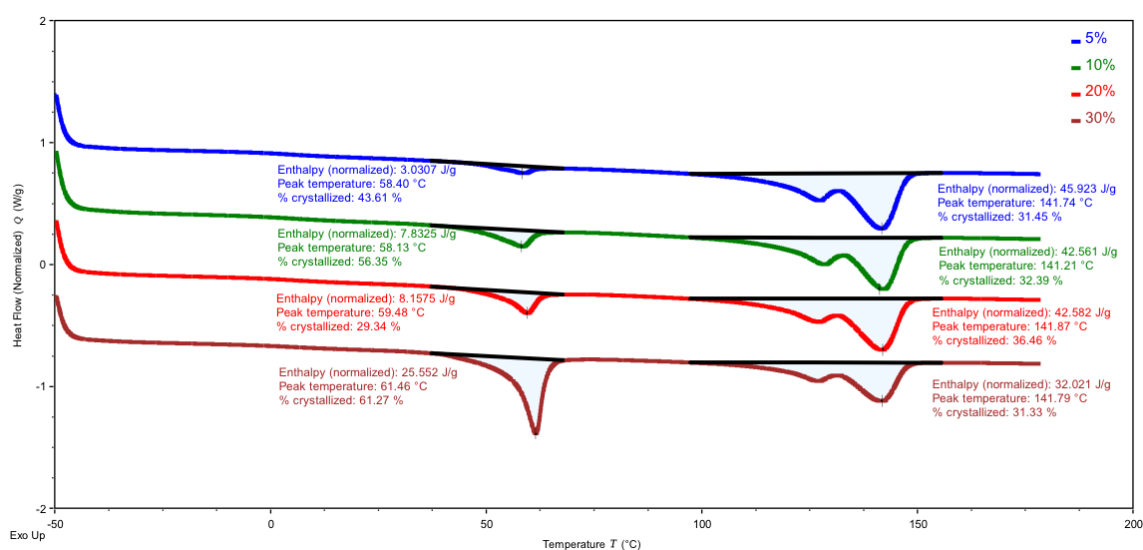


**Figure 2.13:** Melting endotherms of 5, 10, 20, and 30% blends of PCL with PHBHHx (6% Hx)

loading is getting closer to where the added PCL will begin to show a co-continuous phase rather than disperse droplets. Polycaprolactone is distinct from PBAT in that there is an evident melting transition seen at 58°C even at small loadings of 5%. This shows that PCL crystallizes under the injection molding conditions used for the blend even at small loading of 5%. The relative crystallinity of the PCL fraction in the 20% blend is notably lower than all the other blends while the PHA crystallinity is higher than all the other blends. This is also the blend with the lowest elongation at break although the Young's modulus is not as high as the 10% blend. While this is unexpected with the crystallinity of the PHA fraction being 36% this could be due to the remainder of the PCL remaining amorphous thus causing the reduction in the modulus of the blend. Interestingly there is little evidence of a crystallization peak on the cooling curve until a weight loading of 30% where a large exothermic transition of PCL is evident at 26°C. A slight exothermic transition can be seen at 0°C and 10°C for the 10% and 20% blends

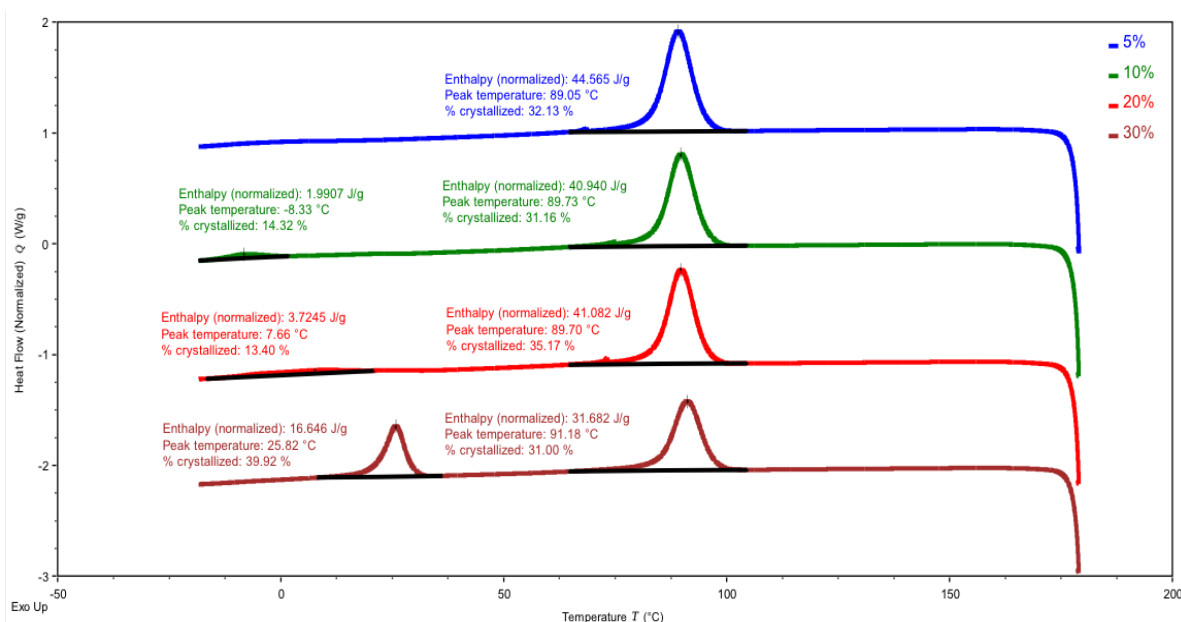


**Figure 2.14:** Exothermic transitions for 5, 10, 20, and 30% PCL blends with PHBHHx (6% Hx)

respectively. The slow crystallization of the PCL could be due to the small droplet size of the blends showing an increased peak  $T_c$  as weight loading increases up to 30%.

PBS behaves very similarly to PCL in that it has no evident crystallization peak until blended at a 30% weight loading, although even at this loading the exothermic transition is much less pronounced in comparison to PCL. There are slight exothermic transitions observed around 0°C and 10°C for the 10% and 20% blends respectively. The decrease in mechanical properties seen for both PCL and PBS at 20% loading cannot be explained through thermal transitions and crystallinity of the blend and likely occurs due to the morphology and size of the immiscible droplets in conjunction with the crystallinity of the blended polymer.

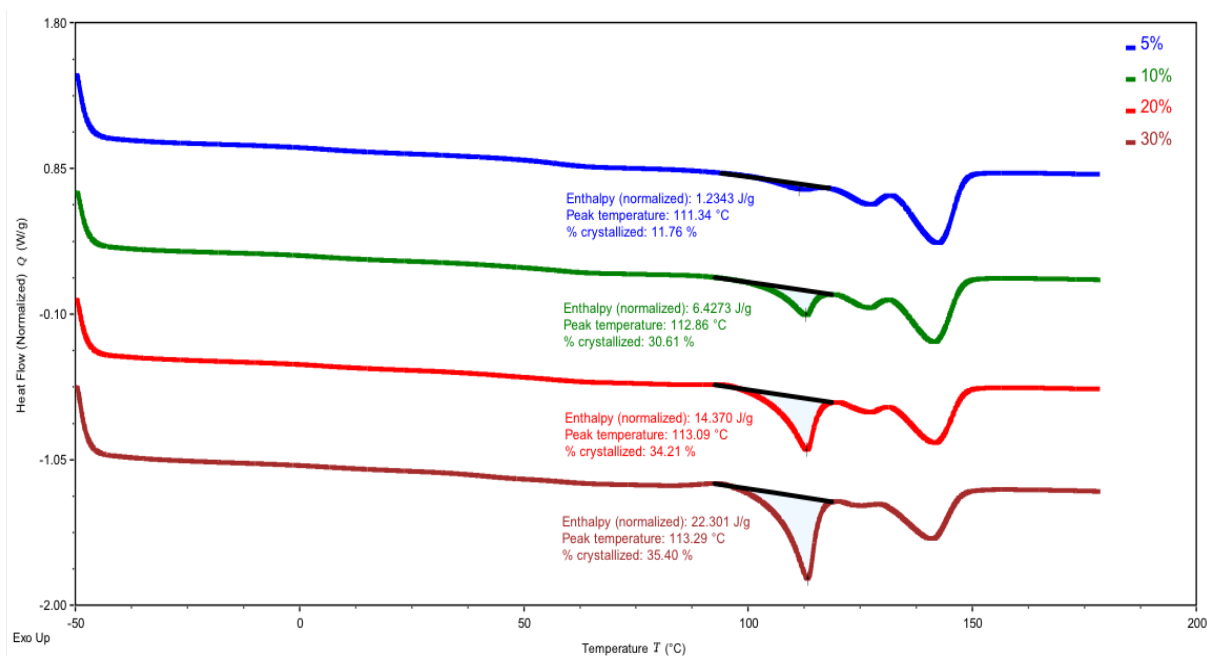


**Figure 2.15:** Melting endotherms for 5, 10, 20, and 30 % blends of PBS with PHBHHx (6% Hx)

PBSA, a less crystalline polymer, shows behavior in between PBAT and PCL/PBS.

Small loadings show an improvement in mechanical properties (125%) with increased

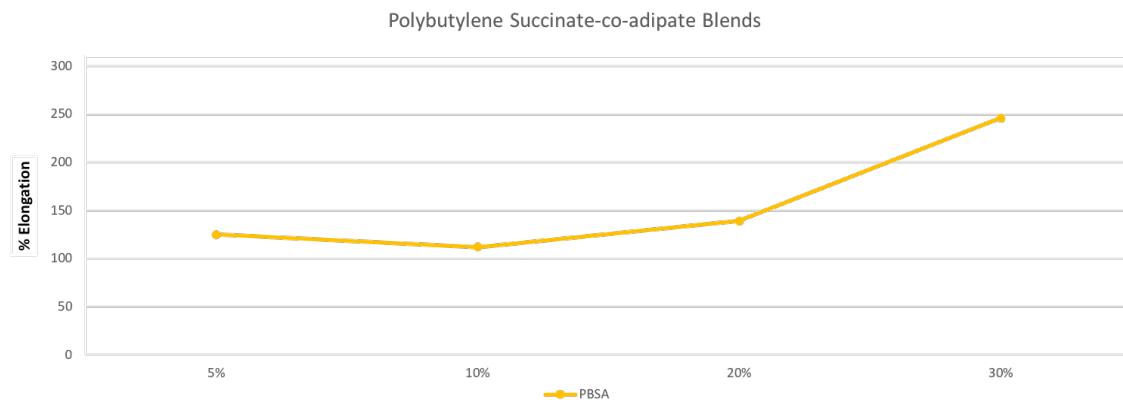


**Figure 2.16:** Elongation at break of 5, 10, 20, and 30% blends of PBSA with PHBHHx (6% Hx)

loadings showing a steady increase in elongation at break to a maximum value of 246% at a 30% weight loading. There is no characteristic drop in mechanical properties at the 20% weight loading like what was observed for PCL and PBS. PBSA also has a more drastic reduction in Young's modulus with increased weight loadings more similar to the behavior of PBAT. This is likely due to the less crystalline and more rubbery nature of

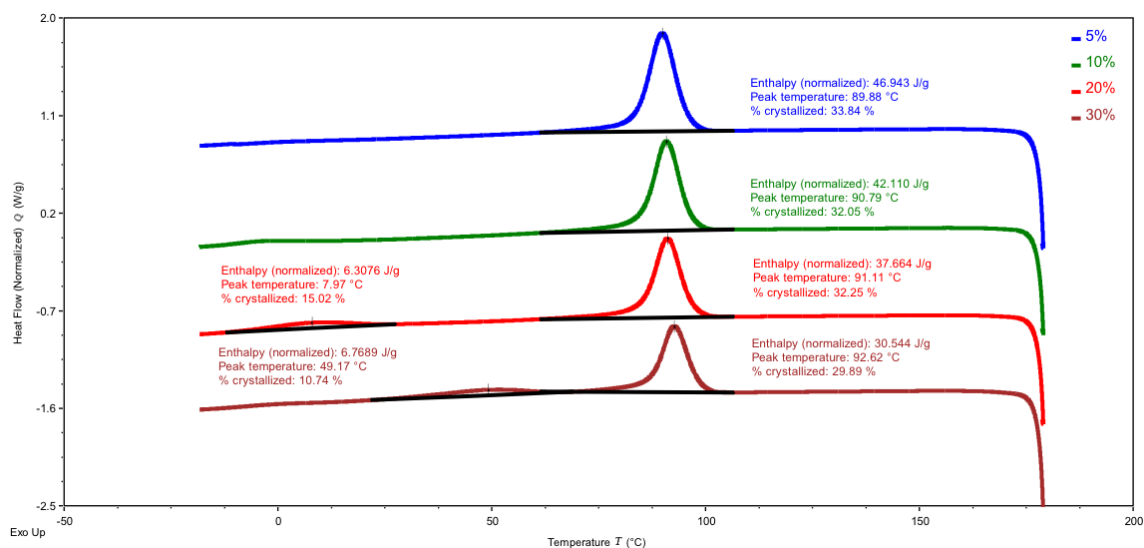


**Figure 2.17:** Crystallization exotherms for 5, 10, 20 and 30% blends of PBSA with PHBHHx (6% Hx)

PBSA due to the incorporation of adipic acid into the polymer. This shows that incorporation of other diacids that disrupt crystallinity of the random copolymer show much promise in being able to tune the final mechanical properties of the PHA blend based on weight percent of the added polymer as well as its relative crystallinity based on the mole percent of comonomer used.

Reactive extrusion was also explored with PHA blends using the previously blended commercially available polyesters (PBAT, PCL, PBS, PBSA). Tert-butyl peroxy benzoate (Luperox P) was used as the reactive compatibilizer at a constant loading of 0.1wt% while blending with 5, 10, 20, and 30% of the polyester additives to see the impact of increasing compatibility between the two components on the final mechanical

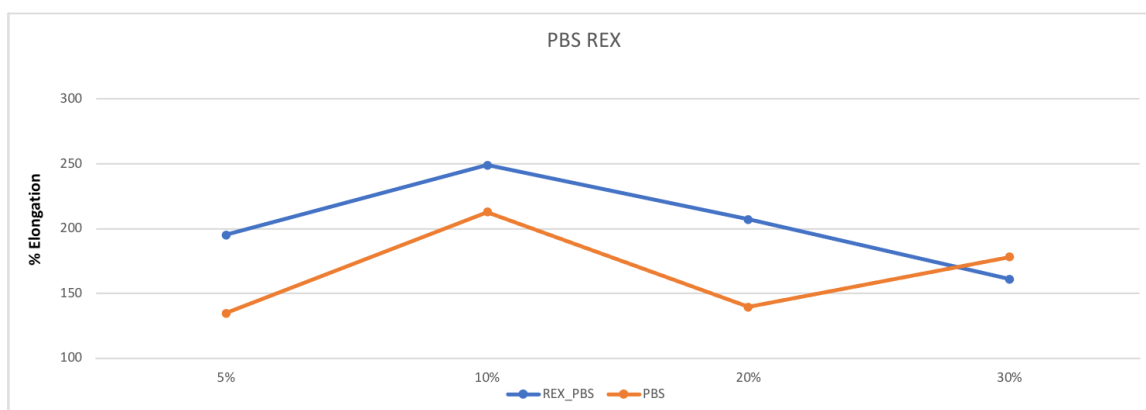


**Figure 2.18:** Elongation at break of 5, 10, 20, and 30% blends of PBS with PHBHHx (6% Hx) with and without peroxide

properties of the PHA blend. The organic peroxide noticeably caused an improvement in the elongation at break of all the polymer blends especially at lower loadings of 5%.

REX\_PBS showed a large improvement of the elongation at break at all loadings except for the 30% blend. REX\_PBS showed a peak elongation at the 10% loading just like the blend alone, yet above 10% there is a rapid drop in the elongation at break. This

is likely due to extensive crosslinking taking place. PBS showed remarkable reactivity towards the peroxide during the extrusion process causing a large increase in torque and pressure as the reaction proceeded. The stress-strain curves, shown in figure 2.19, from the tensile test also support that crosslinking is taking place with increased loadings of PBS indicating that it is the most reactive portion within the blend. As the

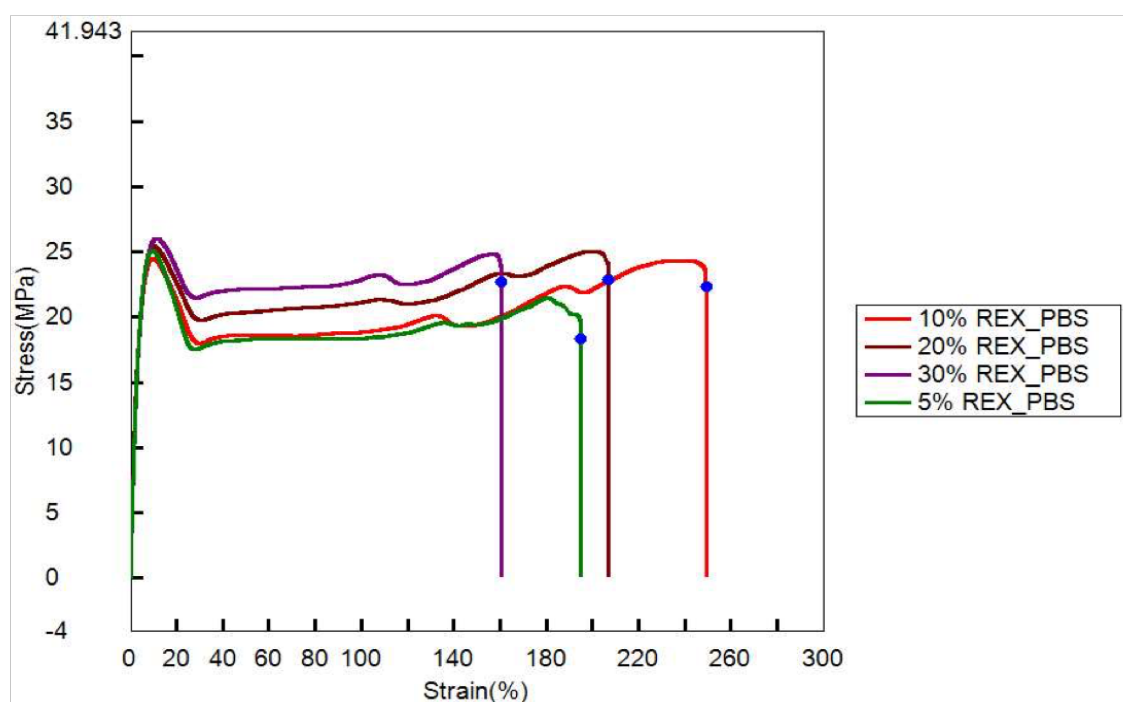


**Figure 2.19:** Stress-Strain curves of 5, 10, 20, and 30% REX blends of PBS with PHBHHx (6% Hx)

loading of PBS increases the elongation at break decreases but the yield point, and tensile strength increase which is consistent with chemical crosslinks being present in the system. PBS has been reported to be more reactive than PHA towards gelation using Dicumyl peroxide as the radical initiator with the gel content being close to the amount of added PBS.<sup>7</sup> As the gel content increases the polymer, while being very strong to tensile deformation, is no longer able to have crystal slippage and interfacial debonding as the polymer chains are now chemically bonded together in a network interspersed

within the PHA matrix. This produces a blend that is not as ductile but is extremely tough. REX causes a slight reduction in the stiffness of the polymer blend (100 MPa) yet interestingly shows the same increase in stiffness at a 20% loading as does the plain blend. The reduction in stiffness is due to the crosslinking of the internal PBS component causing a reduction in its crystallinity. Chemical grafting, at the interface, between the two components also could account for the slight reduction in Young's modulus as the two components form a non-crystalline crosslinked and branched structure with one another.

Interestingly, PBS still shows a melting transition even with very high gel contents expected to be concentrated within the PBS fraction of the polymer blend. In fact, the overall crystallinity of the PBS fraction is only reduced by 10% in comparison to the blend without peroxide compatibilization. One large difference found between REX\_PBS and pure PBS blends was the crystallization exotherm. As previously described, there are slight exotherms of crystallization seen for the PBS component in the 20% and

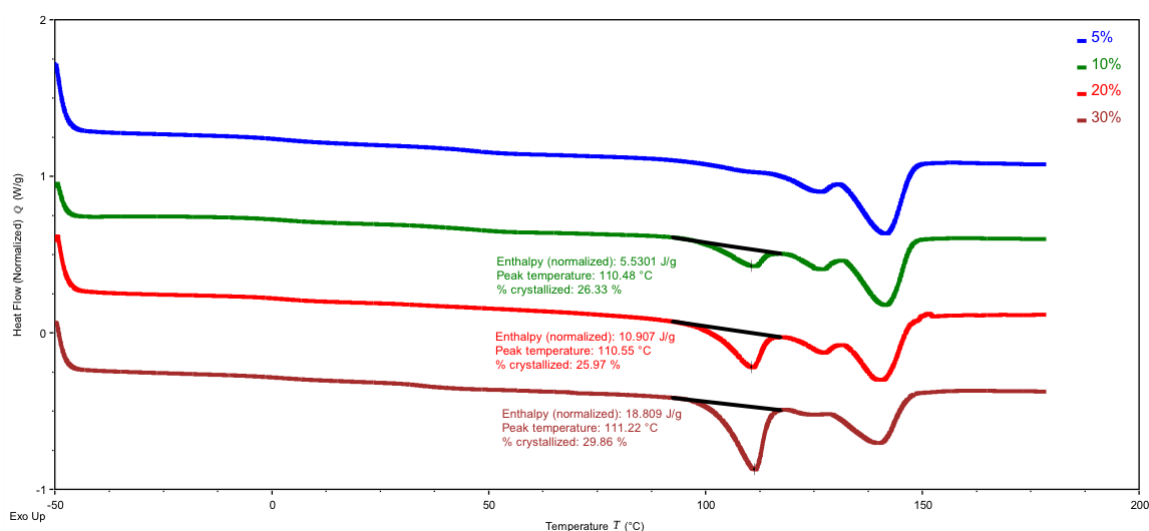


**Figure 2.20:** Melting endotherms for 5, 10, 20, and 30% REX\_PBS blends with PHBHHx (6% Hx)



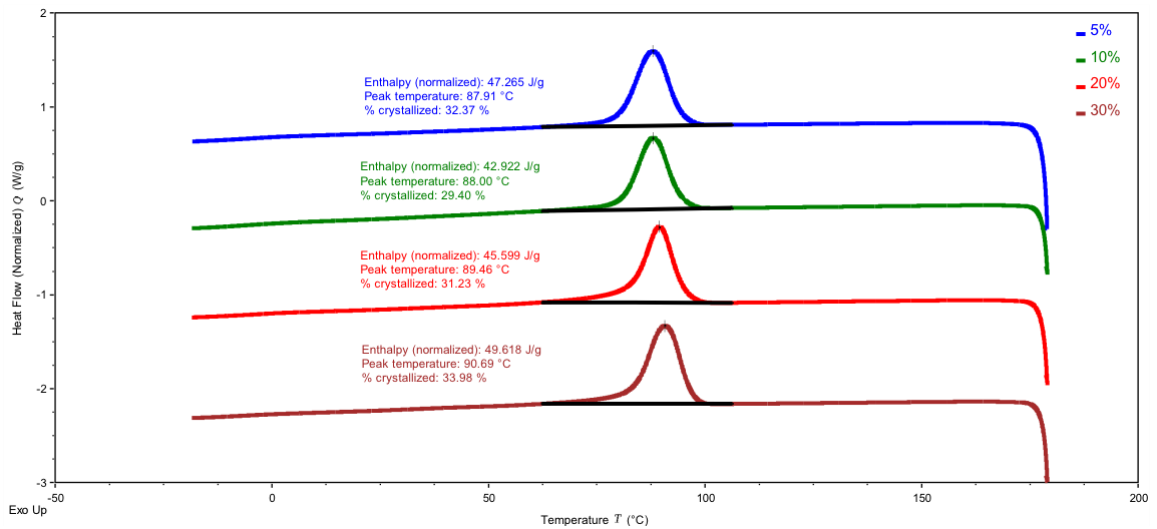


**Figure 2.21:** Crystallization exotherms for 5, 10, 20, and 30% REX\_PBS blends with PHBHHx (6% Hx)

30% blends. These were down shifted to approximately 10°C and 50°C from the usual temperature of crystallization of 89°C likely due to the confinement induced by PHA nucleation prior to the crystallization of the PBS component. Notably there are no exotherms observed in the REX\_PBS blends at equivalent temperatures although there are melting endotherms observed around 110°C. This indicates that the crosslinked PBS component is a mixture of highly branched, crosslinked, and grafted material. It is believed that the branch points can act as molecular defects that induce nucleation. Although, more likely the crosslinked portion of PBS chains are confined to favorable positions at the interface of crystalline lamellae and the crosslinked network. Upon an increase in temperature the crystalline domains melt while the network portion would only swell. This acts as a nucleation site for reformation of the crystalline lamellae as the chains would be held in an optimal lattice position for initiation of crystallization. While no exotherms are seen at lowered temperatures the relative crystallinity calculated from the exotherms seen for PHA are several percent higher than normal and increase

upon increasing PBS loading. This indicates that the crystallization exotherm for the crosslinked PBS is shifted to a peak temperature of 89°C and is hidden in the exothermic transition of PHA crystallization. This would also indicate that the PBS is located in larger enriched domains of crosslinked material as the crystallization is not hindered. This is further exemplified when the 30% blend was heated to 200°C to remove the nucleation efficiency of inherent PHB homopolymer within the PHBHHx copolymer. Upon cooling the PHA exotherm is down shifted and broadened as nucleation becomes poorer without the inherent nucleating agent. Typically, no exotherm is observed for PHA after heating to this temperature indicating that crosslinking in the PHA fraction acts as a nucleating agent similar to PBS. The crystallization of the PBS fraction becomes clearly visible at 93°C which is several degrees higher than typical for PBS. SEM images shown

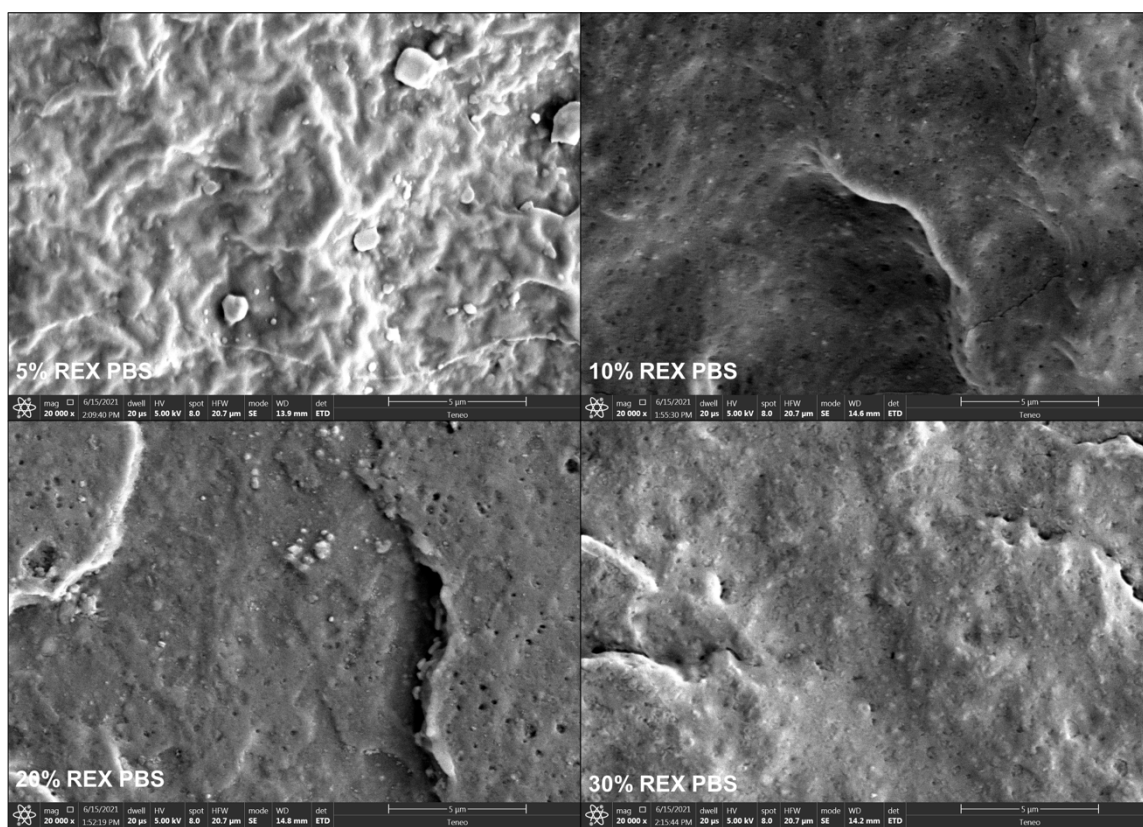


**Figure 2.22:** SEM images of 5, 10, 20, and 30% REX PBS blended with PHBHHx (6% Hx)

in figure 2.22 show that reactive extrusion causes good compatibilization between the two phases as immiscible droplet formation is reduced from what is typically seen for PBS. The domains of PBS are most evident in the 10%\_REX blend which is fitting with the tensile data previously shown in figure 19 which has the best elongation at break. The compatibility that is shown in the 20% and 30% blends is likely due to the high amount of crosslinking that is evident in the tensile data.

Polycaprolactone shows a remarkable improvement in elongation for all loadings when reacted using Luperox P. At low loadings there is a moderate difference between PCL and REX\_PCL of 184% and 200% respectively, but as the loading of PCL increases the difference in elongation becomes more drastic. At a loading of 10% PCL there is an improvement from 150% to 262% and this difference broadens as PCL is increased to a 20% loading (132% to 270%). At a 30% loading of PCL the elongation at break for the blend drastically increases to 260% as the morphology of the PCL portion is beginning to

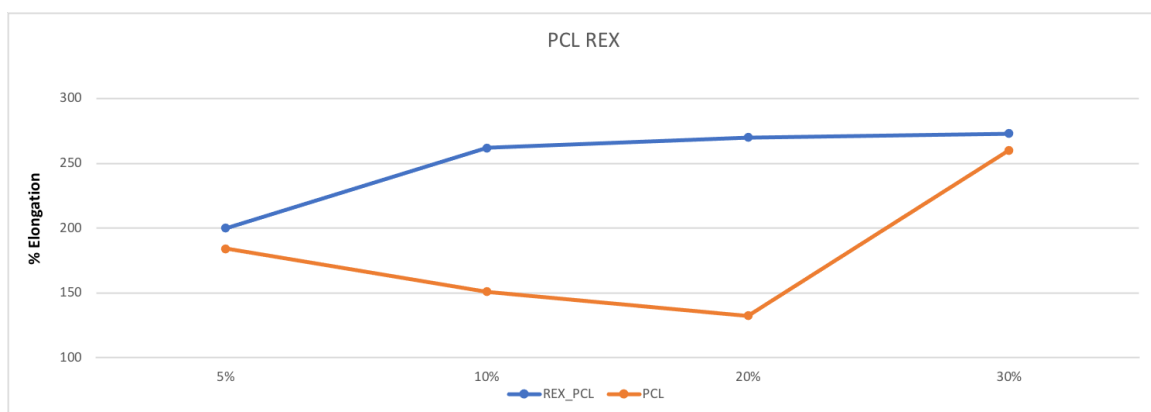


**Figure 2.23:** Elongation at break of 5, 10, 20, and 30% blends of PBS with PHBHHx (6% Hx) with and without peroxide

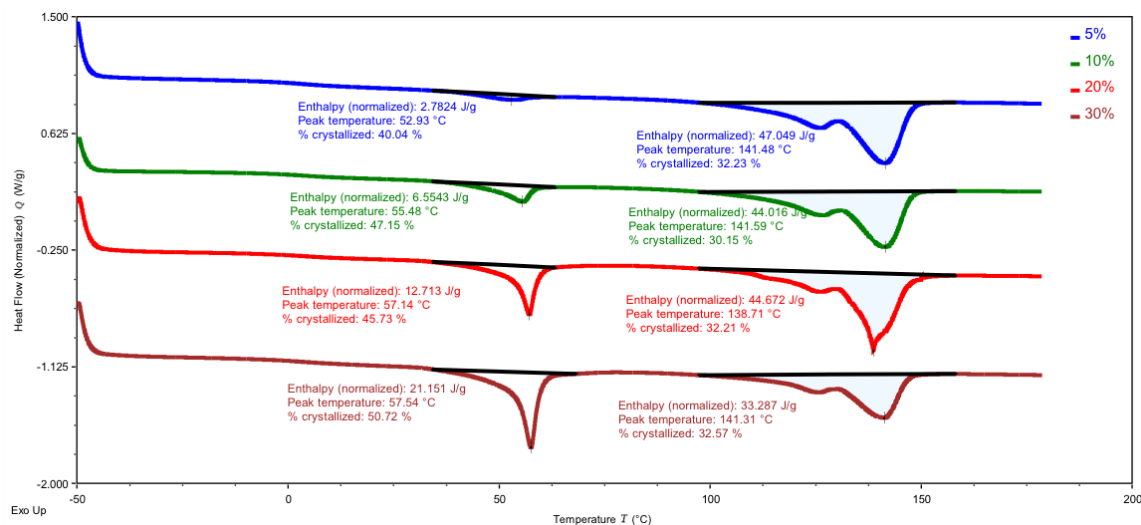


**Figure 2.24:** Melting endotherms of 5, 10, 20, and 30% REX\_PCL blends with PHBHHx (6% Hx)

shift to a co-continuous phase that would be expected in blends of 40, and 50% PCL. The melting transitions shown in figure 24 show that the PCL portion is less crystalline than the blend without reactive extrusion indicating that there may be slight crosslinking occurring within the PCL fraction. Interestingly, the same trend of the 20% blend showing the least amount of crystallinity in the PCL fraction still holds. Although for the REX\_10% blend there is a noticeable drop of relative crystallinity for the PHA fraction of the blend. A melting endotherm is visible even with a PCL loading of 5% which shows complete immiscibility of the blends and that the PCL remains highly crystalline. The crystallization curves for the DSC show no exotherm for the 5% and 10% blends while the crystallization of the PCL portion is very evident in the

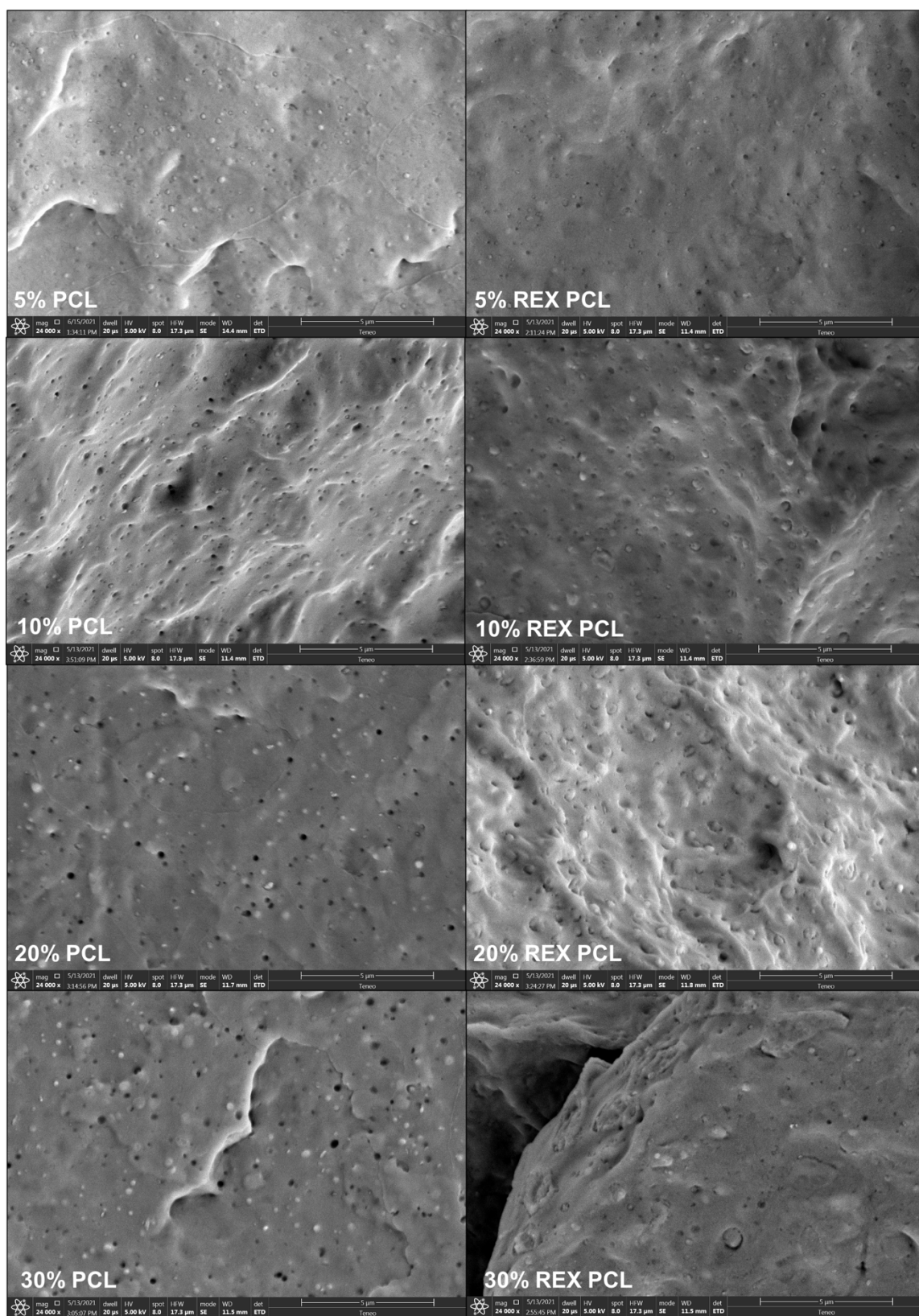


**Figure 2.25:** SEM images showing immiscibility and compatibilization of PCL using reactive extrusion (the scale bar is 5 $\mu$ m)

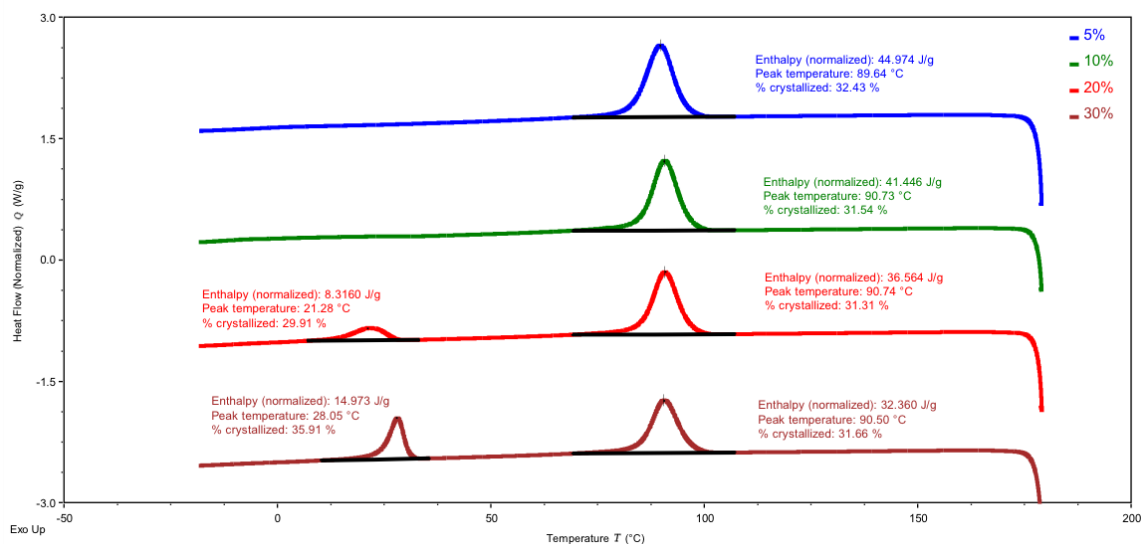


**Figure 2.26:** Crystallization exotherms for 5, 10, 20, 30% REX\_PCL blends with PHBHHx (6% Hx)

20% and 30% blends. The PHA portion remains constant at a relative crystallinity of 31% for all the blends. As can be seen in figure 2.25, SEM shows that there is increased compatibility between the PCL domains and PHA matrix in the REX samples. This is most evident in the 5% blend where the immiscible domains are much harder to see in the REX sample than in the pure blend.

PBSA behaves very similarly to PCL in that the elongation at break remains low (<150%) until the blend loading reaches 30% and elongation drastically improves to

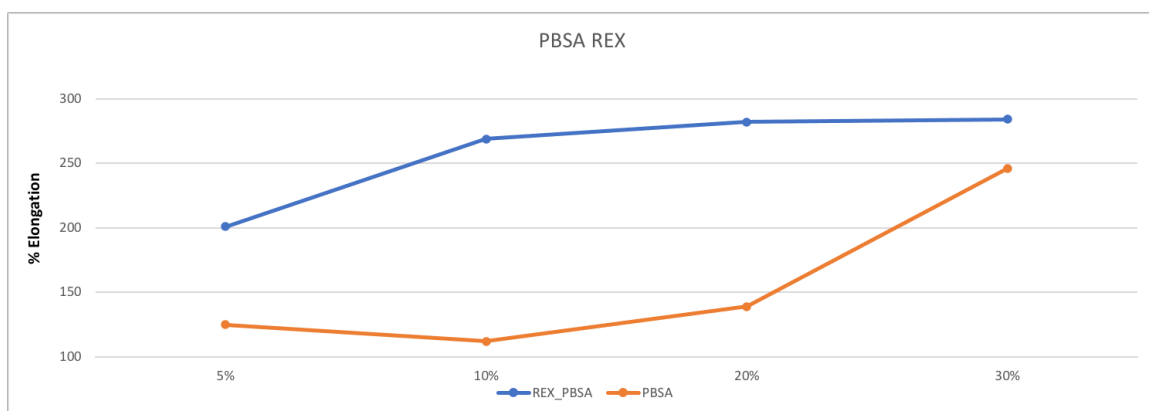


**Figure 2.27:** Elongation at break of 5, 10, 20, and 30% Blends of PBSA with PHBHHx (6% Hx) with and without peroxide

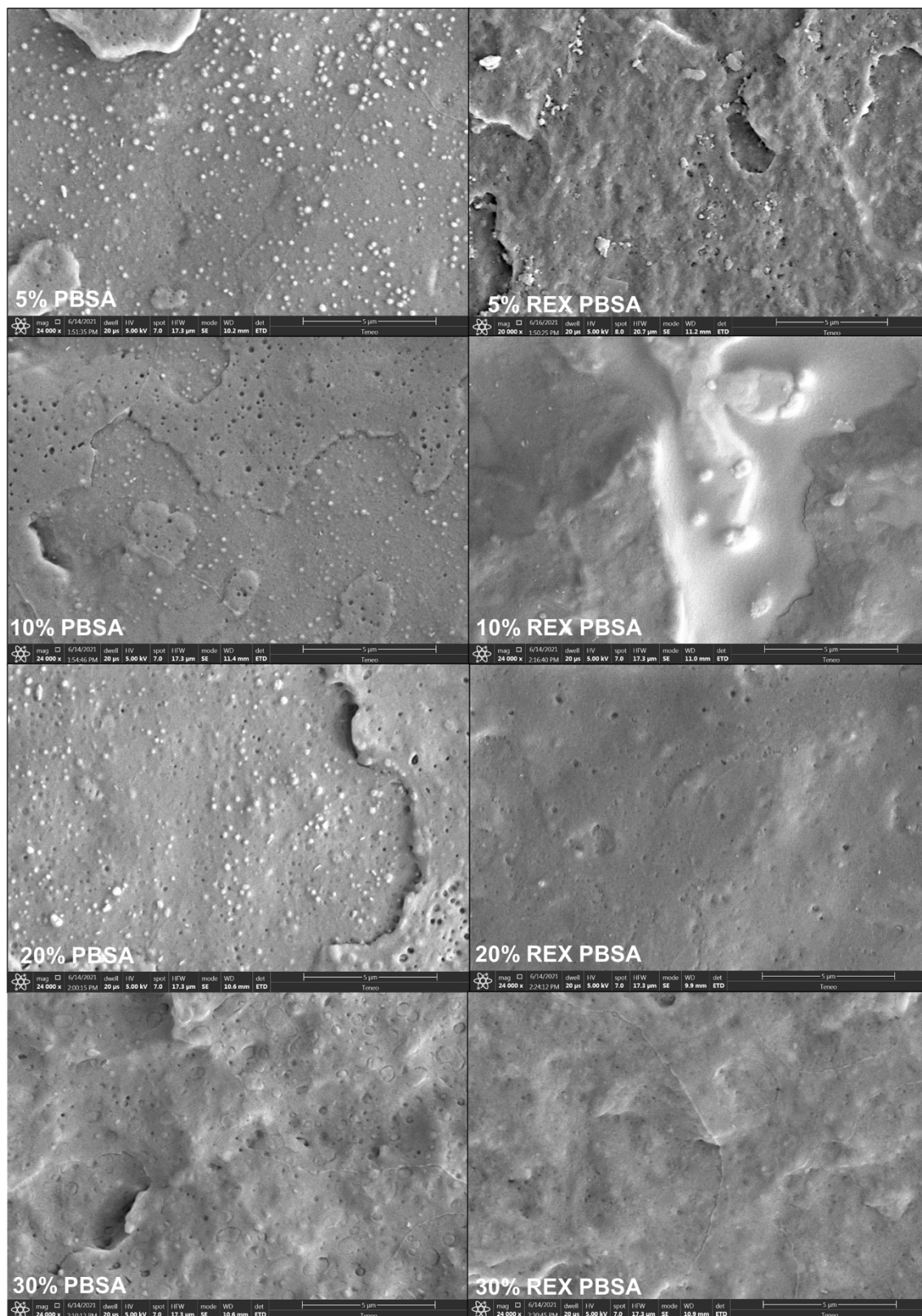


**Figure 2.28:** SEM images showing compatibilization of PBSA with PHBHHx (6% Hx) through reactive extrusion (scale bar is 5µm)

246%. REX PBSA shows much improvement in elongation (201%) even at a 5% loading. The succinate portion of the blend showed high reactivity towards the radical initiator just as PBS did. There was an increase in pressure and torque response as the polymer was extruded. However, unlike PBS the increase in gelation for PBSA led to increased elongation even at a 30% loading. Likely this could be due to the PBSA behaving more like PBAT in the final polymer blend with a larger amorphous fraction, especially when crosslinked in comparison to PBS which still remained fairly crystalline at a 30% loading. This is also reflected in the modulus for REX\_PBSA showing a steady decline to 0.59 GPa at a 30% loading much like the reduction seen for PBAT, while PBS remains fairly constant around 0.67 GPa except for the anomaly at a 20% weight loading. One unique difference about REX\_PBSA is that there was no evidence of crazing or stress whitening during the tensile test. The test area became translucent indicating that there was a unique deformation process that the sample was undergoing. SEM images shown in figure 2.28 confirm that reactive extrusion with PBSA dramatically improved the compatibility between the added polyester and the PHA matrix. Even up to a 30% loading there was little indication of immiscible domains of PBSA for the REX samples. In the 10% blend there are evident, large patches of an immiscible portion believed to be highly crosslinked, PBSA domains.

PBAT shows increased elongation at a 5% loading when compatibilized through reactive extrusion. However, the elongation is still not as good as the other REX polymers. A 10% loading also show better elongation of 246% vs 196% but the blend



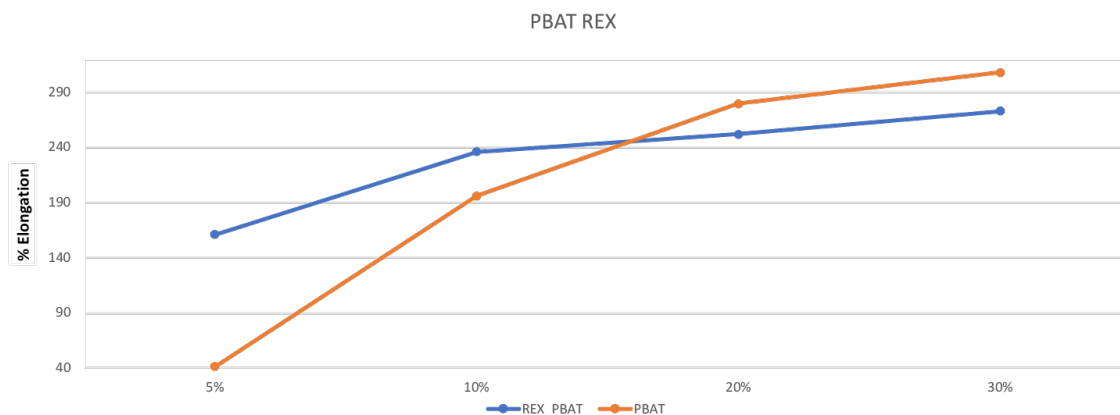


**Figure 2.29:** Elongation at break of 5, 10, 20 and 30% blends of PBAT with PHBHHx (6% Hx) with (blue) and without (orange) peroxide

alone overtakes the REX blend at 20% and 30% loadings. DSC analysis shows that there is very little difference between REX\_PBAT and unreacted blends for the melt and crystallization transitions. In the crystallization exotherms there is a broadening of the crystallization peak, just as was found with the unreacted blends, indicating that there is some crystallinity developing in the PBAT portion of the blend. There is also a dramatic increase in the crystallinity from 34% to 38% indicating that the exotherm for the crystallization of PBAT is hidden behind the crystallization peak of PHA and is only

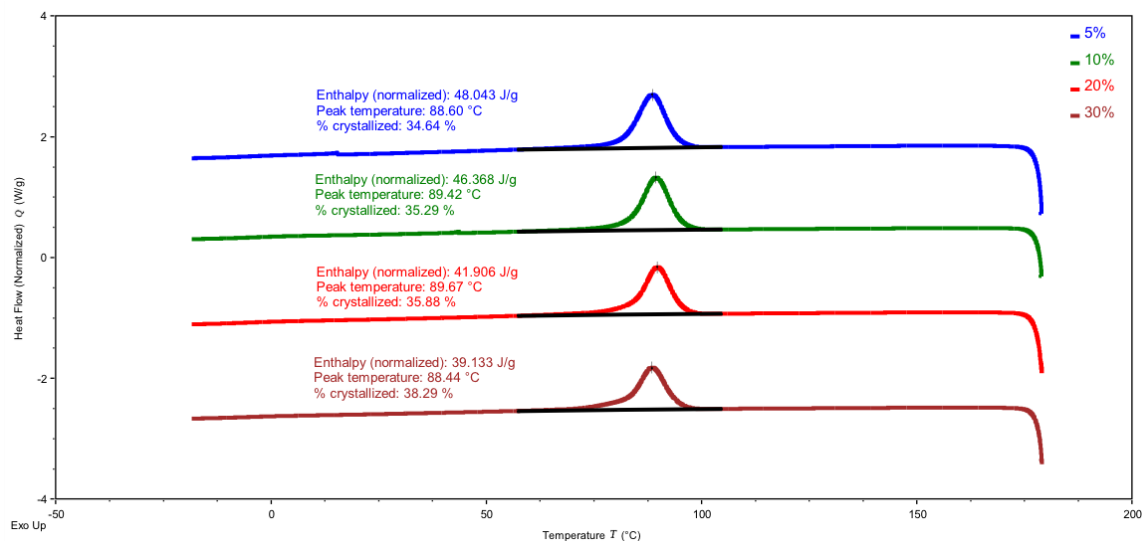


**Figure 2.30:** Crystallization exotherms for 5, 10, 20, and 30% blends of REX PBAT with PHBHHx (6% Hx)

evident at high loadings due to the long tail seen in the 30% blend. SEM analysis for the REX\_PBAT samples shows little difference between the unreacted blends. There appears to be no decrease in the size of the immiscible droplets which is what was expected for the REX samples. The increase in mechanical properties for the lower weight loadings can be attributed to an increase in interfacial adhesion between the immiscible portions which leads to greater compatibility rather than a decrease in particle size.

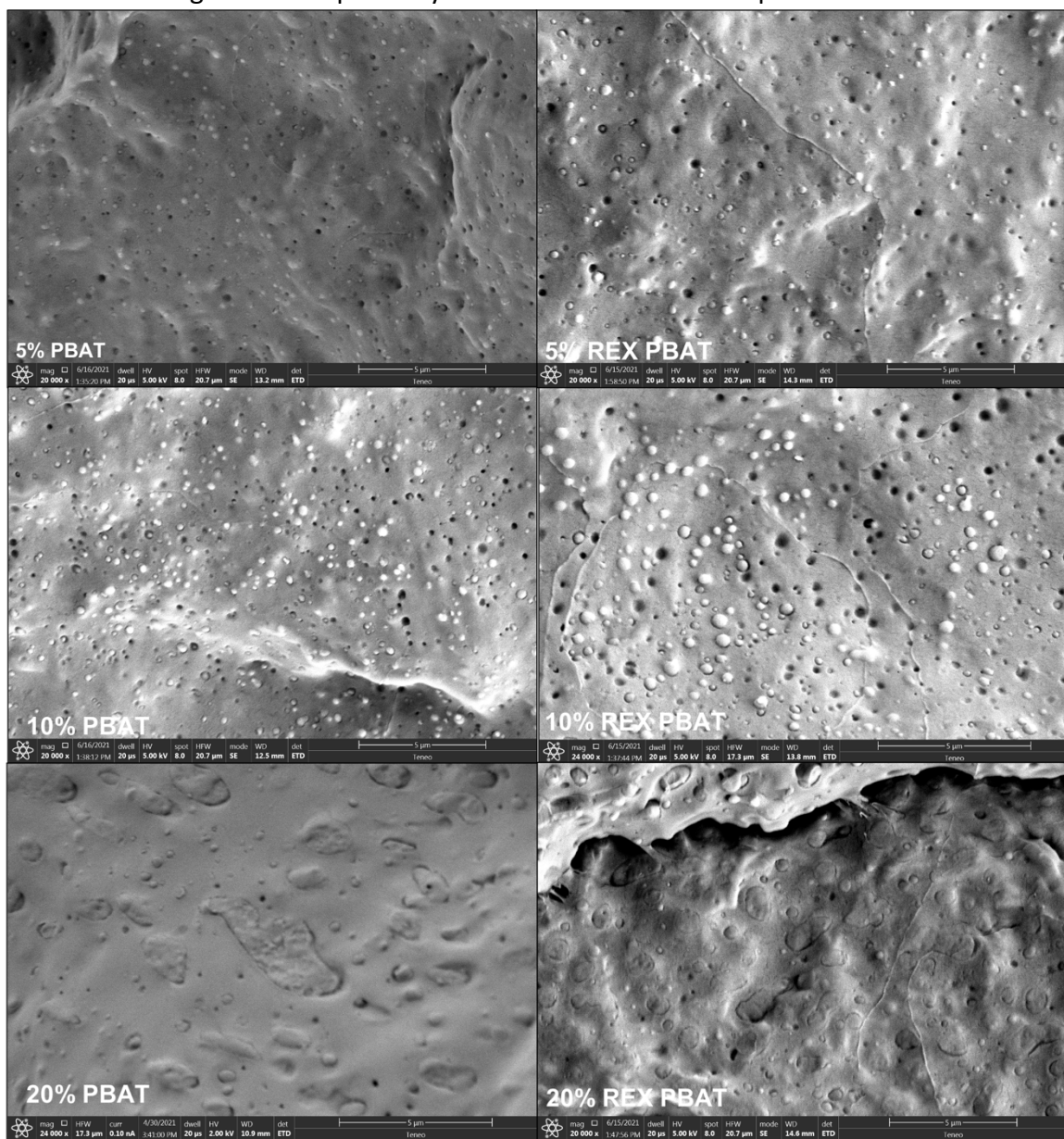


**Figure 2.31:** SEM images comparing REX of 5, 10, and 20% blends of PBAT with PHBHx (6% Hx)

	Youngs Modulus (GPa) 5% Blend	Youngs Modulus (GPa) 10% Blend	Youngs Modulus (GPa) 20% Blend	Youngs Modulus (GPa) 30% Blend
<b>PBS</b>	0.77	0.78	0.80	0.75
<b>REX_PBS</b>	0.69	0.68	0.74	0.67
<b>PCL</b>	0.81	0.77	0.75	0.75
<b>REX_PCL</b>	0.72	0.71	0.70	0.69
<b>PBAT</b>	0.81	0.75	0.63	0.52
<b>REX_PBAT</b>	0.71	0.73	0.64	0.58
<b>PBSA</b>	0.70	0.70	0.64	0.65
<b>REX_PBSA</b>	0.75	0.67	0.64	0.59

**Table 2.2:** Young's Modulus comparison of reactive extrusion blends with PHBHHx (6% Hx)

Blending PHBHHx with other polymers that are not commercially available was also investigated. Polybutylene glutarate (PBG), Polybutylene succinate-co-glutarate (PBSG), and polybutylene adipate (PBA) were synthesized with various molecular weights to see the impact on final mechanical properties of PHA blends. PBG is of particular interest as the biosynthetic pathway for glutaric acid has been recently elucidated, meaning that PBG has the potential to be 100% biobased going forward.<sup>26</sup> Copolymers with succinic acid, which also can be biobased, were investigated to see the impact that changing monomer ratios and crystallinity has on the final mechanical properties of PHA blends.

Polybutylene adipate was synthesized with molecular weights of approximately 30,000, 55,000, and 84,000 Daltons to see the effect of molecular weight on the final mechanical properties of the blends. First the low Mw PBA was blended at 3, 5, 10, 20, and 30 Wt% to see the impact on elongation at break and Young's modulus with

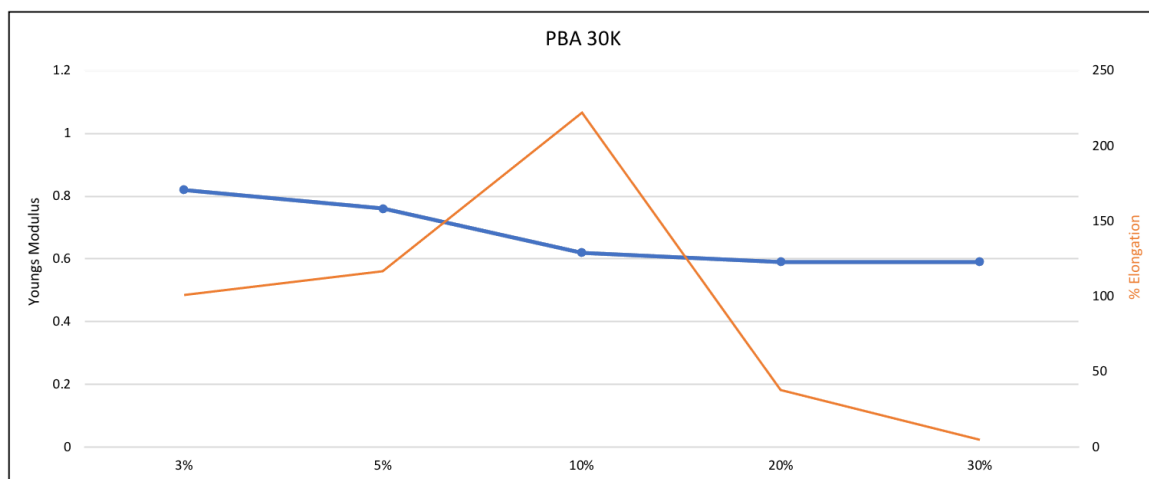


**Figure 2.32:** Young's Modulus and elongation at break of blends with 30,000 Mw PBA and PHBHHx (6% Hx)

increasing weight percent of additive. With commercially available high molecular weight polymers previously shown, 20wt% was a critical point where it is believed that the mechanical properties of the added polymer begin to greatly influence the final mechanical properties of the blend rather than simply the immiscibility of the two causing an increase in elongation due to internal void formation, cavitation, and microfibrils causing toughening. Figure 2.32 shows that there is a peak elongation at break found at 10% weight loading of the PBA component. Above this level the elongation at break severely decreases down to 5%. At this level there is no ductile failure of the sample and only brittle failure of the tensile specimen. The added PBA has very brittle mechanical properties that would be very similar to the brittle failure that is

Polymer	3% Elongation	5% Elongation	10% Elongation	20% Elongation
6Hx + PBA [30k]	101	117	222	38
6Hx + PBA [55k]	111	219	191	14
6Hx + PBA [84k]	46	14	180	125
Polymer	3% Modulus	5% Modulus	10% Modulus	20% Modulus
6Hx + PBA [30k]	0.82	0.76	0.62	0.59
6Hx + PBA [55k]	0.82	0.8	0.75	0.75
6Hx + PBA [84k]	0.76	0.68	0.73	0.64

**Table 2.3:** Elongation at break and Young's modulus for varying molecular weights of PBA blended with PHBHHx (6% Hx)

seen with the 30% blend. It seems that above 10% weight loading the mechanical properties of the added polymer begin to play a larger role in final mechanical properties of the blend up to 30% when the brittle failure of the blend is very similar to the added polymer. Notably, there is little difference between the PBAs of 30k and 55k except the anomaly of the 55k having a peak elongation at a 5% loading. When the molecular weight is increased to 84k the PBA becomes very tough on its own and upon crossing the critical point of 20% the mechanical properties retain elongation above 100% indicating that for each polymer added there is a molecular weight that the polymer reaches for the blend to have optimal mechanical properties above a 20%

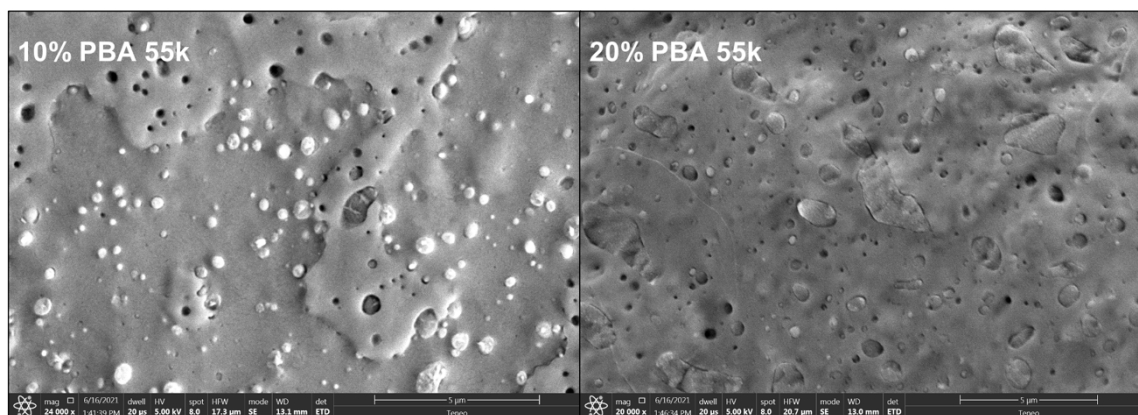


**Figure 2.33:** SEM images showing morphology difference in 10% and 20% blends of PBA 55k with PHBHHx (6% Hx)

loading. This molecular weight is likely different for each polymer as PCL has a molecular weight of only 68,000 but an extremely high elongation of over 800%. This also confirms that 30% and beyond, while still exhibiting droplet formation, is closer to a continuous phase that is expected of 50:50 polymer blends that will have mechanical properties that are largely dependent on the properties of the added polymer. Figure 2.33 also shows a morphology shift when the loading is shifted to 20%. The immiscible droplets lose their spherical shape and begin shifting towards oblong particles that are approaching a co-continuous phase.

PBG and copolymers of PBSG were also investigated for their influence on the mechanical properties of PHBHHx. PBSG [15% glutarate] was made through condensation polymerization with molecular weights of approximately 16,000 daltons and 97,000 daltons. An amorphous PBSG was also made using 70% glutarate with a molecular weight of 21,000 daltons. PBG homopolymer was also made with a molecular weight of 23,000 daltons. Interestingly, PBSG does not follow the same trend in molecular weight as does PBA. The low molecular weight PBSG has an elongation at break of 196% at a 20% loading which is higher than the same polymer at a molecular weight of 97kDa. DSC analysis shows that there is no decrease in crystallinity for the 20% PBSG indicating that the improvement in elongation does not come from a plasticizing effect. The 20% PBSG blend also has a much lower Young's modulus than the 20% blend containing the 97kDa PBSG. For PBG it seems that molecular weight has more to do with the improvement in mechanical properties than chemical structure.

Polymer	3% Elongation (%)	5% Elongation (%)	10% Elongation (%)	20% Elongation (%)
6Hx + 17k PBSG [15G]	62	104	189	196
6Hx + 97k PBSG [15G]	48	117	164	113
6Hx + 21k PBSG [70G]	79	161	172	125
6Hx + 23k PBG	49	107	178	20
Polymer	3% Modulus (Gpa)	5% Modulus (Gpa)	10% Modulus (Gpa)	20% Modulus (Gpa)
6Hx + 17k PBSG [15G]	0.79	0.76	0.67	0.57
6Hx + 97k PBSG [15G]	0.79	0.74	0.71	0.75
6Hx + 21k PBSG [70G]	0.72	0.61	0.65	0.55
6Hx + 23k PBG	0.82	0.72	0.64	0.59

**Table 2.4:** Elongation at break and Young's modulus of varying PBSG blends with PHBHHx (6% Hx)

PBG follows a similar trend to 30k PBA although the impact at lower loadings is not as good as PBA. Interestingly, when loading goes above 20% the elongation at break drastically decreases to 20% due to the low molecular weight and brittle nature of the PBG. It was also found that the crystallinity of the added polymer has a large influence on mechanical properties when molecular weight is lower. PBSG[70G] is a completely amorphous low molecular weight polymer that is very viscous. When loaded at 20wt% there is not the typical reduction in elongation that has been observed with other low molecular weight polymers. In fact, it has better elongation at break (125%) than does the high molecular weight 97k PBSG[15G] which has an elongation of 113% at a 20wt% loading. Blends with PBSG[70] also showed a lower tensile strength as it seems to act as a polymeric plasticizer dispersed within the PHBHHx.

Aging is a problem that is frequently encountered and poorly understood with PHA based materials. A formulation can be extruded, and injection molded into an article and have mechanical properties that are adequate for the desired use, but after a period of time the sample will begin to embrittle and in some cases become completely

unusable. There have been several studies that attempt to elucidate the cause of this problem as well as strategies that prevent or remediate it. Most theories focus on the formation of a rigid amorphous phase due to secondary crystallization in the polymer, and while secondary crystallization is sometimes ruled out as the primary cause of embrittlement due to there being only a 2-3% increase in crystallinity by DSC analysis, the area that is being crystallized is generally not taken in to account.<sup>3</sup> DSC results that show a very small increase in crystallinity that would not normally cause a material to embrittle do not show if the crystallinity is localized within the interlamellar amorphous region, shown in figure 2.34. Depending on the thickness of the amorphous region between crystalline lamellae, small changes in crystallinity could have a large impact on the overall mechanical properties. Although, secondary crystallization leads to a simultaneous aging of the rigid amorphous fraction and they have been cited as being inseparable and indistinguishable from one another and simply seen by the resulting loss in mechanical properties.<sup>27</sup> Rejuvenation is one technique that has been explored

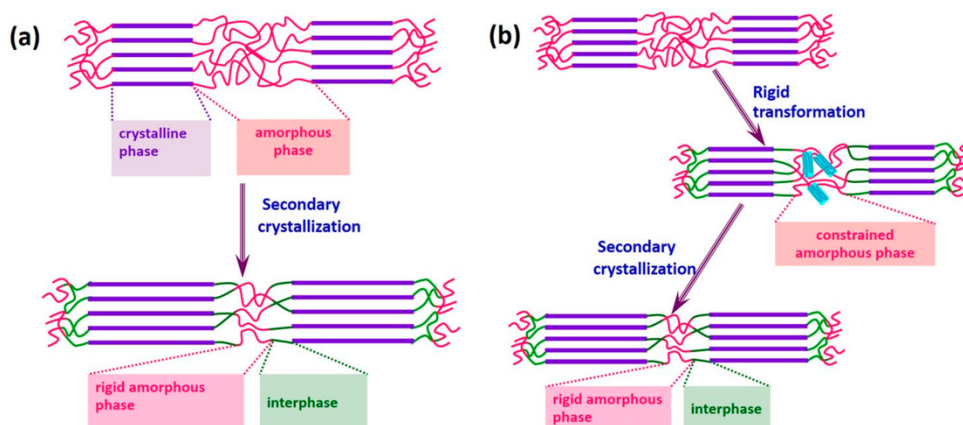


**Figure 2.34:** Schematic of the pathways for aging of PHA. (a) pathway showing development of a rigid amorphous fraction due to secondary crystallization and (b) the pathway showing the development of a constrained amorphous phase that develops a rigid amorphous phase due to secondary crystallization



for PHB. By annealing at 110°C, PHB that was embrittled was able to show recovery of elongation at break even after another subsequent aging process.<sup>4</sup> This showed that from a simple annealing experiment PHB mechanical properties could be retained in a permanent way. Likely this technique of rejuvenation comes from the removal of the rigid amorphous phase that develops close to the interphase between the amorphous and crystalline zones.<sup>28</sup> Other causes could be crystal perfection and lamellar thickening at the annealing temperature. Other techniques for ameliorating the embrittlement problem are the use of various plasticizers.<sup>29, 30</sup> While the rejuvenation technique shows great promise in permanently preventing re-aging of injection molded articles it is not a viable technique for use in an industrial setting as samples would have to be produced and then annealed at high temperatures for extended amounts of time. While this could certainly be done on a small scale it is not viable for large scale production and would not be feasible for many products that are produced as the thermal treatment at high temperature would need to be the last step in the process. The use of plasticizers has had little success in retention of mechanical properties and while they were used with PHBV, this method of preventing embrittlement, while valuable, is not viable for the plasticizers studied. One of the most valuable studies on the aging of PHA's showed that the amount of comonomer included within the copolymer has a drastic effect on the ability of the material to grow brittle over time.<sup>5</sup> When the hexanoate fraction of the copolymer was below 10 mole percent the aging of the polymer films was extreme, yet interestingly when above a threshold value of 10% the copolymers showed much less brittleness after 60 days of aging and also showed only a small loss of elongation over

that amount of time. The increase in the thickness of the interlamellar amorphous region is what is credited for the reduction in embrittlement over time. Although, all the samples undergo secondary crystallization, evidenced by the increase in relative crystallinity during the testing period, those with higher Hx content form thicker amorphous regions that allow for a buffer when it comes to the effect on mechanical properties. The high Hx material accumulates in the interlamellar amorphous zone increasing its thickness with higher Hx content, and this thickness prevents the secondary crystallization from severely constraining the amorphous phase allowing the copolymer to retain its mechanical properties even as it undergoes secondary crystallization. This shows much promise for the use of PHBHHx with varying Hx content for the reduction of embrittlement of the final biodegradable articles. One of the problems with using a copolymer with an Hx content above 10% is the low melting point and the very slow crystallization time, even upon addition of a nucleating agent, which can make it unusable for many applications. What has not been explored is using high Hx content polymers as toughening additives for the reduction of aging in low Hx blends. It would be of much value to develop formulations that have a high modulus and fast crystallization time which are common to low Hx copolymers while retaining the high elongation at break and low embrittlement properties that are available to high Hx content copolymers.

For this study, a blend of PHBHHx (6% Hx) with 10% PBSA was selected as PBSA showed great reactivity and elongation at break using peroxides. PHBHHx (10% Hx) was also used as an additive at a 20% weight loading to see the influence it had on elongation at break after aging. Tensile tests were performed at 24hr, 72hr, and 15 days to see short term and long-term aging of the blends. The mold temperature was also varied from 45°C, which was previously used for all blending, to 70°C as this is close to the optimal crystallization temperature of PHBHHx (6% Hx) under rapid cooling conditions (shown in figure 2.35). It is believed that proper formation of spherulites during the injection molding process can also prevent secondary crystallization from taking place as the samples are stored at room temperature. Interestingly the blends with no high Hx content polymer showed very low aging when the mold was 70°C.

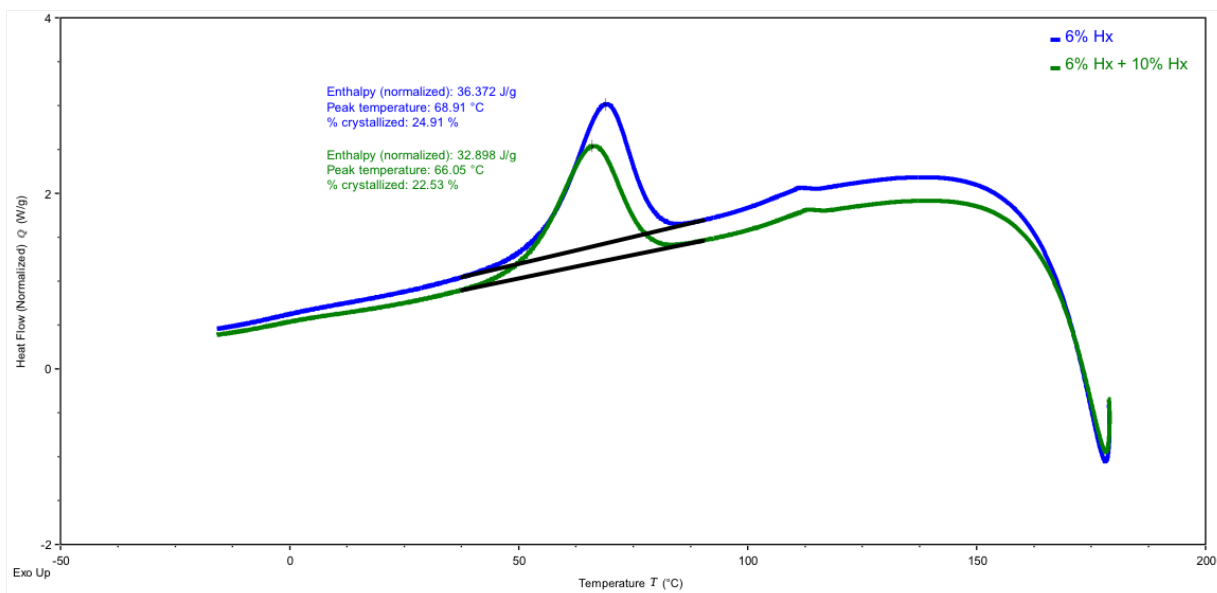


**Figure 2.35:** Crystallization exotherms for rapidly cooled (100°C/min) PHBHHx (6% Hx) alone and blended with PHBHHx (10% Hx)

When the mold is 45°C there is significant aging of nearly 100% in final elongation when comparing to the 72-hour timepoint. The reduction in embrittlement is thought to be due to the optimal crystallization that is allowed to take place when the mold is held at 70°C. At 45 °C the polymer is semi-quenched because the sample is suddenly cooled to 45°C which allows crystallinity to develop but is quickly taken past the optimal temperature for the maximal rate of crystallization to propagate and complete

Blend	24hr Elongation	72hr Elongation	15 day Elongation	Mold temp °C
6Hx + PBSA	156	241	158	45
6Hx + 10Hx + PBSA	231	235	255	45
6Hx + PBSA	303	277	255	70
6Hx + 10Hx + PBSA	371	351	331	70
Blend	24hr Modulus	72hr Modulus	15 day Modulus	Mold temp °C
6Hx + PBSA	0.69	0.79	0.8	45
6Hx + 10Hx + PBSA	0.64	0.75	0.8	45
6Hx + PBSA	0.67	0.69	0.78	70
6Hx + 10Hx + PBSA	0.61	0.67	0.74	70

**Table 2.5:** Young's Modulus and elongation at break after 15 days with blends of PHBHHx (6% Hx), PHBHHx (10% Hx), and PBSA

crystallization cannot take place. Upon storage at room temperature secondary crystallization is able to take place thus causing significant reduction in elongation at break over 15 days. When the mold is held at 70°C optimal crystallization takes place and while some secondary crystallization occurs it is severely reduced allowing for a smaller impact on elongation at break. Interestingly, upon addition of 10Hx copolymer the elongation at break for the 45°C mold sample increases with aging time. Secondary crystallization is taking place as exemplified by the increase in the modulus of the material over time from 0.64 GPa to 0.8 GPa but the increase in crystallinity and formation of a constrained amorphous phase seems to have no negative affect on the elongation.

Noticeably the addition of 10Hx copolymer causes a slight decrease in stiffness at the 24-hour and 72-hour time points. When the mold is held at 70°C there is a lower final modulus of all the materials, especially for those containing the high Hx component. The elongation at break of the 10% Hx blend with a 70°C mold shows some decrease in the elongation at break of 371 to 331%, but even the aged sample shows better peak elongation than any of the other samples at any time point. This indicates that optimal spherulite size and content are formed in the injection molding process to reach these peak elongations, and that secondary crystallization is less severe due to the inclusion of the high Hx copolymer.

Reactive extrusion was also used to see the impact on embrittlement over time using a 10% Hx copolymer. As gel content increases there should be less crystalline material to develop over time as more polymer chains will be crosslinked with the high

Blend	24hr Elongation	72hr Elongation	15 day Elongation	Mold temp
6Hx + 10Hx + PBSA [0.1 LuP]	315	333	317	45°C
6Hx + 10Hx + PBSA [0.1 LuP]	440	452	469	70°C
Blend	24hr Modulus	72hr Modulus	15 day Modulus	Mold temp
6Hx + 10Hx + PBSA [0.1 LuP]	0.69	0.79	0.75	45°C
6Hx + 10Hx + PBSA [0.1 LuP]	0.59	0.69	0.70	70°C

**Table 2.6:** Young's Modulus and elongation at break after 15 days with blends of REX PHBHHx (6% Hx), PHBHHx (10% Hx), and PBSA

Hx component as well as at the interface between the PHA and PBSA components of the blend. Noticeably, the 45°C mold blend follows the same trend as the non-REX sample. The 72-hour time point has the best elongation at break of 333% as well as having the highest Young's modulus of 0.79 in comparison to the 15-day sample of 0.75. While

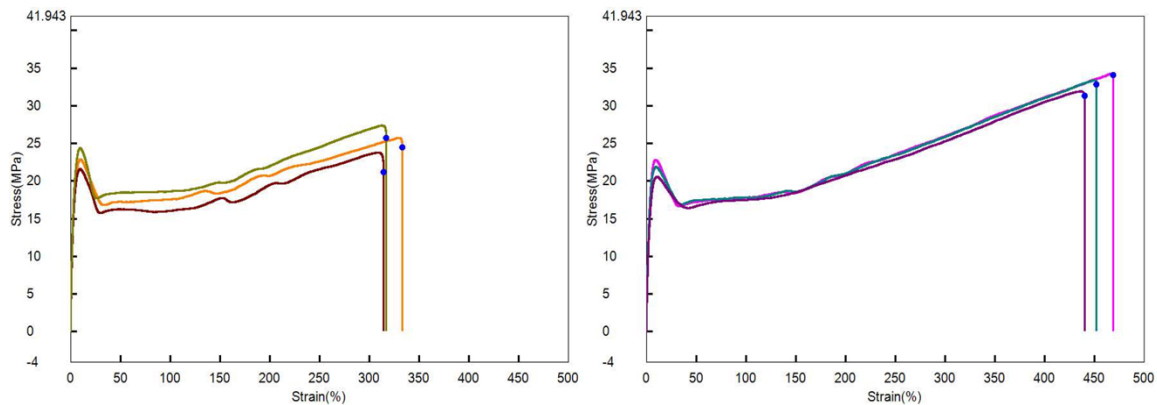


**Figure 2.36:** Stress-Strain curves showing (left) 45° mold and (right) 70°C mold temperatures of REX blends with PHBHHx (6% Hx), PHBHHx (10% Hx), and PBSA

following the same trend in having a peak toughness at 72-hours the elongation at break of the REX formulation is much greater by an average of 80%. Most noticeably the sample injected into a mold held at 70°C has an increasing elongation at break over time and has the highest peak elongation of all the samples tested after 15-days of 469%. Significant strain hardening is also seen as the samples are elongated past 150% (shown in figure 2.36). The addition of a 10% Hx copolymer coupled with a mold temperature of 70°C allows for the most optimal crystallization as the sample is injected as well as

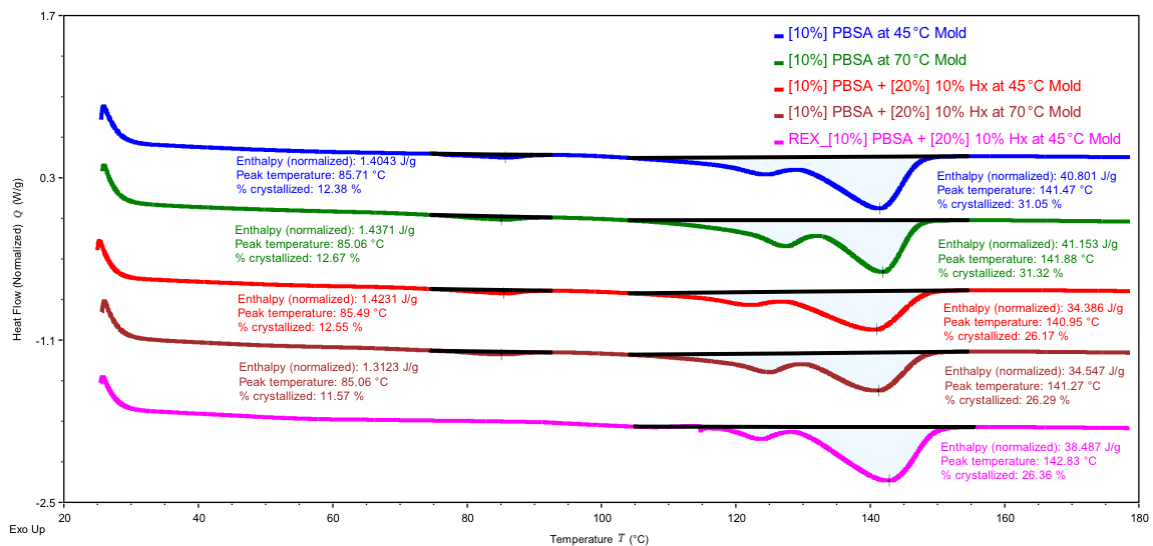


**Figure 2.37:** Melting endotherms for 15-day aged blends with PHBHHx (6% Hx), PHBHHx (10% Hx) and PBSA

preventing significant embrittlement over time. The additional compatibilization induced by the reactive extrusion process allowed for a sample that was extremely tough as well as very ductile. The Young's modulus of these blends is also much lower with a peak stiffness of 0.70 GPa. This is presumably due to the increase in gel fraction that is in the blend due to the high reactivity of the PBSA additive as well as the crosslinking that takes place on a smaller scale within the PHA fraction of the blend. This is clearly shown in figure 2.37 as the crystallinity of the blends reduces when 10Hx is added and the PBSA melting endotherm is no longer visible in the sample that has undergone reactive extrusion. This shows that the majority of the PBSA is no longer semi-crystalline but is highly crosslinked and amorphous within the blend.

A smaller study was repeated using a low molecular weight (30,000 daltons) polybutylene-adipate to see if lower molecular weight polymeric plasticizers could produce elongation at break similar to blends with PBSA. There is a large drop from 222% to 102% with blends of PBA and 6Hx after 15 days, but upon the addition of 10Hx the elongation is able to remain near 200%. This confirms that the 10Hx component does limit the amount of embrittlement that the blends undergo regardless of what semi-crystalline aliphatic polyester additive is used. With the use of Luperox P and TAC, a multifunctional coagent, there is an increase in elongation to 242% after 15 days with a modulus of 0.69. This shows that while low Mw PBA is effective in toughening PHA, especially over shorter time points, the peak elongation is not as good as higher Mw PBSA during reactive extrusion. This is likely due to the gel content being much lower as

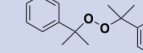
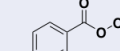
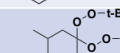
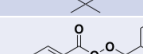

Blend	15 day Elongation (%)	15 day Modulus (Gpa)	Mold temp
[1] 6Hx + PBA	102	0.77	45°C
[2] 6Hx + 10Hx + PBA	198	0.71	45°C
[3] 6Hx + PBA [0.1LuP] [0.2 TAC]	228	0.75	45°C
[4] 6Hx + 10Hx + PBA [0.1LuP] [0.2 TAC]	242	0.69	45°C

**Table 2.7:** Young's modulus and elongation after 15 days of REX blends with PHBHHx (6% Hx), PHBHHx (10% Hx), and PBA

the reactivity of the PBSA additive is much higher based on the torque and pressure increase during extrusion.

To expand the scope of reactive extrusion for PHBHHx, several different radical initiators were also evaluated to see the impact on mechanical properties based on the half-life of the peroxide used. The half-life of each peroxide dictates the extent to which radical decomposition takes place in the duration of the extrusion process. This will also affect the ability of the peroxide to be mixed during extrusion. If the half-life is too short, rapid radical decomposition will take place and localized hot spots will lead to very high crosslinking. If the half-life is slower there is time for adequate mixing as the radicals are generated leading to the development of lightly crosslinked, and highly branched structures within the polymer blends. A range of peroxides were chosen based on half-lives as they related to the extrusion temperature of 150°C. Peroxide concentrations were selected at fixed values of 0.033, 0.067, and 0.10 moles (equivalent to 0.1, 0.2, and 0.3wt% Luperox P). The mold temperature for these blends was fixed at



Peroxide	6 Minute $t_{1/2}$ (°C)	1 Minute $t_{1/2}$ (°C)	Structure
Dicumyl (DCP)	154	171	
Luperox P	150	171	
Luperox 231	126	155	
Benzoyl (BPO)	113	131	
Lauroyl	99	120	

**Table 2.8:** Half-life chart of radical initiators used in REX with PHBHHx (6% Hx)

70°C to reduce bubble formation within the testing area of the tensile bar. This temperature also allows for the most optimal crystallization temperature to give the highest elongation at break. Interestingly, DCP showed the best elongation at break for all concentrations used even though, at 150°C, it has the slowest decomposition time. Lauroyl peroxide (LP) followed a predictable trend as its decomposition is very rapid at 150°C. As the content of LP gets higher the decomposition is so rapid that crosslinking begins taking place even before mixing begins. This gives high areas of localized gel content that causes poor elongation at break at higher loadings. This is also what is seen with benzoyl peroxide which has a reactivity slightly slower than LP but a half-life of approximately 5 seconds at an extrusion temperature of 150°C. Rapid decomposition leading to localized gel contents has also been seen with fast reacting peroxides when blended with PLA.<sup>31</sup> Luperox 231, which has a half-life of one minute at 155°C, seems to have reactivity that is perfectly tuned for the extrusion temperature as it would reach nearly full conversion after 6 minutes within the extruder. But interestingly it does not show the best mechanical properties. This shows that a slow increase in radical generation as well as adequate mixing time, as they are formed, allows for the best

molecular architecture that greatly enhances mechanical properties. It is believed the size of the crosslinked domains would be smaller and more disperse as mixing is allowed to continue during slow radical decomposition rather than large localized hot spots that would occur with more reactive peroxides. One large drawback is that there is not full conversion of the added peroxide at this timescale under these extrusion conditions, but in an industrial setting, a twin screw extruder would have a zone-controlled temperature profile that could be tuned to give optimal mixing during radical evolution while fully converting any remaining peroxide before exiting the die. While DCP has the best mechanical properties under these extrusion conditions, it has a major drawback of producing acetophenone through its decomposition pathway. As a result, all extruded articles have a very strong smell that is not removable and certainly not amendable for food contact applications where PHA is likely to be used. Luperox P provided the best balance between reactivity and mechanical properties.

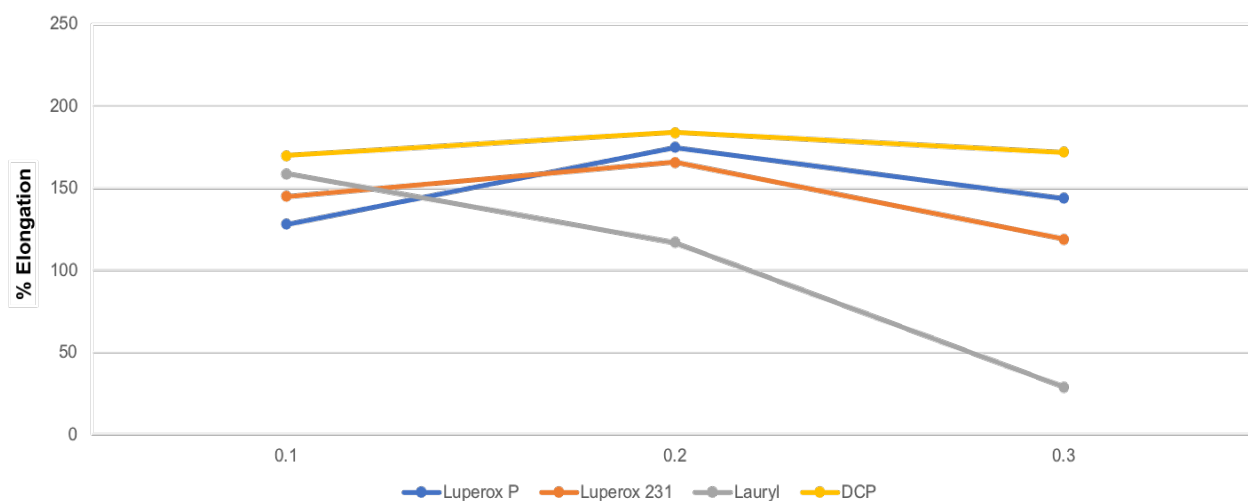


**Figure 2.38:** Elongation at break for increasing peroxide content in blends with PHBHHx (6% Hx) at a mold temperature of 70°C

Multifunctional coagents have been shown to greatly enhance the reactivity of peroxides and have been shown to produce PHB and PLA with enhanced nucleation rates and strain hardening during extensional viscosity experiments.<sup>32-36</sup> Triallyl cyanurate (TAC), pentaerythritol tetraacrylate (PENTA), and hexanediol diacrylate (HDDA) were used at a weight loading of 0.2% to see the impact on the mechanical

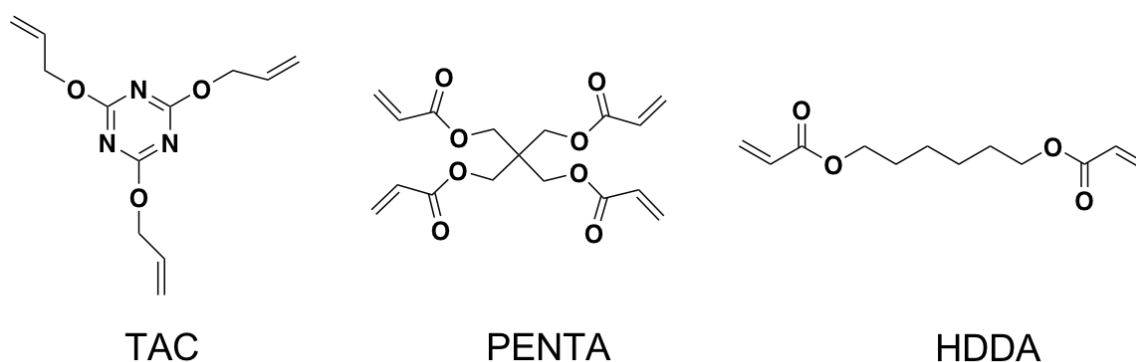


**Figure 2.39:** Chemical structures for crosslinking coagents used in reactive extrusion with Luperox P

properties. Blending was done with 0.1% Luperox P and a mold temperature of 45°C. Higher loadings of peroxide with a coagent can become problematic with other polymers as the extent of crosslinking can get out of control causing the extruder to shut down due to pressure and torque responses. Interestingly, HDDA shows the largest improvement in elongation. One area of concern was the weight loading of the multifunctional coagents. Though they were added based on weight percent rather than fixing a constant mole content, the number of reactive handles is very similar based off the moles of additive used and the equivalents of reactive handles for each coagent. HDDA may lead to more branching and light crosslinking due to it being difunctional rather than tri or tetrafunctional like TAC and PENTA. It also is a low viscosity liquid that

	<b>Elongation at Break (%)</b>
Luperox P	92
Luperox P + Triallyl Cyanurate	101
Luperox P + Pentaerythritol Tetraacrylate	118
Luperox P + Hexanediol Diacrylate	156

**Table 9:** Elongation at break for REX samples using different multifunctional coagents

has good miscibility with PHA leading to better mixing while crosslinking is taking place. PENTA and HDDA both showed better elongation at break than TAC. This could be to the reactivity difference in acrylic and allylic double bonds. Previously it has been reported that PHB has a greater sensitivity to allylic coagents rather than acrylic, but the mechanism was based upon solubility of coagent oligomers in the polymer rather than the reactivity of the additive.<sup>37</sup> The solubility of PENTA and HDDA oligomers also could be higher than TAC. As the oligomers build within the PHA matrix they present more active sites for higher branching and crosslinking efficiency of the PHA matrix.

## **Conclusion**

PHA, while a biologically degradable alternative for many commodity thermoplastics such as polypropylene and polyethylene, has mechanical properties that are not suitable for many applications. Blending with compostable polyesters such as PCL, PBS, PBSA, PBAT, PBA, PBG, and copolymers of PBSEG proved to be an effective method for the improvement in the elongation at break of PHBHHx (6% Hx) without compromising the stiffness of the material. The linear polyester additives were shown to be immiscible and have multiple toughening mechanisms based upon the crystallinity of the added polymer. The mechanical properties in blends of 20% or more were, for the most part, dependent on the final mechanical properties of the additive itself as the immiscible droplets became more densely packed as the domains shifted closer to a co-

continuous phase. PHBHHx embrittlement was also prevented in polymers blends that contained 10Hx copolymers as an additive and had also undergone reactive extrusion. Multifunctional coagents also proved to be an effective method to increase the crosslinking efficiency and increase the toughness of PHBHHx. While PHA has many problems that must be overcome, if it is to be an industrially relevant replacement for plastics such as polypropylene, this chapter has highlighted strategies that allow for mechanical properties to be matched for many polypropylene grades that are currently available and shows much promise for the application of PHA in extruded articles.

## References

1. Noda, I.; Green, P. R.; Satkowski, M. M.; Schechtman, L. A., Preparation and Properties of a Novel Class of Polyhydroxyalkanoate Copolymers. *Biomacromolecules* **2005**, 6 (2), 580-586.
2. Abe, H.; Doi, Y.; Aoki, H.; Akehata, T., Solid-State Structures and Enzymatic Degradabilities for Melt-Crystallized Films of Copolymers of (R)-3-Hydroxybutyric Acid with Different Hydroxyalkanoic Acids. *Macromolecules* **1998**, 31 (6), 1791-1797.
3. Srubar, W. V.; Wright, Z. C.; Tsui, A.; Michel, A. T.; Billington, S. L.; Frank, C. W., Characterizing the effects of ambient aging on the mechanical and physical properties of two commercially available bacterial thermoplastics. *Polymer Degradation and Stability* **2012**, 97 (10), 1922-1929.
4. de Koning, G. J. M.; Lemstra, P. J., Crystallization phenomena in bacterial poly[(R)-3-hydroxybutyrate]: 2. Embrittlement and rejuvenation. *Polymer* **1993**, 34 (19), 4089-4094.
5. Alata, H.; Aoyama, T.; Inoue, Y., Effect of Aging on the Mechanical Properties of Poly(3-hydroxybutyrate-co-3-hydroxyhexanoate). *Macromolecules* **2007**, 40 (13), 4546-4551.
6. Zytner, P.; Wu, F.; Misra, M.; Mohanty, A. K., Toughening of Biodegradable Poly(3-hydroxybutyrate-co-3-hydroxyvalerate)/Poly( $\epsilon$ -caprolactone) Blends by In Situ Reactive Compatibilization. *ACS Omega* **2020**, 5 (25), 14900-14910.
7. Ma, P.; Hristova-Bogaerds, D. G.; Lemstra, P. J.; Zhang, Y.; Wang, S., Toughening of PHBV/PBS and PHB/PBS Blends via In situ Compatibilization Using Dicumyl Peroxide

- as a Free-Radical Grafting Initiator. *Macromolecular Materials and Engineering* **2012**, 297 (5), 402-410.
8. Larsson, M.; Markbo, O.; Jannasch, P., Melt processability and thermomechanical properties of blends based on polyhydroxyalkanoates and poly(butylene adipate-co-terephthalate). *RSC Advances* **2016**, 6 (50), 44354-44363.
  9. Gassner, F.; Owen, A. J., Physical properties of poly( $\beta$ -hydroxybutyrate)-poly( $\epsilon$ -caprolactone) blends. *Polymer* **1994**, 35 (10), 2233-2236.
  10. Hopmann, C.; Adamy, M.; Cohnen, A., Front Matter. In *Reactive Extrusion*, 2017; pp i-xvii.
  11. Jacobsen, S.; Fritz, H. G.; Degée, P.; Dubois, P.; Jérôme, R., Single-step reactive extrusion of PLLA in a corotating twin-screw extruder promoted by 2-ethylhexanoic acid tin(II) salt and triphenylphosphine. *Polymer* **2000**, 41 (9), 3395-3403.
  12. Balakrishnan, S.; Krishnan, M.; Narayan, R.; Dubois, P., Three-arm poly ( $\epsilon$ -caprolactone) by extrusion polymerization. *Polymer Engineering & Science* **2006**, 46 (3), 235-240.
  13. Shi, D.; Yang, J.; Yao, Z.; Wang, Y.; Huang, H.; Jing, W.; Yin, J.; Costa, G., Functionalization of isotactic polypropylene with maleic anhydride by reactive extrusion: mechanism of melt grafting. *Polymer* **2001**, 42 (13), 5549-5557.
  14. Mani, R.; Bhattacharya, M.; Tang, J., Functionalization of polyesters with maleic anhydride by reactive extrusion. *Journal of Polymer Science Part A: Polymer Chemistry* **1999**, 37 (11), 1693-1702.

15. Ku Marsilla, K. I.; Verbeek, C. J. R., Modification of poly(lactic acid) using itaconic anhydride by reactive extrusion. *European Polymer Journal* **2015**, *67*, 213-223.
16. Burton, E.-L.; Woodhead, M.; Coates, P.; Gough, T., Reactive grafting of glycidyl methacrylate onto polypropylene. *Journal of Applied Polymer Science* **2010**, *117* (5), 2707-2714.
17. Graebbling, D., Synthesis of Branched Polypropylene by a Reactive Extrusion Process. *Macromolecules* **2002**, *35* (12), 4602-4610.
18. Chen, C.-Q.; Ke, D.-M.; Zheng, T.-T.; He, G.-J.; Cao, X.-W.; Liao, X., An Ultraviolet-Induced Reactive Extrusion To Control Chain Scission and Long-Chain Branching Reactions of Polylactide. *Industrial & Engineering Chemistry Research* **2016**, *55* (3), 597-605.
19. Barham, P. J.; Keller, A.; Otun, E. L.; Holmes, P. A., Crystallization and morphology of a bacterial thermoplastic: poly-3-hydroxybutyrate. *Journal of Materials Science* **1984**, *19* (9), 2781-2794.
20. Han, C. C.; Shi, W.; Jin, J., Morphology and Crystallization of Crystalline/Amorphous Polymer Blends. In *Encyclopedia of Polymers and Composites*, Palsule, S., Ed. Springer Berlin Heidelberg: Berlin, Heidelberg, 2021; pp 1-19.
21. Bucknall, C. B., The micromechanics of rubber toughening. *Makromolekulare Chemie. Macromolecular Symposia* **1988**, *20-21* (1), 425-439.
22. Liang, J. Z.; Li, R. K. Y., Rubber toughening in polypropylene: A review. *Journal of Applied Polymer Science* **2000**, *77* (2), 409-417.



23. Castillo, L. A.; Barbosa, S. E.; Capiati, N. J., Influence of talc morphology on the mechanical properties of talc filled polypropylene. *Journal of Polymer Research* **2013**, 20 (5), 152.
24. Fujiyama, M.; Wakino, T., Crystal orientation in injection molding of talc-filled polypropylene. *Journal of Applied Polymer Science* **1991**, 42 (1), 9-20.
25. Zhou, Y.; Rangari, V.; Mahfuz, H.; Jeelani, S.; Mallick, P. K., Experimental study on thermal and mechanical behavior of polypropylene, talc/polypropylene and polypropylene/clay nanocomposites. *Materials Science and Engineering: A* **2005**, 402 (1), 109-117.
26. Wang, J.; Wu, Y.; Sun, X.; Yuan, Q.; Yan, Y., De Novo Biosynthesis of Glutarate via  $\alpha$ -Keto Acid Carbon Chain Extension and Decarboxylation Pathway in *Escherichia coli*. *ACS Synthetic Biology* **2017**, 6 (10), 1922-1930.
27. Righetti, M. C.; Aliotta, L.; Mallegni, N.; Gazzano, M.; Passaglia, E.; Cinelli, P.; Lazzeri, A., Constrained Amorphous Interphase and Mechanical Properties of Poly(3-Hydroxybutyrate-co-3-Hydroxyvalerate). *Frontiers in Chemistry* **2019**, 7 (790).
28. Righetti, M. C.; Tombari, E.; Di Lorenzo, M. L., The Role of the Crystallization Temperature on the Nanophase Structure Evolution of Poly[(R)-3-hydroxybutyrate]. *The Journal of Physical Chemistry B* **2013**, 117 (40), 12303-12311.
29. Barbosa, J. L.; Perin, G. B.; Felisberti, M. I., Plasticization of Poly(3-hydroxybutyrate-co-3-hydroxyvalerate) with an Oligomeric Polyester: Miscibility and Effect of the Microstructure and Plasticizer Distribution on Thermal and Mechanical Properties. *ACS Omega* **2021**, 6 (4), 3278-3290.

30. Umemura, R. T.; Felisberti, M. I., Modeling of the properties of plasticized poly(3-hydroxybutyrate) as a function of aging time and plasticizer content. *Materials Today Communications* **2020**, 25, 101439.
31. Takamura, M.; Nakamura, T.; Takahashi, T.; Koyama, K., Effect of type of peroxide on cross-linking of poly(l-lactide). *Polymer Degradation and Stability* **2008**, 93 (10), 1909-1916.
32. Tiwary, P.; Kontopoulou, M., Rheological characterization of long-chain branched poly(lactide) prepared by reactive extrusion in the presence of allylic and acrylic coagents. *Journal of Rheology* **2018**, 62 (5), 1071-1082.
33. Tiwary, P.; Kontopoulou, M., Tuning the Rheological, Thermal, and Solid-State Properties of Branched PLA by Free-Radical-Mediated Reactive Extrusion. *ACS Sustainable Chemistry & Engineering* **2018**, 6 (2), 2197-2206.
34. Nerkar, M.; Ramsay, J. A.; Ramsay, B. A.; Kontopoulou, M., Dramatic Improvements in Strain Hardening and Crystallization Kinetics of PLA by Simple Reactive Modification in the Melt State. *Macromolecular Materials and Engineering* **2014**, 299 (12), 1419-1424.
35. Nerkar, M.; Ramsay, J. A.; Ramsay, B. A.; Vasileiou, A. A.; Kontopoulou, M., Improvements in the melt and solid-state properties of poly(lactic acid), poly-3-hydroxyoctanoate and their blends through reactive modification. *Polymer* **2015**, 64, 51-61.

36. Kolahchi, A. R.; Kontopoulou, M., Chain extended poly(3-hydroxybutyrate) with improved rheological properties and thermal stability, through reactive modification in the melt state. *Polymer Degradation and Stability* **2015**, *121*, 222-229.
37. Dawidziuk, K.; Simmons, H.; Kontopoulou, M.; Parent, J. S., Peroxide-initiated graft modification of thermoplastic BioPolyesters: Introduction of long-chain branching. *Polymer* **2018**, *158*, 254-261.

## CHAPTER 3

### MELT MISCIBLE AND HETEROGENEOUS NUCLEATING AGENTS FOR ENHANCED CRYSTALLIZATION RATES OF POLYHYDROXYBUTYRATE-CO-HYDROXYHEXANOATE<sup>1</sup>

---

<sup>1</sup> Crane, Grant. To be submitted to Journal of Polymer Chemistry Part A

## ABSTRACT

With mismanaged plastic waste rising and deleterious effects being discovered for macro and micro plastics within the environment, there is a growing need for completely biodegradable alternatives for commercial thermoplastics.

Polyhydroxyalkanoates show much promise for their biodegradation in a variety of natural environments as well as having mechanical properties that can be tuned for the desired end use of the produced articles such as bottles, cup lids, straws, cutlery, and fiber. Although PHA can be tuned to meet the mechanical property needs for some current commodity plastics such as polypropylene, it has several drawbacks on the processing side that, if unsolved, prevent it from being applicable in many extrusion applications. PHAs are notorious for their slow nucleation rate after complete melting, and for most applications, rapid nucleation is needed for processing to be feasible. The addition of nucleating agents can greatly increase the rate of crystallization for PHA. Typically, heterogeneous nucleating agents such as talc or boron nitride have been used but for many applications, such as fiber production, melt miscible nucleating agents are desirable to prevent clogging of processing equipment during production.

## Introduction

PHAs have a crystallinity range from completely amorphous to highly crystalline (65%) depending on the copolymer type or percent within the polymer backbone, and the mechanical properties of the copolymer are largely dictated by the final crystallinity of the polymer after processing. But while crystallinity is important for final mechanical properties, nucleation and crystallization rate are paramount when it comes to fast processing of PHA copolymers. While PHAs show much promise for end-of-life degradation as well as having mechanical properties that can be tuned for replacing many commodity thermoplastics, they are notorious for their slow nucleation rate after complete melting. It can be very useful to increase the ductility by increasing the amount of comonomer, such as hydroxy hexanoate, within the copolymer. Unfortunately, as the amount of comonomer is increased the nucleation and crystallization rates decrease as a result. If the amount of comonomer is increased too high the polymer can remain amorphous for long periods of time and prevent rapid processing for extrusion applications.<sup>1</sup> The toughness of PHAs can also be affected if a nucleating agent is not used. The spherulites formed from a melt cooled sample of PHA are quite large and lead to a material that is very stiff and brittle after crystallization has taken place from a tacky, flexible amorphous material. The use of a nucleating agent can greatly enhance the ability of PHA to crystallize during melt processing as well as affecting the size and morphology of PHA spherulites.

Heterogeneous nucleating agents can act as a foreign surface within the polymer melt that can change the crystallization rate, spherulite size, and density.

Heterogeneous agents should not dissolve at the processing temperature of the polymer and should have a favorable interaction that allows for an optimal orientation of the polymer that is similar to its crystal structure.<sup>2</sup> It is also thought to be helpful if the lattice parameters of the added nucleating agent are similar to the crystal structure of PHB. The unit cell of PHB, although having slight variations between studies, is orthorhombic with two antiparallel chains per cell and with lattice parameters of  $a = 5.76 \text{ \AA}$ ,  $b = 13.20 \text{ \AA}$ , and  $c = 5.96 \text{ \AA}$  (fiber axis).<sup>3, 4</sup> Increasing the comonomer content of hydroxy hexanoate generally causes a slight increase in the lattice parameters.<sup>5, 6</sup> Several heterogeneous nucleating agents have been studied with various PHAs including ammonia chloride,<sup>7</sup> boron nitride,<sup>8, 9</sup> talc,<sup>9, 10</sup> cyclodextrin,<sup>11</sup> cyanuric acid,<sup>12</sup> and orotic acid.<sup>13-15</sup> While many of these, such as orotic acid, have been specifically proven to nucleate PHBHHx there has been little work done on optimizing the type and amount of nucleating agent to produce a blend of polymers for injection molding applications. More specifically the size of the nucleating agents is frequently ignored which can drastically impact spherulite size and crystallization rate and density. Investigating metal salts of orotic acid to see the influence of changing the crystal structure on the impact in nucleation using PHBHHx would be of much benefit. Also finding an optimal nucleating agent particle size for efficient crystallization would be beneficial in designing a formulation for injection molding applications.

There are some applications, such as melt blown fibers, where the use of a heterogeneous nucleating agent becomes prohibitive. Melt blown fibers are produced by extrusion processing coupled with a blast of hot air that produces fibers that are in

the 1-10 $\mu$ m range in diameter.<sup>16, 17</sup> Taking a heterogeneous nucleating agent down to this size, while possible, is frequently labor and cost prohibitive and even particles around 1 $\mu$ m can impact the final properties of the fiber or cause a breakage of the fiber during processing. For applications such as this where an insoluble particle is not amendable for the processing conditions, melt miscible nucleating agents can be of great benefit. Melt miscible agents either dissolve or melt within the polymer during processing and either recrystallize as discrete crystals or self-assemble into three dimensional networks as the polymer is cooled giving a surface upon which polymer nucleation can initiate. Oxalamides have been studied for self-assembling mechanisms for nucleation of isotactic polypropylene (iPP) but have only lightly been studied for their applicability in PHAs.<sup>18-21</sup> Pentaerythritol was found to be a good nucleating agent for PHB and PHBHHx copolymers, and while previously thought to be a heterogeneous nucleating agent, this work highlights its melt-miscible nucleation mechanism. Pentaerythritol is unique in that the morphology of its recrystallization within the PHA melt is controlled via concentration to give dendritic or particle morphology that influences the subsequent nucleation of the PHA at its crystallization temperature.

PHBHHx copolymers are made up of a distribution of different comonomer concentrations that give a weighted average for molar percent of the hydroxy hexanoate repeat unit that is typically reported from nuclear magnetic resonance (NMR) or gas chromatography (GC). Depending on the culture media, bacteria type, fermentation conditions, and feed ratio a complex polymeric mixture can be obtained of homopolymers and copolymers.<sup>22</sup> This can greatly affect the final crystalline properties



of the produced copolymer, and while PHBHHx is typically treated as a random copolymer of narrow monomeric distribution this is not always the case. Fractionation using mixtures of chloroform and heptane is the typical method to determine the distribution of copolymers within the matrix<sup>23, 24</sup> but is not industrially viable and comonomer distribution is typically ignored. One area that this distribution can become important is the nucleation and crystallization of the copolymer. Typically, a PHBHHx copolymer will have a small fraction of pure PHB homopolymer. While the amount of pure homopolymer can vary, it can be so small as to not have any visible transition by DSC analysis, yet it can greatly influence the ability of the material to nucleate. For the 6Hx material used in this study, when heated above 180°C in DSC analysis the sample will no longer nucleate without an added nucleating agent. PHB has a crystal structure that is nearly identical to the copolymer allowing for optimal nucleation. This can be of great advantage when designing a nucleation package for any PHBHHx formulations as inherent or added PHB can be used to initiate nucleation at a higher temperature than the typical T<sub>c</sub> for the random copolymer.

## **Materials and Methods**

### *Materials*

Polyhydroxybutyrate-co-hydroxyhexanoate (6% Hx) with a molecular weight of 930,000 daltons and 1,000,000 daltons and polyhydroxybutyrate-co-hydroxyhexanoate (11% Hx) were produced through fermentation and both were supplied by the New Materials Institute at the University of Georgia. Talc (3CA) was purchased from Imerys and had a d<sub>50</sub> of 1 µm. Nano boron nitride (<150nm), Pentaerythritol, anhydrous orotic

acid, orotic acid, and cyanuric acid were purchased from Sigma Aldrich. Zinc orotate, potassium orotate, calcium orotate, Magnesium orotate, and zinc glycinate were purchased from bulk supplements and used as received. Diethyl oxalate was purchased from oakwood chemical and used without further purification. Hexane diamine and dodecyl amine were purchased from TCI chemicals and used without further purification.

#### *Extrusion procedure*

6.5g total formulation was added to a Haake minilab II corotating twin screw extruder using a manual feeder. Melt blending was carried out at 150°C, 100 rpm screw speed, and a cycle time of 6 minutes to ensure adequate blending or peroxide decomposition. Type V tensile bars were injection molded from a 150°C cylinder using 660 bar of pressure for 5 seconds into a 45°C mold. Tensile bars were aged for at least 24 hours prior to testing.

#### *Mechanical and Thermal Properties*

Tensile testing was done using a Shimadzu AGS-X tensile tester. Type V dogbones were tested at a strain rate of 5 mm/min. Thermal properties were measured using a TA Discovery 250 differential scanning calorimeter. Samples were taken from the bottom portion of the tensile bar to best represent the crystallinity of the injection molded sample. Samples were heated at 10°C/min to 180°C and cooled at 10°C/min to -20°C. For samples where nucleation was being examined the first heating run was done to 200°C to melt any inherent PHB found in the sample. Melting enthalpy, melting peak

temperature, and percent crystallinity were calculated using TA software on the instrument. Percent crystallinity was calculated using equation 1.

$$X_c (\%) = \frac{\Delta H}{\Delta H_c * \phi} * 100 \quad (1)$$

Where  $\Delta H$  is the specific enthalpy of fusion of the sample taken from the peak area on the program software (J/g), and  $\Delta H_c$  is the enthalpy of fusion for a 100% crystalline material (assumed to be 146 J/g for PHB)<sup>25</sup> and  $\phi$  is the weight fraction of the polymer. Crystallization was observed using a Nikon polarized optical microscope. Small samples were cut from the extruded article and were heated to a peak temperature of 180°C or 200°C and cooled at a rate of 20°C/min to observe blend morphology, crystallization and spherulite morphology.

#### *Synthesis of N<sup>1</sup>,N<sup>1'</sup>-(hexane-1,6-diyl)bis(N<sup>2</sup>-undecyloxalamide)*

2.0g (17.2 mmol) of hexane diamine was dissolved in 20ml of THF and slowly dripped through an addition funnel into a 250 ml round bottom flask containing excess diethyl oxalate. The reaction was stirred overnight, and the white precipitate was filtered and rinsed twice with THF. 2.244g (7.78 mmol) of product was refluxed in chloroform with 4.56g (24.5 mmol) of dodecylamine for 16 hours. The white precipitate was filtered and washed several times with hot chloroform to remove any unreacted starting material.

#### *Particle Size analysis*

Particle size for added nucleating agents was taken using a Malvern Mastersizer 3000 with a hydro MV automated dispersion attachment. DI water was used as the

mobile phase and all measurements were taken in triplicate. For samples that had water solubility an Aero S dry powder dispersion unit was used

## Results and Discussion

Optimal spherulite formation is paramount for the development of PHBHHx with good mechanical properties. If the polymer is completely melted and allowed to cool and crystallize the formed spherulites are very large as the rate of crystallization is much

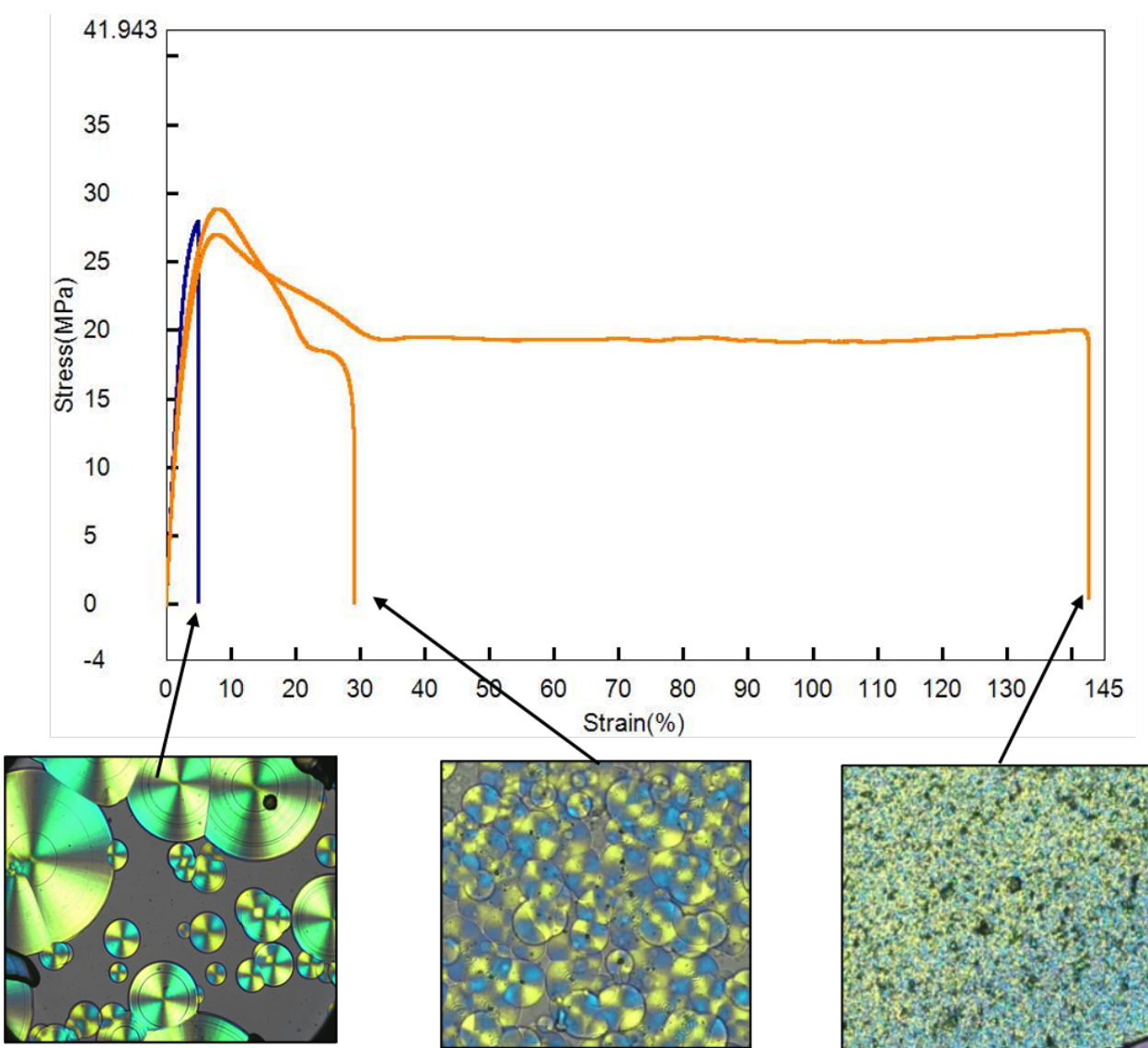


**Figure 3.1:** Representative image for the effect of spherulite size and crystallization conditions on the final mechanical properties of PHBHHx (6% Hx)

faster than the rate of nucleation events. The large spherulites have much fewer polymer tie chains at the interface of the spherulites leading to a stiff polymer that is very brittle as shown in figure 3.1. Adding a nucleating agent increases the rate of nucleation events leading to much smaller and more uniform spherulite formation and reducing the size of the added nucleating agent allows for the formation of very small spherulites produces a polymer that is more ductile while retaining much of the stiffness. Optimal crystallization for mechanical properties is achieved by matching the peak crystallization temperature to the rate of cooling during the processing step to achieve the most rapid crystallization. Increasing the peak crystallization temperature as well as decreasing the time to complete crystallization allows for a polymer that not only can be processed rapidly but also has good final mechanical properties for the extruded article. Without an added or inherent nucleating agent there can be no optimizing of the processing conditions due to the extraordinarily slow crystallization of PHA. Cyanuric acid (CA) was explored as a heterogeneous nucleating agent for PHBHHx

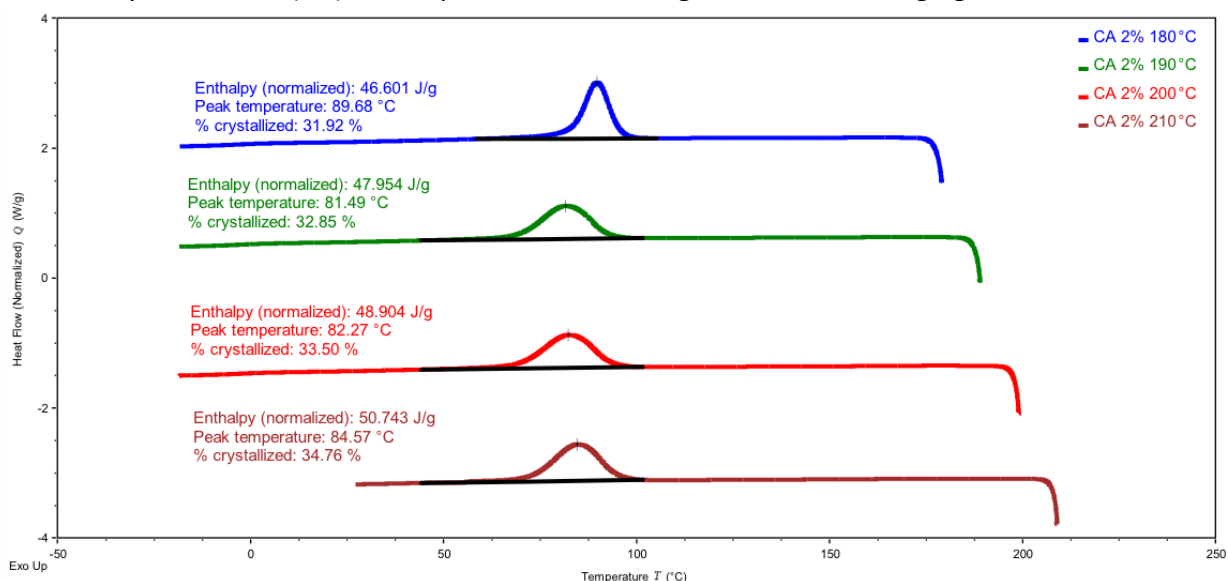


**Figure 3.2:** Crystallization exotherms of 2% cyanuric acid blended with PHBHHx (6% Hx)

(6% Hx). Initially 2% of CA was melt blended with PHA to see the peak crystallization temperature of the nucleated PHA. When heating to 180°C the crystallization exotherm is narrow and at a higher temperature of 90°C due to the inherent PHB within the copolymer acting as the primary nucleating agent. Upon heating to 190°C and higher the inherent PHB is melted and all nucleation activity is coming from the un-melted crystals of cyanuric acid. There is a decrease of nearly 10°C in peak crystallization temperature as the CA becomes the primary nucleating agent in the blend. Upon heating to a peak temperature of 210°C, the crystallization temperature increases by 5°C. This is thought to be due to thermal degradation of the polymer under these conditions allowing for more rapid alignment of the polymer chains leading to a faster crystallization event. This phenomenon is noticed in nearly all of the nucleating agents that are used within this study. The broadness of the crystallization exotherms shows that the rate of crystallization is rather slow for CA, and after analysis using POM the slow rate is

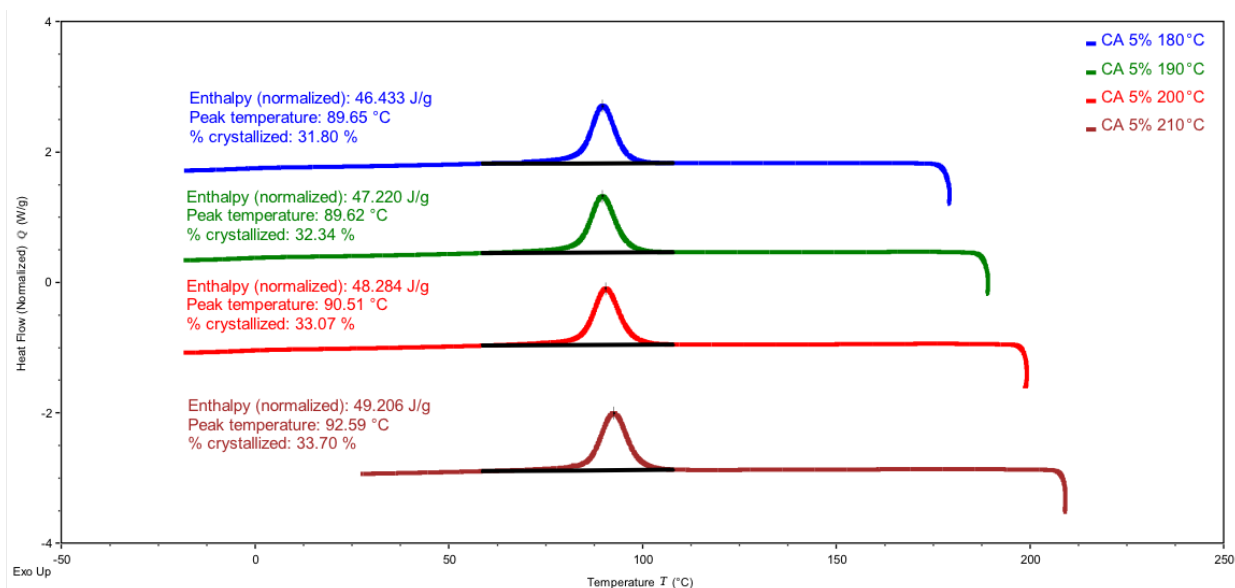


**Figure 3.3:** Crystallization exotherms of 5% cyanuric acid blended with PHBHHx (6% Hx)

attributed to the large particle size of the CA crystals. While efficiently nucleating the PHBHHx on the crystal surface of CA the dispersed nucleating agent, at a loading of 2%, does not allow for rapid crystallization as the spherulite density is rather small and crystallization proceeds from large particle to large particle. Upon increasing the loading of CA to 5% the density of nucleating agent is greatly increased and allows for much better crystallization temperatures to be achieved. The peak crystallization temperature of a 5% CA blend stays at 90°C even upon heating above the melting point of PHB. It is also evident that the peak shape becomes narrower than the 2% blend. This is due to the increased number of CA particles acting as a surface to initiate the crystallization of PHBHHx. More nucleation events and having particles more tightly packed within the PHA matrix allows for faster coverage and impingement of propagating spherulites and more rapid crystallization. One of the concerns for a blend using 5% is the amount of

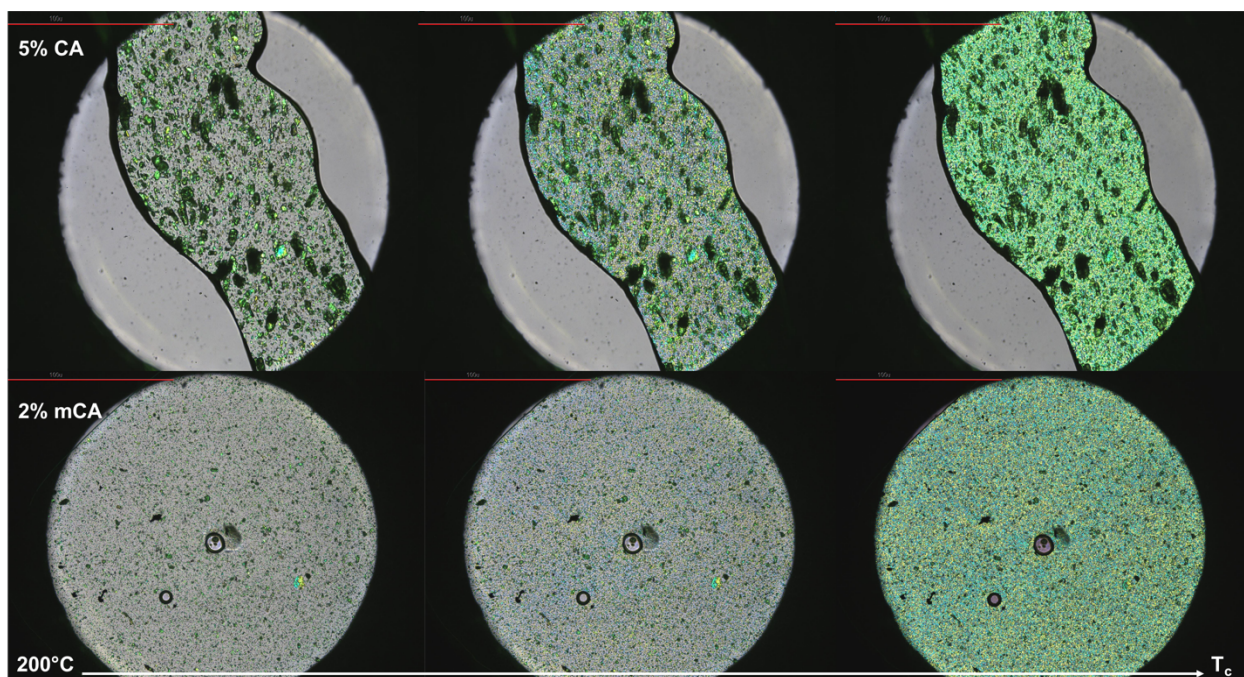


**Figure 3.4:** Polarized microscopy images comparing blends of 5% and milled 2% cyanuric acid with PHBHHx (6% Hx)

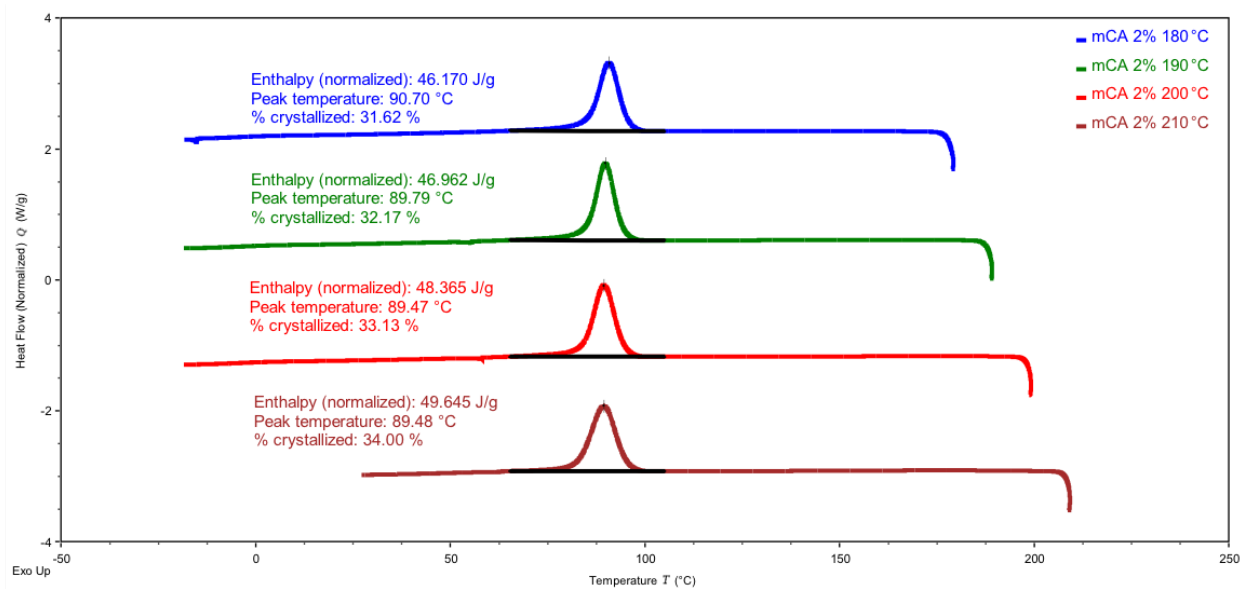


**Figure 3.5:** Crystallization exotherms for 2% milled cyanuric acid blended with PHBHHx (6% Hx)

nucleating agent that is added to the polymer. As can be seen in figure 3.4, 5% CA is quite a lot of large particles within the PHA matrix. Not only does this increase the cost of the blend it can attribute to a roughness of the extruded article as well as affect the mechanical properties as it behaves similar to a filler. Reducing the particle size allows for the addition of much less nucleating agent to achieve the same efficiency seen at a 5% loading. Milling the large granular crystals of cyanuric acid down to a particle size of  $d_{90} = 263\mu\text{m}$  allowed for good nucleation using a 2% loading. The peak crystallization temperature increases above what was seen for the 5% blend and the peak becomes narrower as the rate of crystallization completion increases due to the small and well dispersed particles of mCA within the PHA matrix.

Orotic acid was also evaluated as a heterogeneous nucleating agent for PHBHHx. Orotic acid has a crystal structure with lattice parameters of  $a=9.561$ ,  $b=7.261$ , and  $c=5.895\text{ \AA}$  which were originally put forward in 1973<sup>26</sup> and were updated in 2008 to



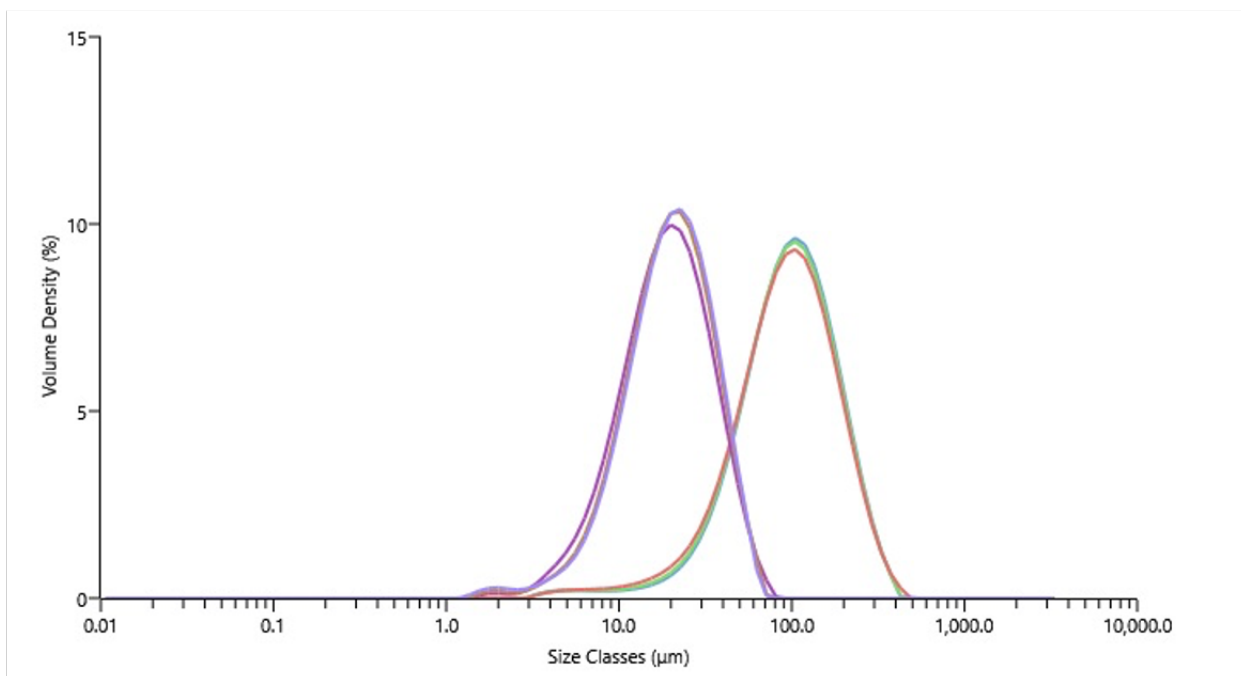


**Figure 3.6:** Particle size analysis of orotic acid monohydrate before and after milling

$a = 5.898$ ,  $b = 6.929$ ,  $c = 9.591 \text{ \AA}$ .<sup>27</sup> It has been previously reported that there is lattice matching between the  $(100)_{\text{PHB}} // (001)_{\text{OA}}$  planes which shows an excellent lattice match between the cell parameters of  $a_{\text{OA}}$  and  $c_{\text{PHB}}$ .<sup>14</sup> Not only is there good lattice matching between orotic acid and the PHB unit cell, there is also the ability to form hydrogen bonding between the two surfaces allowing for good interaction and alignment of PHB chains to initiate crystallization. While the epitaxial mechanism of orotic acid is already known there has been little attention paid to the particle size of the orotic acid used as well as its performance in an extrusion environment rather than in a solvent cast or hot-pressed film. The particle size was taken before and after milling and was reduced from  $d_{x(90)} = 207 \mu\text{m}$  to  $d_{x(90)} = 40 \mu\text{m}$ . Interestingly the particle size of  $207 \mu\text{m}$  still has efficient nucleation at a 2% loading. When the particle size is reduced the loading is able to be decreased to 0.5% with a very small impact on peak crystallization temperature. It has

been reported that anhydrous orotic acid had a slightly better impact on crystallization for PHBV (5% V) in comparison to the monohydrate version. This was attributed to the layer of bound water inhibiting the interaction between the nucleating agent and the hydrophobic polymer.<sup>15</sup> This study also controlled for particle size difference between the two agents through SEM analysis, but nucleation was studied using cast films from chloroform and not through melt blending in an extrusion environment. Monohydrate and anhydrous versions of orotic acid were compared through extrusion blending using PHBHHx (6Hx). For blends of 2% the monohydrate version showed slightly higher peak crystallizing temperatures even when heated above the melting point of PHB although the difference is nearly negligible. This different result can be attributed to the preparation method of the samples. In extrusion any bound water on orotic acid will be removed due to the extended time at 150°C under high shear. In the study with PHBV there was observation of dehydration of the monohydrate observed through DSC analysis at 144°C. For melt extruded samples any endotherm from the removal of water would be hidden behind the melting peak of the PHBHHx. There is also a solubility difference between the two forms of orotic acid in chloroform. When extruded samples of 2% OAm were dissolved in chloroform and passed through a 0.22µm PTFE syringe the

NA	180°C T <sub>c</sub>	190°C T <sub>c</sub>	200°C T <sub>c</sub>	210°C T <sub>c</sub>	180°C X <sub>c</sub> (%)	190°C X <sub>c</sub> (%)	200°C X <sub>c</sub> (%)	210°C X <sub>c</sub> (%)
OAm 0.5%	90.7	89.8	89.5	89.5	31.9	32.4	34.0	34.2
OAm 1%	92.4	92.5	93.4	94.8	34.5	34.9	35.8	36.8
OAm 2%	92.1	92.1	93.5	95.5	35.0	35.6	36.2	37.3
Milled OAm 2%	92.8	93.1	94.4	96.6	33.9	34.5	34.5	36.2
OAa 2%	91.8	91.6	92.7	94.5	36.2	36.7	37.6	38.7

**Table 3.1:** Peak crystallization temperature and relative crystallinity for various forms of orotic acid heated to different peak temperatures

samples were still able to nucleate even after heating above the melting temperature of PHB although the rate was reduced. Under POM imaging there was no observation of orotic acid crystals within the melt likely indicating that a small amount of OA was solubilized in the chloroform and upon drying precipitated as nano sized particles that cannot be seen under the magnification of the POM microscope. When just orotic acid was treated to the same dissolution and filtration step a thin white film was evident upon evaporation of the solvent. This indicates that if there is any difference in solubility between OAm and OAa the final particle concentration could skew the DSC results in favor of whichever agent has more solubility in chloroform. While there is no significant difference between the two nucleating agents for PHBHHx (6Hx) the resulting removal of water during the extrusion process can lead to a greater reduction in molecular weight through hydrolysis. Great care is taken to thoroughly dry the polymer before extrusion to prevent this and adding in a nucleating agent that contains bound water must be taken into consideration. Anhydrous orotic acid allows for control of this although the cost difference between the two could make the benefit of retaining molecular weight negligible.

Metal salts of orotic acid were also evaluated as potential nucleating agents for PHBHHx. It would be of much interest to see how changing the crystal structure of orotic acid by complexing with metals such as potassium, zinc, magnesium and calcium affects the ability of the chemical to nucleate PHA. Figure 3.7 shows that zinc and magnesium orotate both have a bimodal distribution and similar particle sizes while

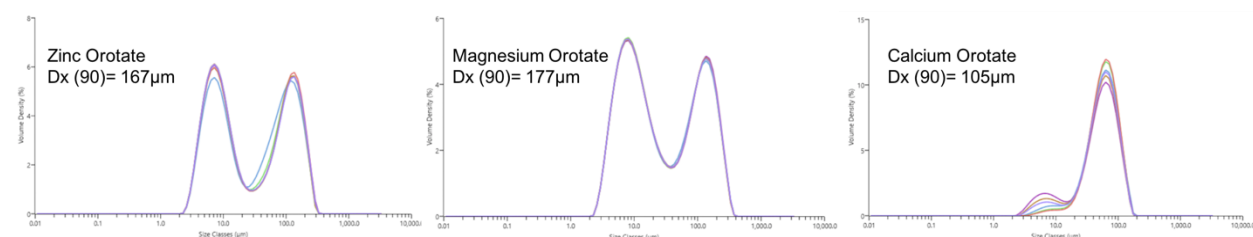


**Figure 3.7:** Particle size analysis for zinc, magnesium, and calcium orotate

calcium orotate has a much smaller  $dx(90)$  of 105  $\mu\text{m}$  and more uniform distribution of particle sizes. Potassium orotate has a reported crystal structure of  $a = 6.842$ ,  $b = 12.535$ ,  $c = 7.685$ .<sup>28</sup> Although there is good lattice matching of the  $b_{\text{KOA}}$  with  $b_{\text{PHB}}$  the ability to nucleate is very poor with peak crystallization values around 70°C after melting the inherent PHB within the sample. Interestingly, Zinc orotate showed the best ability to nucleate PHA. The peak crystallization temperatures stay around 89°C when heating to a temperature above the melting point of PHB. This is very close to the peak temperatures of orotic acid monohydrate. One of the difficulties in determining the effect of crystal structure on nucleation efficiency are the wide variety of structures that each metal orotate can have. There are two crystal structures both featuring the same  $\text{Zn}(\text{Or})(\text{H}_2\text{O})_4$  units<sup>29, 30</sup> as well as another unique crystal structure for the bis-orotate version  $\text{Zn}(\text{Or})_2 \cdot 8\text{H}_2\text{O}$ .<sup>31</sup> The structure is dependent on the method of preparation and mono-orotates can predominate even when stoichiometric ratios should favor bis-orotates. Direct synthesis and crystal structure characterization would be of much value when comparing nucleating efficiency for PHA and would provide a direct method for changing the crystal structure while retaining the same chemical compound. For this study, zinc orotate was analyzed under POM to see if there was dissolution of the zinc

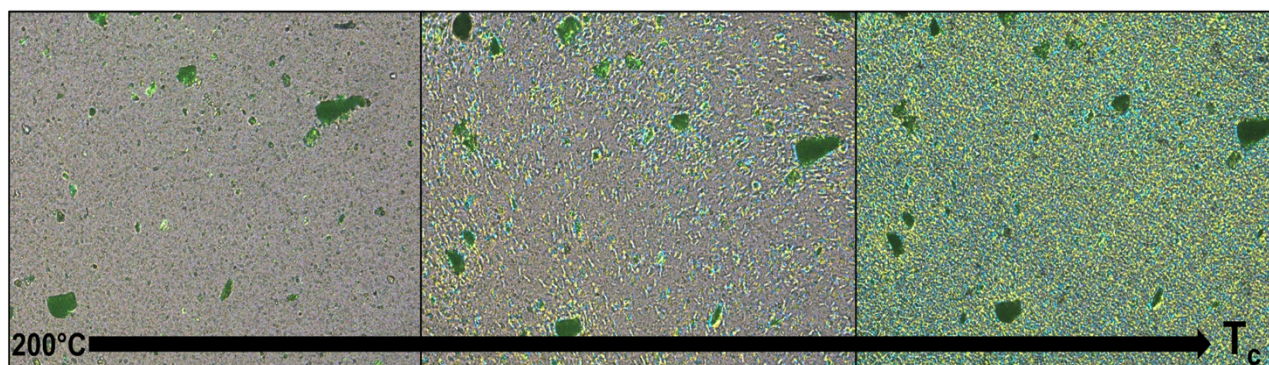


**Figure 3.8:** Polarized optical microscopy images of Zinc orotate blends with PHBHHx (6% Hx) cooling from a melt temperature of 200°C

salt allowing for precipitation of orotic acid from the melt. As can be seen in figure 3.8, the zinc orotate crystals have a broad size distribution of particles, and they remain intact within the melted PHA and initiate crystallization very clearly from the surface of each crystal which indicates an epitaxial mechanism from the crystal structure of zinc orotate. Calcium and magnesium orotate both show poorer nucleation than the zinc salt with calcium having the lowest peak crystallization temperatures. This shows that lattice matching, while not the sole dictator of whether a heterogeneous material can nucleate PHBHHx, is extremely important as each of these metal orotates have a different crystal structure but possess the same hydrogen bonding capabilities.

NA	180°C T <sub>c</sub>	190°C T <sub>c</sub>	200°C T <sub>c</sub>	210°C T <sub>c</sub>	180°C X <sub>c</sub> (%)	190°C X <sub>c</sub> (%)	200°C X <sub>c</sub> (%)	210°C X <sub>c</sub> (%)
OAm 0.5%	90.7	89.8	89.5	89.5	31.9	32.4	34.0	34.2
OAm 1%	92.4	92.5	93.4	94.8	34.5	34.9	35.8	36.8
OAm 2%	92.1	92.1	93.5	95.5	35.0	35.6	36.2	37.3
Milled OAm 2%	92.8	93.1	94.4	96.6	33.9	34.5	34.5	36.2
OAa 2%	91.8	91.6	92.7	94.5	36.2	36.7	37.6	38.7
KOA 2%	89.8	67.7	69.7	72.2	34.8	32.5	33.3	34.2
ZnOA 2%	90.3	88.6	88.8	89.3	29.0	31.5	33.4	35.0

**Table 3.2:** Peak crystallization temperature and relative crystallinity for various forms of orotic acid heated to different peak temperatures

To expand on the hydrogen bonding capabilities of amino acid-like structures with the thermal stability of zinc salts, zinc glycinate was investigated as a potential nucleating agent for PHBHx. Typically, amino acids, such as glycine, would cause severe degradation of PHA during the extrusion processing step. And while N-acetyl glycine possesses good hydrogen bonding potential and less reactivity than glycine, it dissolves within the PHA at elevated temperatures thus not providing a surface upon which nucleation can happen. Complexing the amino acid glycine with zinc gives the thermal stability and insolubility needed to be a heterogeneous nucleating agent as well as retaining hydrogen bonding potential for good interfacial activity between the polymer and crystal surface. Most recently the crystal lattice of zinc glycinate is reported as having parameters of  $a=15.006$ ,  $b=10.420$ , and  $c=9.772$  Å.<sup>32</sup> Although, there are many varying structures put forward in the literature.<sup>33-35</sup> Figure 3.9 shows that zinc glycinate Dx(90)=292µm is able to nucleate PHBHx although when heating to temperatures

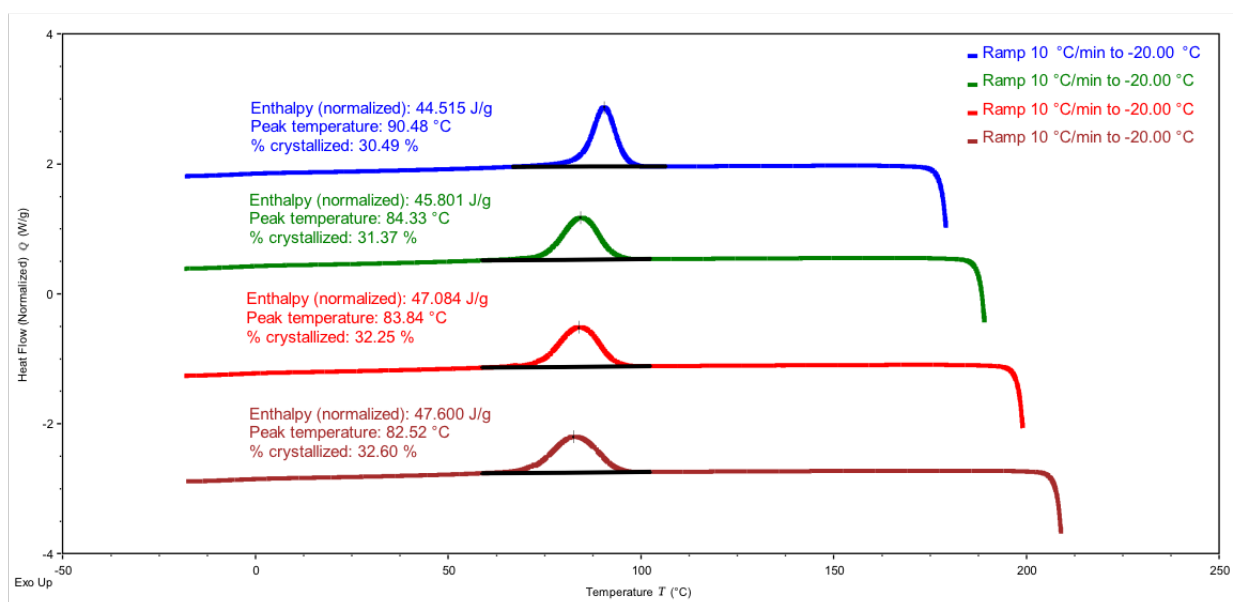


**Figure 3.9:** Crystallization exotherms of zinc glycinate blended with PHBHx (6% Hx)

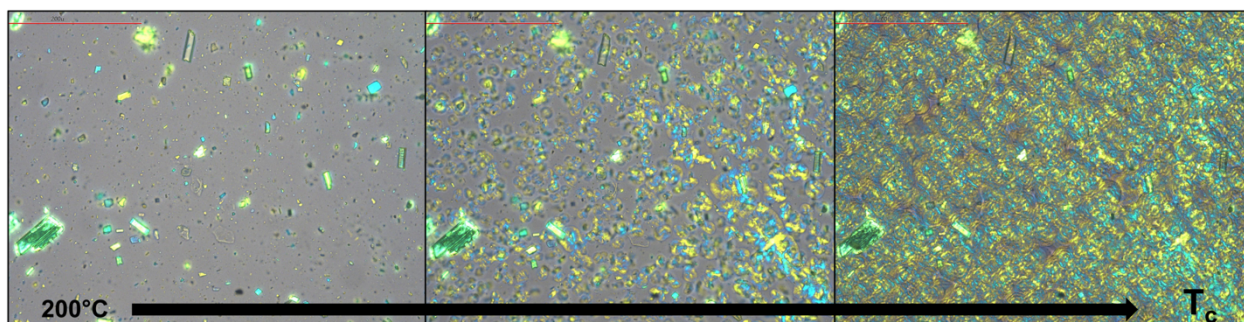


**Figure 3.10:** Polarized optical microscope images of epitaxial nucleation of PHBHHx (6% Hx) on the surface of zinc glycinate crystals

above the melting point of PHB the exothermic transitions shift down and begin to broaden. POM imaging was done to preclude the possibility that the compound is dissolving within the PHA and causing degradation that would result in a lowering and broadening of the crystallization exotherm. As can be seen in figure 3.10, zinc glycinate seems to be completely insoluble within the PHA matrix and stays as discrete crystals at elevated temperatures that allow for epitaxial nucleation upon cooling. This shows that there is potential for coordination complexes using zinc with a wide variety of amino acids as well as other amine bearing compounds for their potential use as nucleating agent for PHA.

Boron nitride has been reported as an excellent nucleating agent for PHB with decreasing efficiency as the amount of hydroxy hexanoate comonomer is increased.<sup>8,9,13</sup> And while for many studies compounds such as orotic acid were shown to be better at nucleating PHBHHx there was no control of the particle size of the added nucleating agents. In this study nano particles of boron nitride (<150nm) were used to see the efficiency of this nucleating agent at low weight percent loadings. As shown in figure 3.11, nucleation of the PHBHHx is achieved with as little as 0.1% addition of nBN



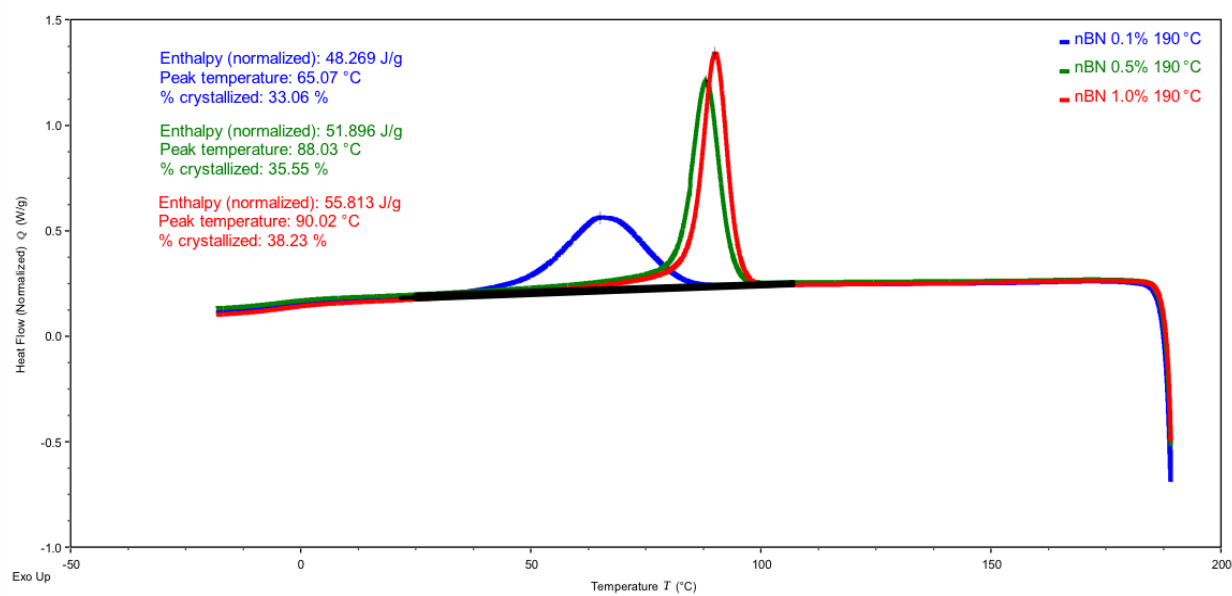


**Figure 3.11:** Crystallization exotherms showing 0.1, 0.5, and 1.0% nano boron nitride blends with PHBHHx (6% Hx)

although the peak crystallization is 65°C and the peak is very broad indicating a slow completion of crystallization. This is likely from agglomeration of the nanoparticles within the PHA causing the effective particle size to increase. Rapid nucleation is achieved with 0.5 and 1.0% addition of nBN. This shows that orotic acid has better

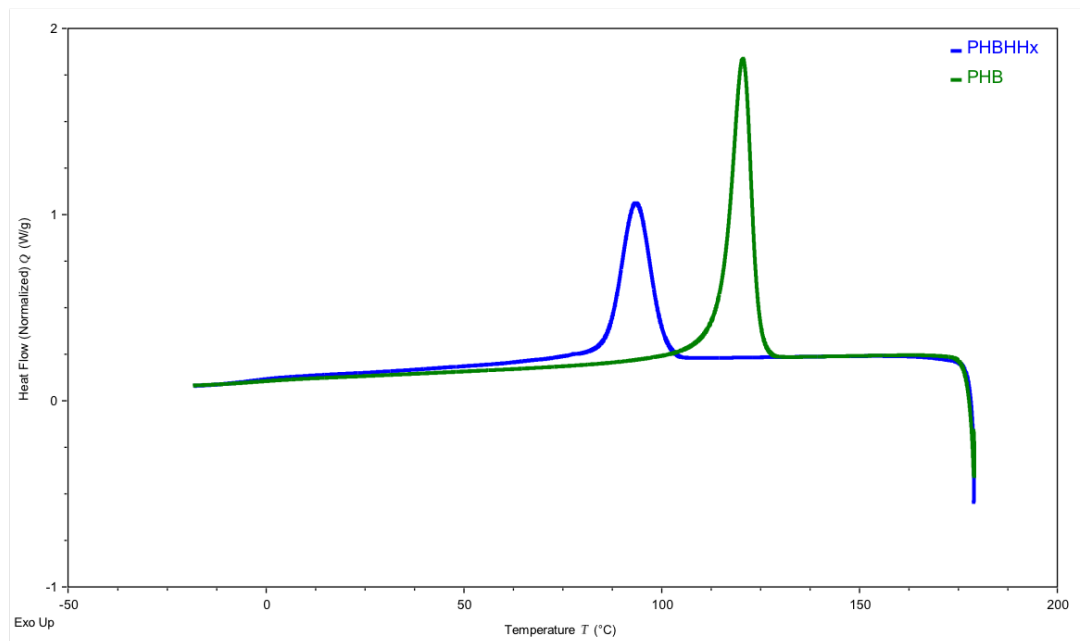


**Figure 3.12:** Crystallization exotherms comparing the peak crystallization temperature of a PHB homopolymer against a PHBHHx (6% Hx) copolymer



nucleation even with particle sizes 200x that of nBN. PHB homopolymer, due to its high stereoregularity and monomer purity, has a higher melting temperature and very rapid nucleation at an elevated temperature above the crystallization temperature of PHBHHx copolymers (shown in figure 3.12). It can be used as a nucleating agent for PHA copolymers like what is seen when heating to 180°C on DSC analysis. The un-melted PHB crystals have a perfect lattice match for the epitaxial nucleation of the PHBHHx copolymer. The effectiveness of this nucleation pathway can be expanded by adding a nucleating agent such as boron nitride to selectively nucleate the pure PHB homopolymer at an elevated temperature thus generating a cascade of more surfaces for the PHBHHx copolymer to nucleate on. When 10% of a PHB homopolymer is added to a blend with PHBHHx and nBN at a 1% weight loading the peak crystallization temperature is raised by nearly 10°C. The first crystallization peak appears broad and to have low crystallinity. This is due to the PHB fraction remaining mostly un-melted at a

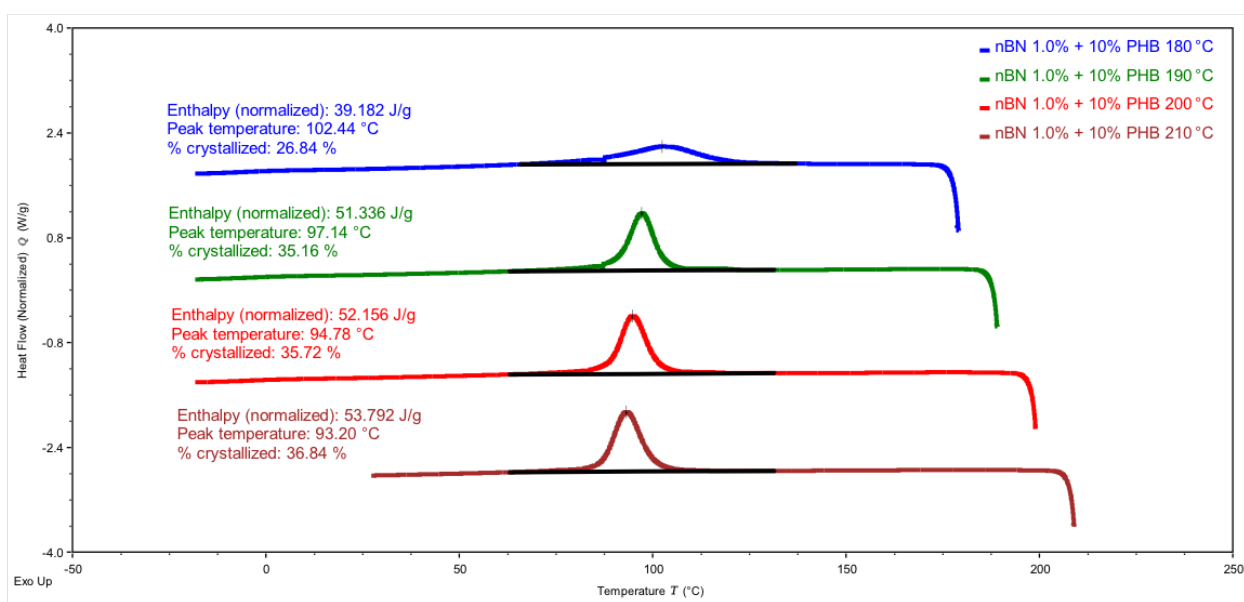


**Figure 3.13:** Crystallization exotherms of 1% nano boron nitride blended with a PHB homopolymer and a PHBHHx (6% Hx) copolymer

peak temperature of 180°C and subsequently recrystallizing on itself upon cooling. As the blend is heated to 190°C the PHB is completely melted and co-crystallizes with the PHBHHx copolymer giving one sharp exothermic transition at 97°C. POM images also corroborate that the PHB remains largely un-melted and acts as a cascading nucleating agent in the blend. Isothermal DSC experiments were also performed to show the difference in rate between nBN with and without PHB homopolymer as a co-nucleating agent. Milled cyanuric acid was also used to compare efficiency of nucleation against nBN. The large exotherm seen before the time point of 20 minutes is due to the rapid cooling to the hold temperature of 105°C. As can be seen in figure 3.14, nBN at 1% shows slow nucleation at the holding temperature but the rate of crystallization is greatly increased by the addition of 10% homopolymer. Surprisingly milled cyanuric acid shows nearly as rapid nucleation as does the nano particles of boron nitride. The isothermal study highlights the difference in crystallization time that adding PHB

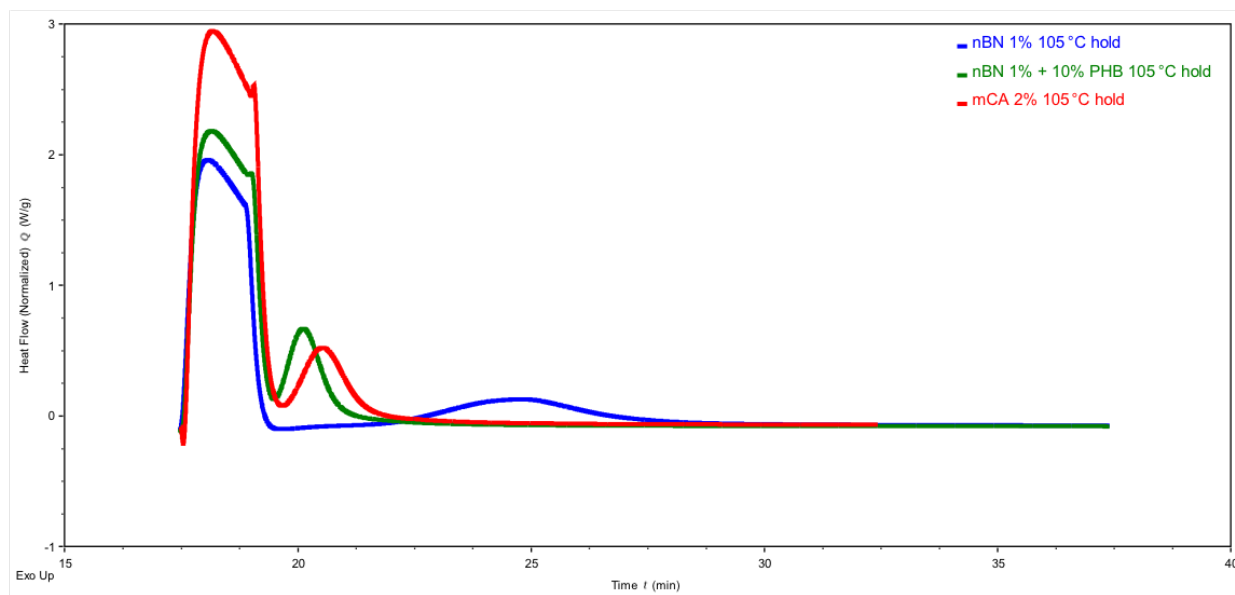


**Figure 3.14:** Isothermal crystallization at a hold temperature of 105°C comparing nano boron nitride with and without PHB homopolymer against milled cyanuric acid.

homopolymer can achieve and also shows the value of using a cascading strategy for rapidly nucleating an extruded article during fast processing conditions. This study also indicates the boron nitride is a better nucleating agent for PHB than PHBHHx copolymers.

While pentaerythritol (PE) has been described in the patent literature as a crystal nucleating agent for PHA<sup>36</sup> there has been little work done on describing the mechanism associated with its nucleation. The unit cell of Pentaerythritol is reported as tetragonal with lattice parameters of  $a=6.10$  and  $c=8.73$  Å.<sup>37</sup> This shows good lattice matching between  $a_{PE}$  and  $c_{PHB}$  which shows a viable method of epitaxial nucleation.

Pentaerythritol is also unique in that it undergoes a phase change at a temperature of 185.5°C where PE shifts from the tetragonal  $\alpha$  phase to the orientationally disordered face-centered cubic  $\gamma$  phase.<sup>38</sup> Understanding the influence on crystal structure change on the nucleation ability as well as the nucleation mechanism can broaden the scope of this nucleating agent as well as the viability of PHA for multiple applications. Initially PHBHHx was blended with pentaerythritol at a weight loading of 2% and DSC and POM analysis were used to see thermal transitions and spherulite morphology. Interestingly, as can be seen in figure 3.15 there are two exotherms seen on the cooling curve indicating multiple crystallization events taking place. The first exotherm is constant at a temperature of 133°C while the main crystallization exotherm of PHA is seen between 87-93°C. Upon melting there is also an endothermic transition observed around 157°C. This indicates that pentaerythritol is undergoing a dissolution/recrystallization event at much lower temperatures than its phase transition temperature and melting point.

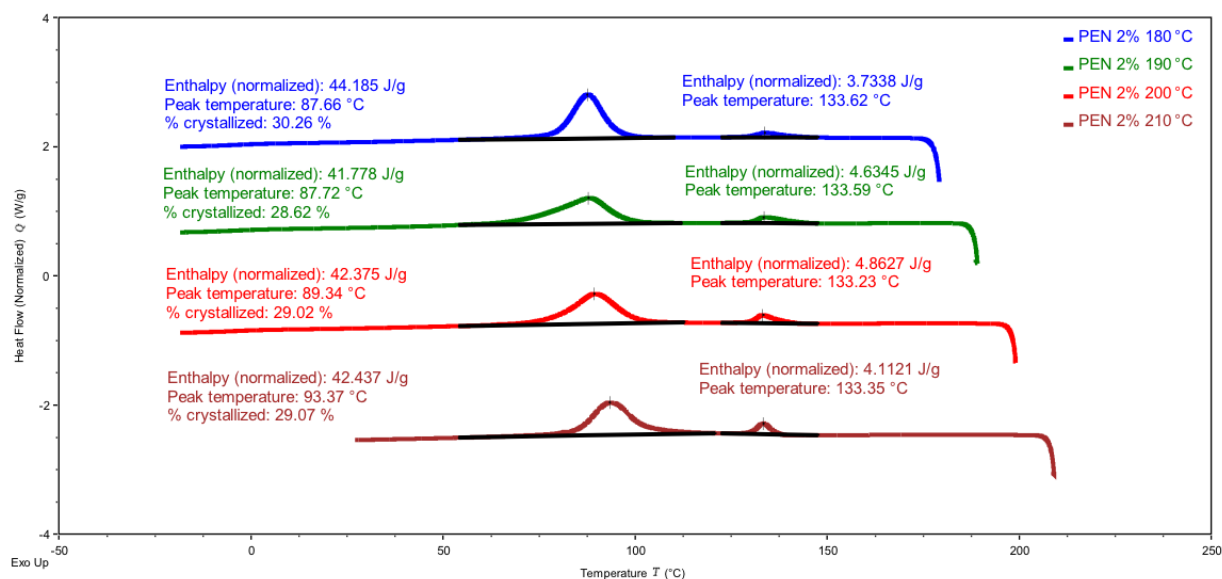


**Figure 3.15:** Crystallization exotherms for blends of 2% pentaerythritol with PHBHHx (6% Hx)

Addition of other polyhydric alcohols to blends of PE has been shown to drastically shift its solid-state transition with temperature shifts depending on the molar ratio and type of alcohol blended.<sup>39</sup> DSC analysis does not show if interaction with the polymer matrix causes a phase shift in the polymer that leads to dissolution although it does indicate that crystal dissolution is happening of the added PE with subsequent recrystallization at a temperature above the crystallization of the PHA component. POM analysis was used to further probe the dissolution and recrystallization of the added PE. Figure 3.16 shows that most of the PE dissolves within the polymer matrix with some larger particles not showing complete dissolution at the holding time of 1 minute at the elevated temperature. The larger particles act as seeds for a feather-like recrystallization of PE that is subsequently followed by crystallization of the PHA on the generated surfaces of PE. This also explains why the first crystallization exotherm at 133°C is smaller than the subsequent heatings as not all of the PE is melted when heating to a peak temperature

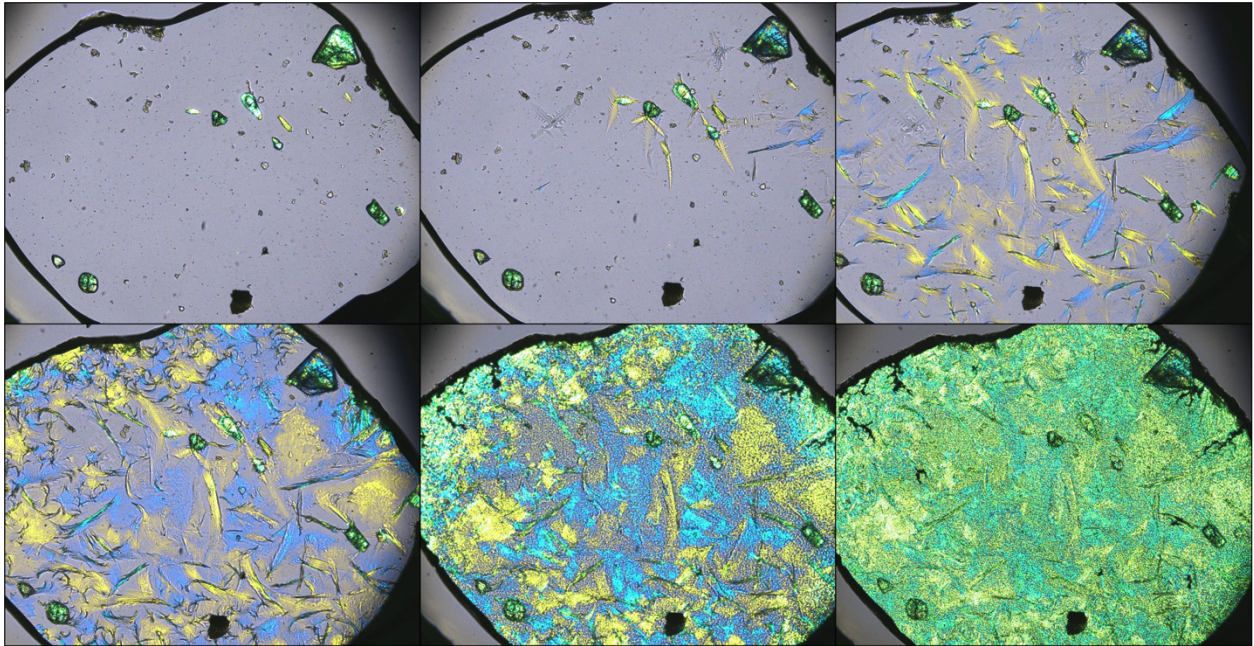


**Figure 3.16:** Polarized optical microscope images showing the feather-like recrystallization of PE in blends with PHBHHx (6% Hx) followed by epitaxial nucleation of the polymer component

of 180°C. Upon further heating complete dissolution of the PE component is achieved resulting in more being recrystallized upon subsequent cooling. This is the first indication that PE is a melt miscible nucleating agent for PHA. To see the impact of crystal structure phase change on the solubility and nucleating efficiency of pentaerythritol within the PHA it was annealed overnight to induce a shift to the  $\gamma$  phase. Observation of the shift was evident through POM imaging as well as the physical transformation of the PE in the annealing dish. Before annealing PE was a white granular particle and after 24 hours of annealing at 200°C the physical structure had shifted to large snowflake-like structures. This was then ground into a fine white powder and blended with the PHA. At an extrusion temperature of 150°C there was no evidence of enhanced dissolution of the  $\gamma$  PE indicating that a phase shift in crystal structure is not responsible for the dissolution of the PE within the PHA. In fact, there was no difference

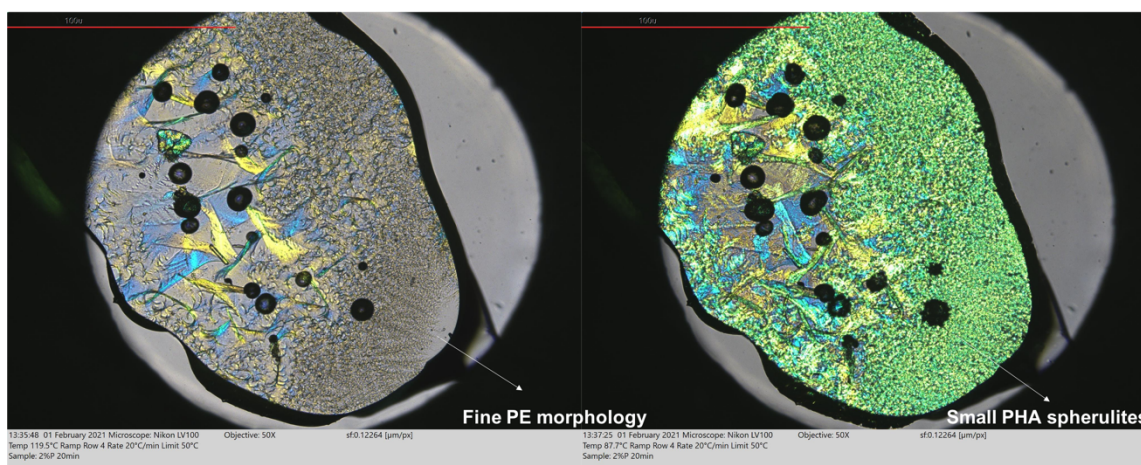


**Figure 3.17:** POM images showing that decreasing concentration of PE allows for finer fibrillar formation that leads to much smaller PHA spherulites.

in the annealed sample in comparison to unannealed PE indicating that upon recrystallization it is likely in its  $\alpha$  phase once again. This shows that PE is a melt miscible nucleating agent above a processing temperature of 155°C which for many PHAs is optimal. It was noticed that heating to higher temperatures caused the dissolved PE to spread out within the polymer matrix and recrystallize as thin tendrils rather than large feather like structures (shown in figure 3.17). This is desirable as the large crystalline PE structures could compromise the mechanical integrity of the extruded article as well as having reduced nucleation efficiency due to the decreased surface area of the larger feather-like 3D structure in comparison to the thin tendril-like structure. To try and dictate the PE superstructure formed different concentrations of PE were added. The extrusion temperature was also varied to completely melt the PE during processing to see the impact on the recrystallization structure as the PE would be melt dispersed within the polymer rather than having localized areas of high concentration as the crystals melt during the DSC and POM analysis. Decreasing the weight loading of PE to 1% caused a shift in the recrystallization temperature from 133°C to just above the



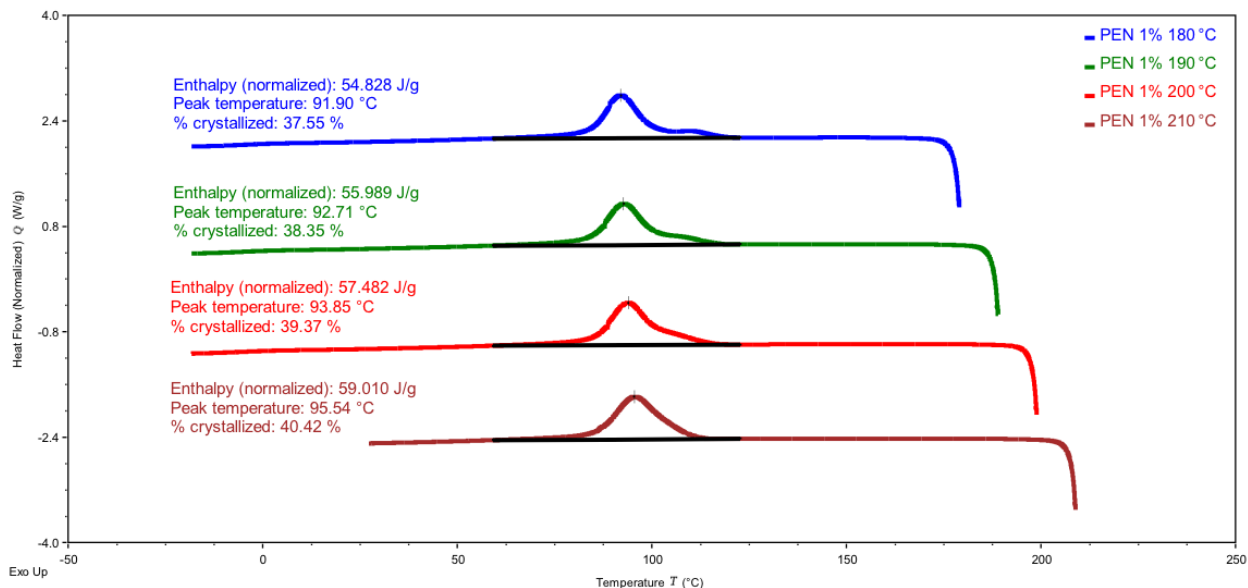


**Figure 3.18:** Crystallization exotherms for 1% pentaerythritol blended with PHBHHx (6% Hx)

recrystallization temperature of PHA evidenced by a shoulder just above the crystallization temperature of PHA in figure 3.18. As the concentration of PE is lowered within the blend the ability to recrystallize is diminished, Yet the peak crystallization temperature of the PHA component of the blend is slightly higher than the blend with

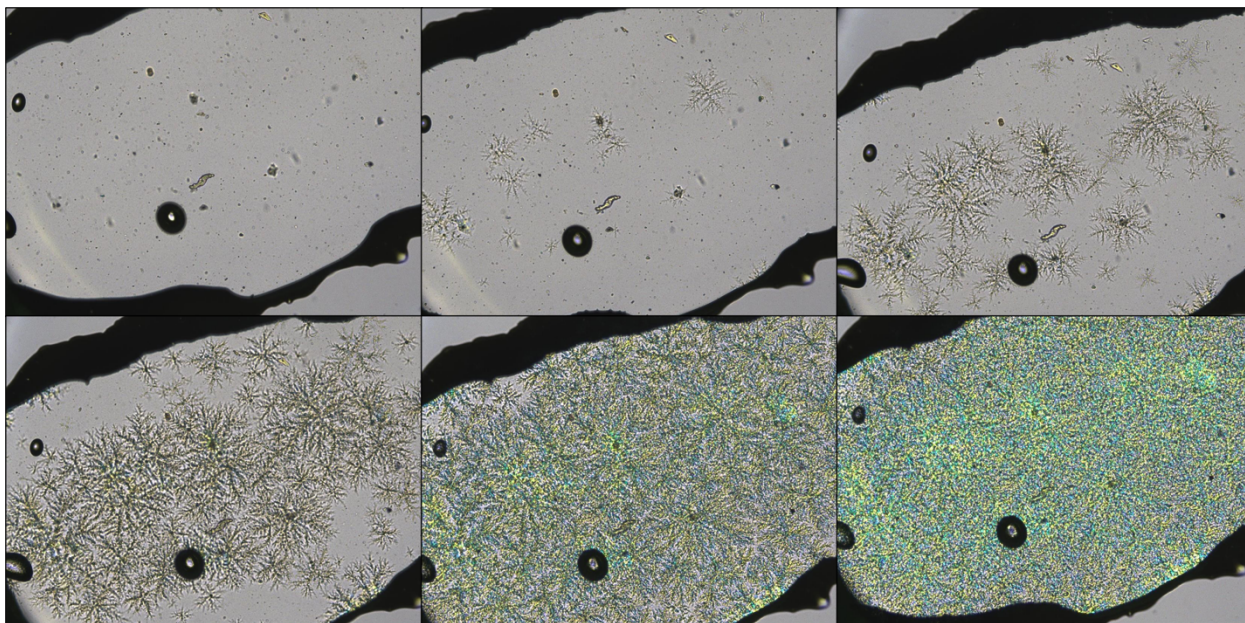


**Figure 3.19:** Polarized optical microscope images showing the morphology of recrystallization for 1% pentaerythritol blended with PHBHHx (6% Hx)

2% PE. This is likely due to the smaller surface area of the recrystallized PE. The 2% blend recrystallizes as large feather like sheets that do not initiate nucleation as well as the PE crystal structures that develop from a lowered concentration of nucleating agent. To further see the impact on PE morphology during recrystallization the weight loading was reduced to 0.5%. At this loading the crystallization of PHA is severely inhibited when heating above the melting point of inherent PHB within the sample. With 0.5% PE the concentration of nucleating agent particles is so low that the recrystallization process of the miscible nucleating agent is hindered until much lower temperatures of approximately 55°C. From the DSC analysis there is no evidence of separate crystallization exotherms for the nucleating agent and the polymer. There is one broad exotherm seen for the polymer indicating that the recrystallization is taking place simultaneously with the PHA polymer. The POM images shown in figure 3.21 also corroborate that the PE, at this concentration, is recrystallizing and immediately

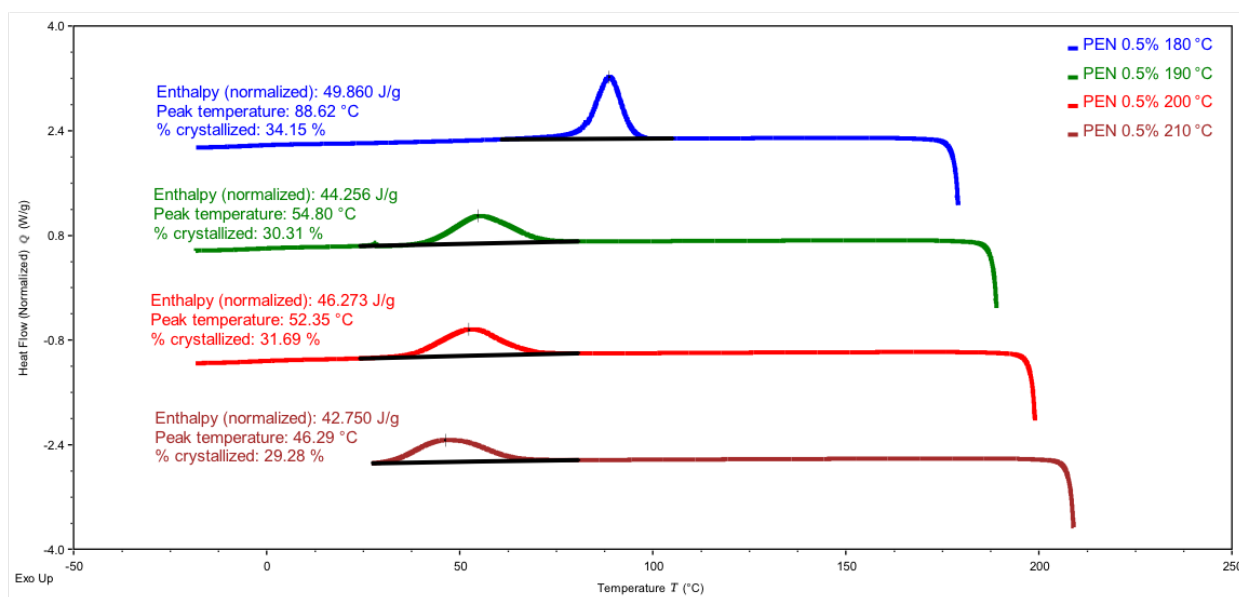


**Figure 3.20:** Crystallization exotherms for 0.5% pentaerythritol blends with PHBHHx (6% Hx)



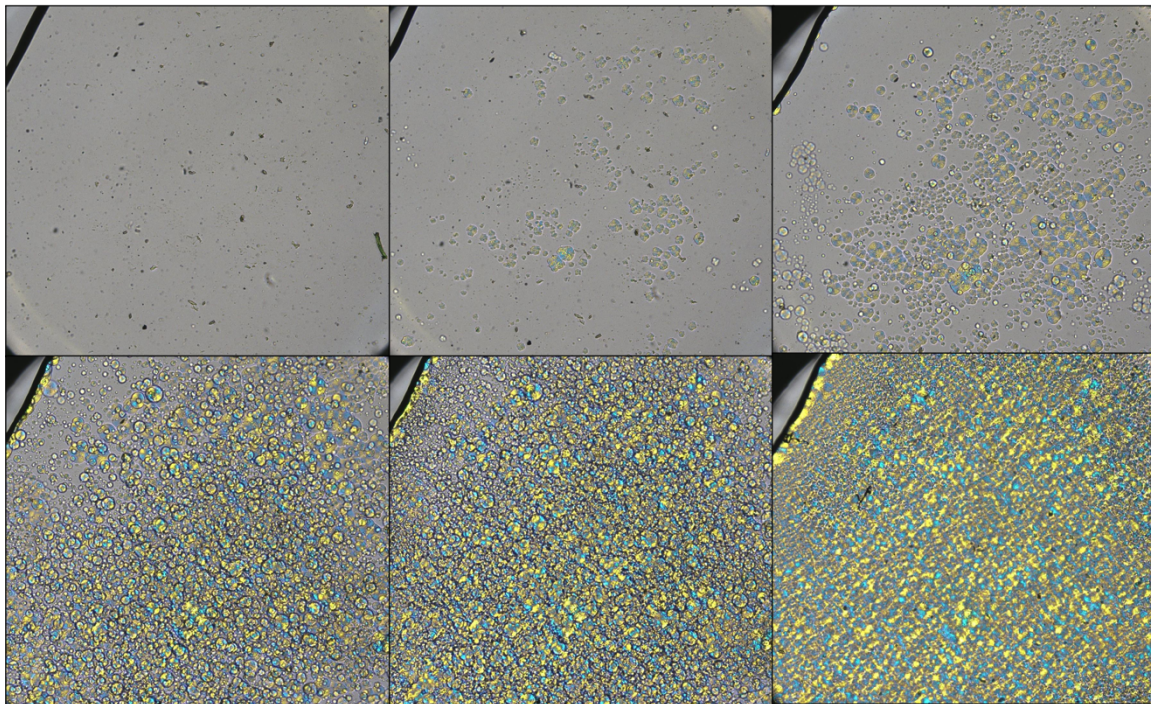


**Figure 3.21:** POM images showing discrete PE crystals with simultaneous PHA nucleation for blends of 0.5% PE with PHBHHx (6% Hx)

nucleating the PHA component as small spherulites. Interestingly the lowered concentration of nucleating agent prevents the development of a PE network like what is seen in the 1% and 2% blends. Instead, the PE recrystallizes as discrete, small crystals that subsequently nucleate PHA. This shows that there is a concentration dependence that must be met for the formation of the 3D network and efficient nucleation of the PHA. For all of these studies the extrusion temperature was kept constant at 150°C, and at this temperature not all of the nucleating agent is dissolving in the polymer matrix. Although for the 0.5% blend there was no evidence of left-over nucleating agent crystals under POM. In an attempt to facilitate the thinnest microfibril structure of PE a blend was extruded at a temperature of 165°C which is 10°C above the dissolution temperature of PE in PHA. When melt mixed at this temperature there are no localized

spots of high PE concentration from un-melted crystals within the PHA and upon recrystallization the peak crystallization temperature is nearly the same as the 1% and 2% blends extruded at 150°C, but there is no observation of a separate exotherm for PE although a slight broadening of the peak is observed with an onset temperature of approximately 110°C. The broadening is especially noticeably for the crystallization curve from a peak temperature of 180°C. It has a slight skew towards higher temperatures indicating a more noticeable exotherm for PE at this temperature. As the peak temperature is increased the PE distributes within the PHA more freely as the viscosity is reduced and allows for a finer network to form at the crystallization temperature of PHA. This indicates that the concentration of nucleating agent is high enough for efficient nucleation of the PHA fraction but not localized and the recrystallization of PE is right before the nucleation of the PHA. POM analysis also shows that PHA crystallization takes place from thinner dendritic fiber structures as soon as

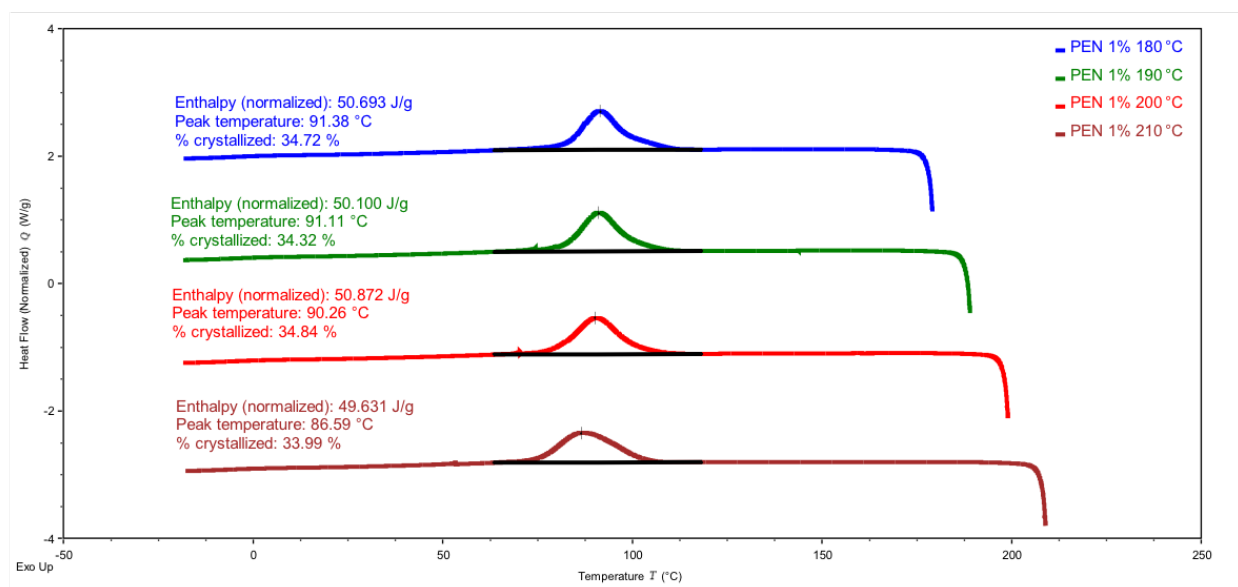


**Figure 3.22:** Crystallization exotherms for 1% pentaerythritol melt blend at 165°C with PHBHHx (6% Hx)

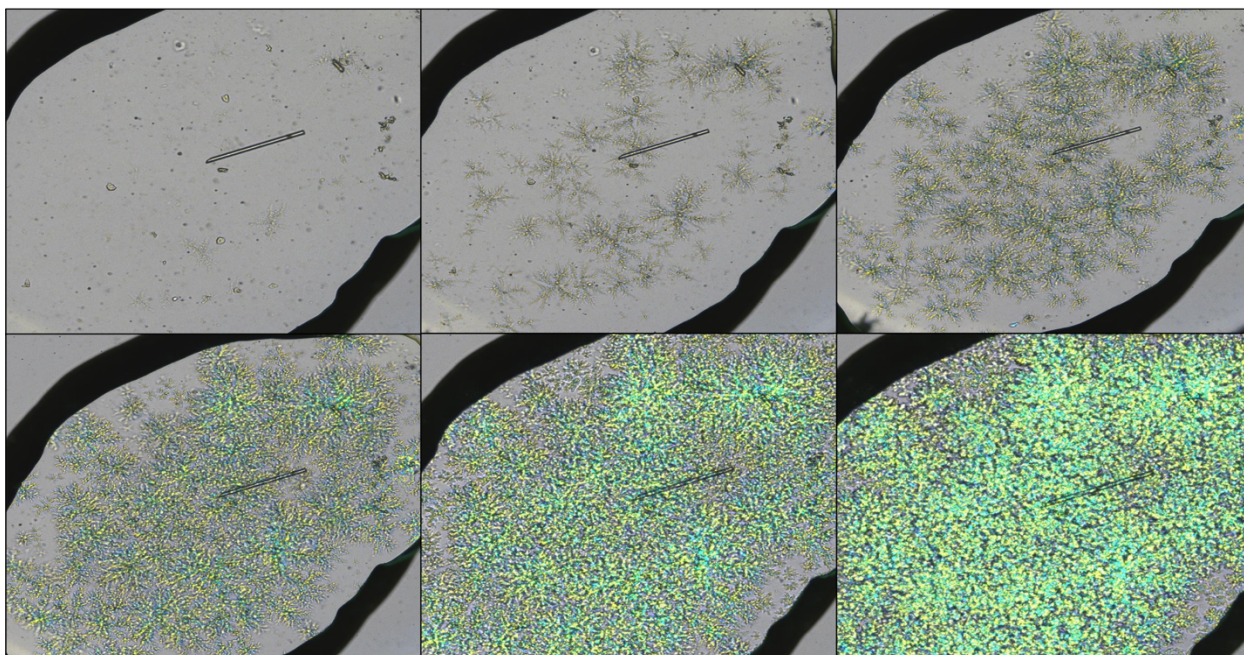


**Figure 3.23:** Polarized optical microscope images showing 1% pentaerythritol melt blended with PHBHHx (6% Hx) at 165°C

they are formed. 2% PE was also extruded at 165°C to see if finer more uniform fibrillar network formation could be achieved. Interestingly there was no difference seen between the 2% blends extruded at 150°C and 165°C except no remaining crystals of PE were seen in the 165°C extruded sample. There was still a large concentration of PE that gave feather like crystal structures indicating that at this weight loading there is a constant concentration of PE throughout the polymer matrix during melt blending that leads to high concentrations of PE during POM analysis. Upon subsequent heating to 200°C there was much finer fibrillar network formation due to the reduction in viscosity of the polymer as well as flow of the PE within the polymer. This seems to indicate that PE morphology can be dictated by concentration and viscosity of the polymer used.

To date, pentaerythritol is the only non-nitrogen containing, self-assembling, melt miscible nucleating agent for PHAs. Other self-assembling compounds such as

dihydrazides make us of toxic precursors for their synthesis such as hydrazine. Recently, oxalamides with varying structures have been shown to nucleate PHA as well as polypropylene. The large hydrogen bonding potential of the oxalamide motif allows for good self-assembly in the melt, and the temperature of self-assembly can be dictated by the internal carbon chain between the two oxalamide motifs as well as the length and structure of the terminal chain on each side of the compound. It has been shown that for PHBHHx with 6% Hx content there is better nucleation when the terminal group is cyclohexyl and benzyl rather than aliphatic<sup>40</sup> as well as when the carbon spacer between the two oxalamide groups has a length of greater than 4.<sup>18</sup> Typically comparing nucleating agents for PHA through literature is difficult as polymer purity, polymer microstructure and chemical distribution, polymer downstream processing conditions, nucleating agent particle size, thermal processing conditions, and testing conditions can greatly vary the results even for a PHA with identical Hx content. To compare the nucleation efficiency of melt miscible pentaerythritol to reported self-assembling nucleating agents, an oxalamide with a carbon spacer of 6 units and a terminal aliphatic unit of 12 carbons was synthesized (shown in figure 3.24). When the oxalamide (Ox) was blended with PHBHHx at a 2% loading there is a slight exotherm seen at 160°C showing the recrystallization of Ox, but the peak crystallization is downshifted to 66°C after heating to a peak temperature above the melting temperature of PHB. Decreasing the

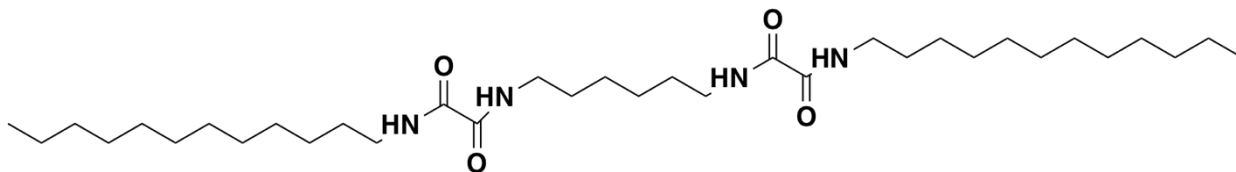


**Figure 3.24:** Structure of synthesized, melt miscible, oxalamide nucleating agent (Ox)



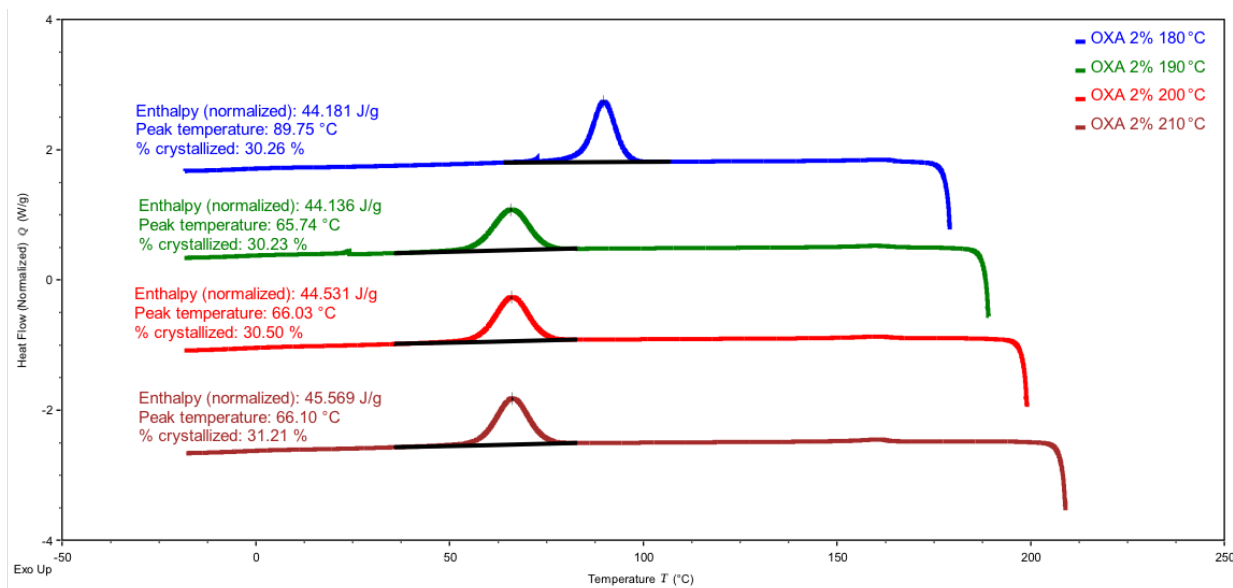


**Figure 3.25:** Crystallization exotherms for 2% aliphatic oxalamide blended with PHBHHx (6% Hx)

weight loading to 1% has little effect on the peak crystallization temperature in comparison to the 2% loading, but upon decreasing to 0.5% a drop of 10°C is seen as well as a broadening of the crystallization exotherm. It is also noticed that the crystal morphology of Ox is very different from PE. Instead of a 3D network structure Ox recrystallizes as many discrete, densely packed crystals (figure 3.26). There is also no observation of epitaxial nucleation from the surface of the oxalamide but rather the formation of many individual, round PHA spherulites. This could indicate that the hydrogen bonding potential of the oxalamide groups is the primary force behind the nucleation seen with this specific chemical structure. The crystal structure of many

NA	180 T <sub>c</sub> (°C)	190 T <sub>c</sub> (°C)	200 T <sub>c</sub> (°C)	210 T <sub>c</sub> (°C)	180 X <sub>c</sub> (%)	190 X <sub>c</sub> (%)	200 X <sub>c</sub> (%)	210 X <sub>c</sub> (%)
Ox 0.5%	88	51	54	56	34.1	24.1	30.2	32.6
Ox 1.0%	87	63	64	65	33.3	31.0	33.2	34.6
Ox 2.0%	90	66	66	66	30.3	30.2	30.5	31.2

**Table 3.3:** Peak crystallization temperatures and relative crystallinity for 0.5, 1, and 2% blends of Ox with PHBHHx (6% Hx)

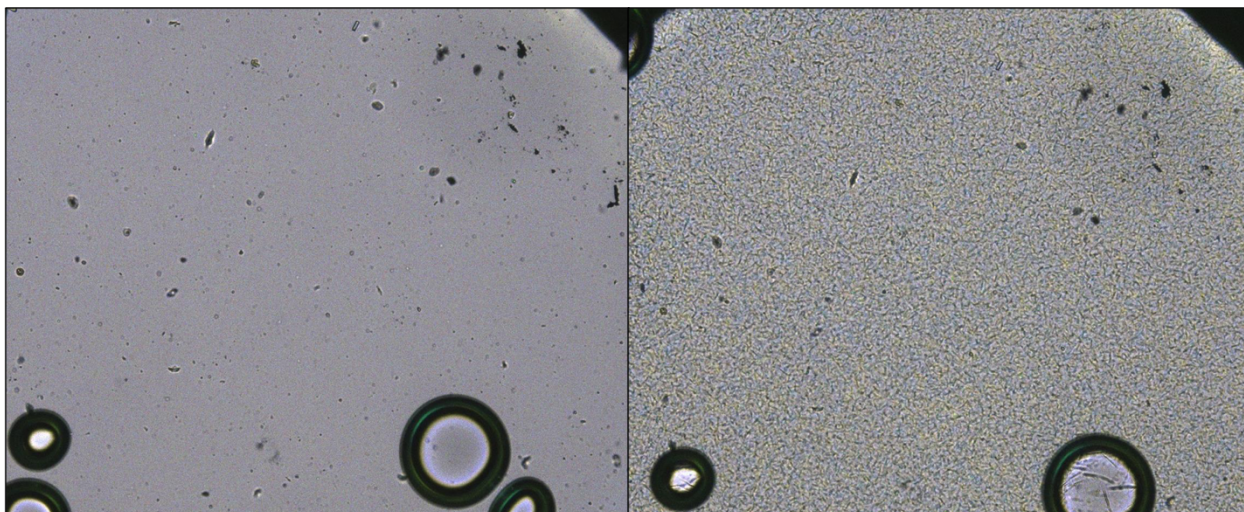


**Figure 3.26:** Polarized optical microscope images showing the recrystallization of Ox as small fiber like crystals upon cooling from the melt

oxalamides has not been reported on and data is not available for the synthesized Ox in this study. Understanding the crystal structure and lattice mismatch with PHB would help to elucidate the mechanism of crystallization. Likely there is a greater mismatch for such a low peak crystallization temperature similar to what is seen for talc. So far, no evidence of lattice matching has been proposed for oxalamide based nucleating agents, and the wide variety that have been made, while having different nucleating efficiency for PHA, all seem to nucleate in some capacity. This supports that while lattice matching is important, it is not the sole dictator of nucleation efficiency with PHA. While the aliphatic structure of the synthesized oxalamide is not optimal for nucleation of PHA based on literature results which showed better nucleation with terminal aromatic or cyclohexyl groups, the synthesized Ox had peak crystallization temperatures comparable to reported values for terminal aromatic and cyclohexyl analogs. This shows that pentaerythritol is the most efficient, reported melt miscible nucleating agent for PHA and has great promise for expanding the application scope of PHBHHx copolymers.

## Conclusion

Many industrial melt processing techniques such as injection molding, extrusion blow molding, and melt blown fibers require rapid crystallization of the polymer being processed. PHA is severely inhibited from being a viable thermoplastic replacement due to its slow nucleation and crystallization speed. The addition of heterogeneous nucleating agents such as cyanuric acid and boron nitride were shown to greatly increase the crystallization rate of a PHBHHx copolymer containing 6% hydroxy hexanoate. In addition, decreasing the particle size of the added nucleating agent was shown to be able to greatly increase the efficiency of the added nucleating agent. Orotic acid was shown to be a highly efficient nucleating agent for PHA especially when milled down to a small particle size of  $<100\mu\text{m}$ . Anhydrous and monohydrate versions show very little difference in peak crystallization temperatures when extrusion processed presumably due to the dehydration of the monohydrate under high shear and temperature. Metals salts of orotic acid using zinc, calcium and magnesium were also shown to efficiently nucleate PHA with zinc showing the closest match to orotic acid monohydrate. POM analysis was used to show that no dissolution of the metal salts was occurring during melting of the polymer indicating that while these salts have different crystal structures, they are still able to effectively nucleate PHBHHx. For some applications, such as melt blown fibers, the addition of a heterogeneous nucleating agent can be problematic. Pentaerythritol was shown to be an excellent melt-miscible nucleating agent for PHA. The spherulite morphology of the 3D PE network was shown to be concentration dependent and good nucleation could be achieved with as little as 1% added nucleating

agent. An aliphatic bis-oxalamide was used in comparison to PE and was shown to nucleate PHA much less efficiently as well as having a different recrystallization structure.



## References

1. Satkowski, M. M.; Melik, D. H.; Autran, J.-P.; Green, P. R.; Noda, I.; Schechtman, L. A., Physical and Processing Properties of Polyhydroxyalkanoate (PHA) Copolymers. In *Biopolymers Online*, 2005.
2. Beck, H. N., Heterogeneous nucleating agents for polypropylene crystallization. *Journal of Applied Polymer Science* **1967**, *11* (5), 673-685.
3. Cobntbekt, J.; Mabchessault, R. H., Physical properties of poly- $\beta$ -hydroxybutyrate: IV. Conformational analysis and crystalline structure. *Journal of Molecular Biology* **1972**, *71* (3), 735-756.
4. Yokouchi, M.; Chatani, Y.; Tadokoro, H.; Teranishi, K.; Tani, H., Structural studies of polyesters: 5. Molecular and crystal structures of optically active and racemic poly ( $\beta$ -hydroxybutyrate). *Polymer* **1973**, *14* (6), 267-272.
5. Doi, Y.; Kitamura, S.; Abe, H., Microbial Synthesis and Characterization of Poly(3-hydroxybutyrate-co-3-hydroxyhexanoate). *Macromolecules* **1995**, *28* (14), 4822-4828.
6. Sato, H.; Murakami, R.; Zhang, J.; Ozaki, Y.; Mori, K.; Takahashi, I.; Terauchi, H.; Noda, I., X-ray diffraction and infrared spectroscopy studies on crystal and lamellar structure and cho hydrogen bonding of biodegradable poly(hydroxyalkanoate). *Macromolecular Research* **2006**, *14* (4), 408-415.
7. Organ, S. J.; Barham, P. J., Nucleation of poly(hydroxy butyrate) by epitaxy on nitrogen-containing compounds. *Journal of Materials Science* **1992**, *27* (12), 3239-3242.

8. Puente, J. A. S.; Esposito, A.; Chivrac, F.; Dargent, E., Effect of boron nitride as a nucleating agent on the crystallization of bacterial poly(3-hydroxybutyrate). *Journal of Applied Polymer Science* **2013**, *128* (5), 2586-2594.
9. Kai, W.; He, Y.; Inoue, Y., Fast crystallization of poly(3-hydroxybutyrate) and poly(3-hydroxybutyrate-co-3-hydroxyvalerate) with talc and boron nitride as nucleating agents. *Polymer International* **2005**, *54* (5), 780-789.
10. Vandewijngaarden, J.; Murariu, M.; Dubois, P.; Carleer, R.; Yperman, J.; D'Haen, J.; Peeters, R.; Buntinx, M., Effect of ultrafine talc on crystallization and end-use properties of poly(3-hydroxybutyrate-co-3-hydroxyhexanoate). *Journal of Applied Polymer Science* **2016**, *133* (45).
11. He, Y.; Inoue, Y., Effect of  $\alpha$ -cyclodextrin on the crystallization of poly (3-hydroxybutyrate). *Journal of Polymer Science Part B: Polymer Physics* **2004**, *42* (18), 3461-3469.
12. Pan, P.; Shan, G.; Bao, Y.; Weng, Z., Crystallization kinetics of bacterial poly(3-hydroxybutyrate) copolyesters with cyanuric acid as a nucleating agent. *Journal of Applied Polymer Science* **2013**, *129* (3), 1374-1382.
13. Jacquel, N.; Tajima, K.; Nakamura, N.; Miyagawa, T.; Pan, P.; Inoue, Y., Effect of orotic acid as a nucleating agent on the crystallization of bacterial poly(3-hydroxybutyrate-co-3-hydroxyhexanoate) copolymers. *Journal of Applied Polymer Science* **2009**, *114* (2), 1287-1294.
14. Jacquel, N.; Tajima, K.; Nakamura, N.; Kawachi, H.; Pan, P.; Inoue, Y., Nucleation mechanism of polyhydroxybutyrate and poly(hydroxybutyrate-co-

hydroxyhexanoate) crystallized by orotic acid as a nucleating agent. *Journal of Applied Polymer Science* **2010**, *115* (2), 709-715.

15. Tsui, A.; Frank, C. W., Comparison of anhydrous and monohydrated forms of orotic acid as crystal nucleating agents for poly(3-hydroxybutyrate-co-3-hydroxyvalerate). *Polymer* **2014**, *55* (24), 6364-6372.

16. Gupta, B. S.; Edwards, J. V., 3 - Textile materials and structures for topical management of wounds. In *Advanced Textiles for Wound Care (Second Edition)*, Rajendran, S., Ed. Woodhead Publishing: 2019; pp 55-104.

17. Purchas, D. B.; Sutherland, K., CHAPTER 3 - Non-woven Fabric Media. In *Handbook of Filter Media (Second Edition)*, Purchas, D. B.; Sutherland, K., Eds. Elsevier Science: Amsterdam, 2002; pp 81-116.

18. Xu, P.; Cao, Y.; Lv, P.; Ma, P.; Dong, W.; Bai, H.; Wang, W.; Du, M.; Chen, M., Enhanced crystallization kinetics of bacterially synthesized poly(3-hydroxybutyrate-co-3-hydroxyhexanoate) with structural optimization of oxalamide compounds as nucleators. *Polymer Degradation and Stability* **2018**, *154*, 170-176.

19. Ma, P.; Deshmukh, Y. S.; Wilsens, C. H. R. M.; Ryan Hansen, M.; Graf, R.; Rastogi, S., Self-assembling process of Oxalamide compounds and their nucleation efficiency in bio-degradable Poly(hydroxyalkanoate)s. *Scientific Reports* **2015**, *5* (1), 13280.

20. Deshmukh, Y. S.; Wilsens, C. H. R. M.; Leoné, N.; Portale, G.; Harings, J. A. W.; Rastogi, S., Melt-Miscible Oxalamide Based Nucleating Agents and Their Nucleation

Efficiency in Isotactic Polypropylene. *Industrial & Engineering Chemistry Research* **2016**, 55 (45), 11756-11766.

21. Wilsens, C. H. R. M.; Hawke, L. G. D.; Troisi, E. M.; Hermida-Merino, D.; de Kort, G.; Leoné, N.; Saralidze, K.; Peters, G. W. M.; Rastogi, S., Effect of Self-Assembly of Oxalamide Based Organic Compounds on Melt Behavior, Nucleation, and Crystallization of Isotactic Polypropylene. *Macromolecules* **2018**, 51 (13), 4882-4895.

22. Laycock, B.; Halley, P.; Pratt, S.; Werker, A.; Lant, P., The chemomechanical properties of microbial polyhydroxyalkanoates. *Progress in Polymer Science* **2013**, 38 (3), 536-583.

23. Yoshie, N.; Menju, H.; Sato, H.; Inoue, Y., Complex composition distribution of poly(3-hydroxybutyrate-co-3-hydroxyvalerate). *Macromolecules* **1995**, 28 (19), 6516-6521.

24. Pederson, E. N.; McChalicher, C. W. J.; Srienc, F., Bacterial Synthesis of PHA Block Copolymers. *Biomacromolecules* **2006**, 7 (6), 1904-1911.

25. Barham, P. J.; Keller, A.; Otun, E. L.; Holmes, P. A., Crystallization and morphology of a bacterial thermoplastic: poly-3-hydroxybutyrate. *Journal of Materials Science* **1984**, 19 (9), 2781-2794.

26. Takusagawa, F.; Shimada, A., The Crystal Structure of Orotic Acid Monohydrate (Vitamin B13). *Bulletin of the Chemical Society of Japan* **1973**, 46 (7), 2011-2019.

27. Portalone, G., Redetermination of orotic acid monohydrate. *Acta Crystallogr Sect E Struct Rep Online* **2008**, 64 (Pt 4), o656-o656.

28. Kanunnikova, O. M.; Aksenova, V. V.; Karban, O. V.; Muhgalin, V. V.; Senkovski, B. V.; Ladjanov, V. I., Mechanical activation effect on structure, physicochemical, and biological properties of potassium/magnesium orotates. *IOP Conference Series: Materials Science and Engineering* **2017**, 283, 012004.
29. Kumberger, O.; Riede, J.; Schmidbaur, H., Orotate Complexes, II1) Preparation and Crystal Structures of Calcium and Zinc Orotate(2-) Hydrates. *Chemische Berichte* **1991**, 124 (12), 2739-2742.
30. Karipides, A., Thomas, B., The structures of tetraaqua(uracil-6-carboxylate)zinc(II) monohydrate (A) and tetraaqua(uracil-6-carboxylato)nickel(II) monohydrate (B). *Acta crystallographica. Section C* **1986**, 47, 1705-1707.
31. Kumberger, O.; Riede, J.; Schmidbaur, H., Preparation and Crystal Structure of Zinc Bis[orotate(1-)] Octahydrate. *Zeitschrift für Naturforschung B* **1993**, 48 (7), 961-964.
32. Abendrot, M., Chęcińska, Lilianna, Kusz, Joachim, Lisowska, Katarzyna, Zawadzka, Katarzyna, Felczak, Aleksandra, Kalinowska-Lis, Urszula, Zinc(II) Complexes with Amino Acids for Potential Use in Dermatology: Synthesis, Crystal Structures, and Antibacterial Activity. *Molecules* **2020**, 25 (4).
33. Low, B. W.; Hirshfeld, F. L.; Richards, F. M., Glycinate Complexes of Zinc and Cadmium. *Journal of the American Chemical Society* **1959**, 81 (16), 4412-4416.

34. Newman, J. M., Bear, C. A., Hambley, T. W., Freeman, H. C., Structure of bis(glycinato)zinc(II) monohydrate, a five-coordinate zinc(II) complex. *cta Crystallographica Section C* **1990**, 46.
35. Konar, S.; Gagnon, K.; Clearfield, A.; Thompson, C.; Hartle, J.; Ericson, C.; Nelson, C., Structural determination and characterization of copper and zinc bis-glycinates with X-ray crystallography and mass spectrometry. *Journal of Coordination Chemistry* **2010**, 63 (19), 3335-3347.
36. Rachelle Arnold, A. J. Crystal nucleating agents for polyhydroxyalkanoates. 2017.
37. Shiono, R., Cruickshank, D. W. J., Cox, E. G., A refinement of the crystal structure of pentaerythritol. *Acta Crystallographica* **1958**, 11 (6), 389-391.
38. Feng, B.; Tu, J.; Sun, J.-W.; Fan, L.-W.; Zeng, Y., A molecular dynamics study of the effects of crystalline structure transition on the thermal conductivity of pentaerythritol as a solid-solid phase change material. *International Journal of Heat and Mass Transfer* **2019**, 141, 789-798.
39. Benson, D. K.; Burrows, R. W.; Webb, J. D., Solid state phase transitions in pentaerythritol and related polyhydric alcohols. *Solar Energy Materials* **1986**, 13 (2), 133-152.
40. Xu, P.; Feng, Y.; Ma, P.; Chen, Y.; Dong, W.; Chen, M., Crystallization behaviours of bacterially synthesized poly(hydroxyalkanoate)s in the presence of oxalamide compounds with different configurations. *International Journal of Biological Macromolecules* **2017**, 104, 624-630.

## CHAPTER 4

### CONCLUSIONS AND FUTURE OUTLOOK

In this dissertation the mechanical properties of polyhydroxybutyrate-co-hydroxyhexanoate were improved through reactive and non-reactive blending with various polyesters. Nucleating agents were also investigated for enhancing the crystallization rate of the polymer. In chapter 2, melt blending of PHBHHx with commercially available polymers was investigated for improvement in elongation at break and it was found that PBAT behaved differently than the other semi-crystalline polymers. PBAT remained mostly amorphous when blending and had a more linear increase in elongation at break with higher loading of the polymer. It also decreased the Young's modulus most significantly of all the polymers especially at high loadings of 30%. PCL and PBS were shown to improve the mechanical properties especially at low loadings. PBS had a peak elongation at break when added at a 10% loading while PCL had a peak elongation at a 30% loading. PBSA was shown to behave more like PBAT due to its less crystalline nature. Starch was also reactively and non-reactively incorporated into the PHA by pre-blending with commercially available polyesters. It was found that PBAT was able to compatibilize starch the best, but the young's modulus decreased significantly. High lamellar talc was used to increase the stiffness of starch blends and it was shown that increasing the surface area was more effective than decreasing the

particle size. Chapter 2 also addressed the aging problem that is so common with PHA. 10% Hx was incorporated into formulations and was shown to significantly reduce the embrittlement over a period of 15 days. Reactive extrusion with 10% Hx content in the formulation was also shown to totally remove any embrittlement over a period of 15 days. Multifunctional coagents were also used to extend the reactivity and lifetime of the organic peroxides during the reactive extrusion cycle. All agents were shown to increase the elongation at break indicating an enhanced branched and crosslinked structure due to the increased sites for reactions to take place.

Chapter 3 investigated both heterogeneous and melt miscible nucleating agents for the improvement in the crystallization rate of PHBHHx. It was shown that for heterogeneous agents particle size is important when considering nucleation efficiency. Smaller particles of the same nucleating agent were able to nucleate the PHA much more effectively allowing for the amount of added agent to be significantly reduced. When particle size was reduced too small the increase in nucleation activity plateaued. At nanometer sized particles of nucleating agent, the particles tended to agglomerate and a loading of 0.5% showed worse activity in comparison to other nucleating agents in the micron size range. PHB homopolymer was also shown to greatly enhance the crystallization rate of PHA when coupled with a heterogeneous nucleating agent. Unmelted crystals of PHB were shown to act as nucleating agents when kept below 180°C, but when heated above the melting point of PHB, the heterogeneous nucleating agent first causes PHB to crystallize which subsequently nucleates the PHBHHx copolymer at a higher peak temperature. Pentaerythritol was shown to be an excellent



melt miscible nucleating agent for PHA. It was shown that PE recrystallized into a 3D structure within the PHA matrix that had good lattice matching for epitaxial growth of PHA crystals. It was also shown that the morphology of recrystallized PE could be changed by shifting its concentration within the PHA matrix. Reducing the concentration led to finer, threadlike structures of PE rather than larger feather like crystals. Reducing the concentration too low caused the 3D structure to collapse into discrete crystals of PE which severely inhibited the overall crystallization of the PHA.

### **Future directions**

In chapter 2 improvement in mechanical properties of PHA was accomplished through melt blending and reactive extrusion, but only elongation at break and Young's modulus were examined. While these two criteria are extremely important for PHA, there are others that also need to be addressed that are not directly related to tensile measurements. Elongation at break under relatively slow deformation rates, while important, does not address impact strength of the extruded article. As deformation rates increase no rearrangement of the polymer chains can take place resulting in much poorer toughness. Investigating impact strength is important for PHA because an extruded article could have a very high elongation at break under a slow deformation rate but have poor impact strength that could lead to a part failure. This is particularly important for articles such as a water bottle that must be able to pass a drop test from a height of 6ft without any cracks forming. Re-examining the best formulations from chapter 2 using notched izod impact testing would be of much value in determining a relationship between elongation at break and impact strength. Furthermore,

investigating properties that pertain to film applications would be of much benefit.

Elmendorf tear testing as well as dart drop testing would help to determine the suitability of formulations, that have good elongational properties, for film applications.

Chapter 2 also showed that blending of aliphatic polyesters with PHA produced immiscible droplet morphology within the blends resulting in improved elongation at break. It was particularly evident that above a 20% loading the mechanical properties of the added polymer become important for the final properties of the blend. Future work in understanding how droplet size, morphology, and interparticle distance affect the final mechanical properties of the blends would be of much value. It was also evident that amorphous polymer additives behaved differently than semi-crystalline additives. Probing the effect of amorphous polymers on PHA toughness as well as aging would also give valuable insight into producing useable PHA articles to replace commodity thermoplastics.

Reactive extrusion was shown to greatly enhance the mechanical properties of PHA blends and produce a gel content that was able to act as a nucleating agent. Further work needs to be done on characterizing the amount of branching as well as the gel content of the REX blends. Gel permeation chromatography can be used to see an increase in the molecular weight distribution as well as to determine information on the amount of branching within the polymer. It is also still unknown how the gel particles are able to nucleate even after heating to temperatures that would normally result in poor crystallization for PHA. Rheology can also help determine the extent of branching and crosslinking as well as help elucidate the effect on viscosity. While radical based

reactive extrusion was explored in this dissertation it would be beneficial to extend to other reactive chemistries that are more controlled to give precise molecular architecture or chain extension rather than random branching and crosslinking.

One area that was not explored in this thesis was the use of small molecule plasticizers for the improvement in polymer ductility. While the impact on mechanical properties for plasticizers would be valuable, it would be of much benefit to begin understanding the melt rheology of the polymer blends from chapter 2 as well as how to tune the viscosity of the blend to be desirable for processing as well as for certain application such as melt blown fibers or film formation. Processing aids, slip agents, and plasticizers can be used to help scale extrusion of PHA to larger set ups rather than the small lab scale extruder used in this dissertation. Viscosity control as well as molecular weight preservation will become extremely important for large scale extrusion applications and there remains a significant gap between lab scale and industrial extrusion particularly for reactive extrusion formulations.

Chapter 3 investigated both heterogeneous and melt miscible nucleating agents for PHA. While significant improvement in crystallization rate was achieved there remains a gap in understanding on lattice matching of the added nucleating agent with the PHB unit cell for final nucleation efficiency. There is a general trend of matching the a and c parameters of the PHB unit cell and also containing hydrogen bonding capabilities such as nitrogen with the ability of a given compound to act as a nucleating agent but understanding this further so that nucleating agents can be picked based on structure and lattice parameters alone without trial and error would be of much benefit

in the industrial applicability of PHA as a replacement for current commodity thermoplastics. Investigating chemical and melt miscible nucleating agents would be very valuable for fiber applications where heterogeneous nucleating agents are not amendable.

Finally, one of the most important future directions for the work outlined in this dissertation is end of life testing for formulations that are developed for optimal crystallization and mechanical properties. Respirometry can be used to examine how chemical crosslinking and fillers such as talc, calcium carbonate, and other polyesters affect the degradation rate of the formulated polymer blend. Adding fillers such as starch are predicted to increase the rate of degradation but when blended into PHA with other polyesters that present a core shell morphology it is unknown if it will increase the rate of degradation. Addition of other additives that increase the rate of degradation, especially in marine environments, would be very valuable, and while respirometry is a powerful technique for investigation of the end-of-life properties of blends it is imperative that it is coupled with field studies such as testing of the fully formed article in the ocean.

### **Final Remarks**

PHA offers an immense amount of potential as a biologically degradable alternative to many of the current commodity plastics used in the single packaging sector. With further development in mechanical properties and processing techniques it has the potential to displace many of the plastics that are used once and then persist in the environment. As PHA begins to be used more in the marketplace for current

persistent plastics used in single use items and as other techniques advance such as mechanical and chemical recycling become more industrially viable the plastic pollution load on the environment will slowly begin to dissipate. PHA is the catalyst in the plastic and packaging sector for proper stewardship of the earth while maintaining human flourishing by allowing the continued use of products that are so beneficial to modern life in an ecologically responsible fashion. This thesis has highlighted the beginnings of what this material is capable of after proper formulation and crystallization techniques.